Observational Cosmology

Lectures on the topic:

Cosmology with galaxy clusters

(K. Basu)

Course website:

http://www.astro.uni-bonn.de/~kbasu/ObsCosmo

Cluster mass and observables

Cosmology with galaxy clusters

- Growth of cosmic structure from cluster number counts (use of halo mass function)

- Measuring the large-scale angular clustering of clusters ("clustering of clusters")

- Measuring distances using clusters as standard candles (joint X-ray/SZE)

- Using the gas mass fraction in clusters to measure the cosmic baryon density

- Measuring the large-scale velocity fields in the universe from kinematic SZE

- Constraints from SZ effect power spectrum

- and many other..

Windows to galaxy clusters

- Optical: σ_v , N_{gal}

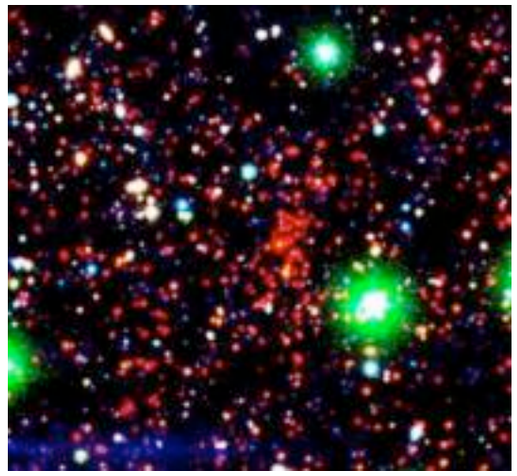

- X-ray: L_X, T_X

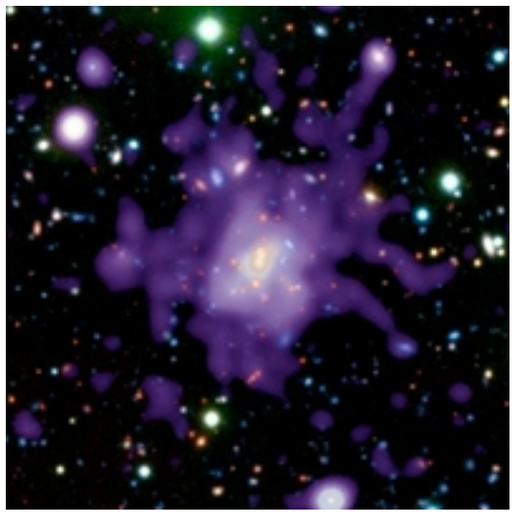

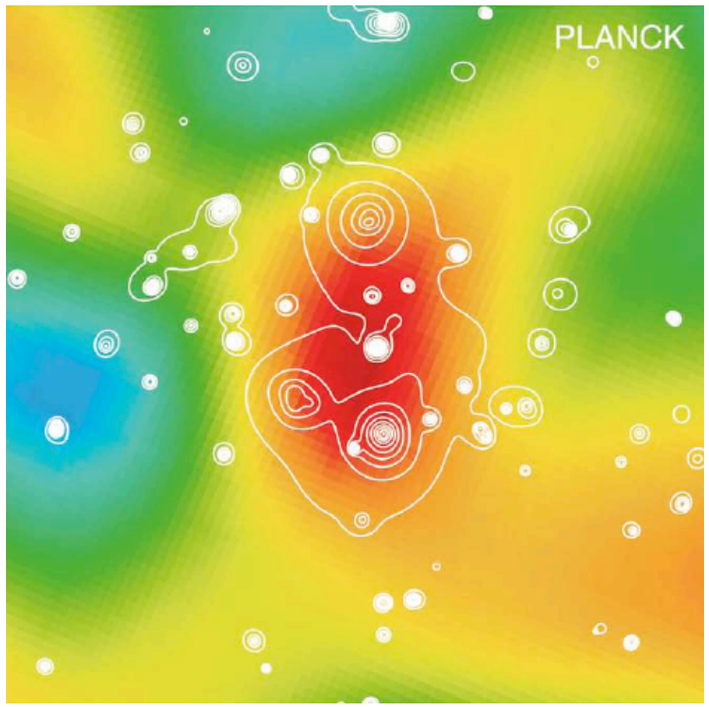

- Millimeter: Y_{SZ}

- Optical: Red sequence, lensing shear

- Radio: halo, relic, etc.

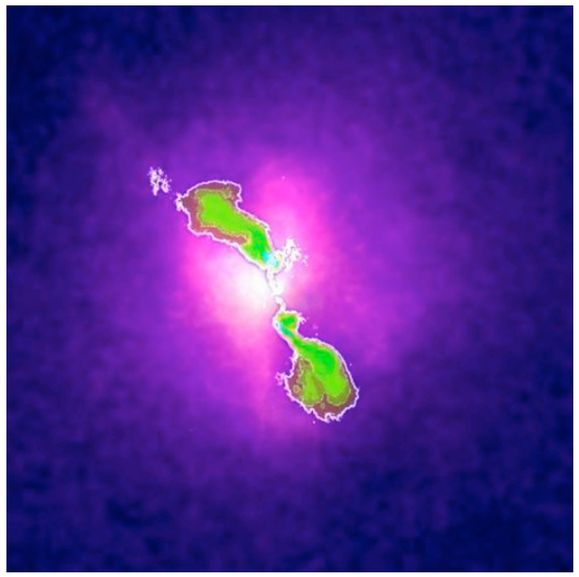

Mass budget in galaxy clusters

(The name "galaxy clusters" is a misnomer)

- ~2% mass in galaxies
- ~13% in the hot, ionized intra-cluster plasma (baryon that didn't make it to the galaxies)
- ~85% dark matter

Example: Coma cluster

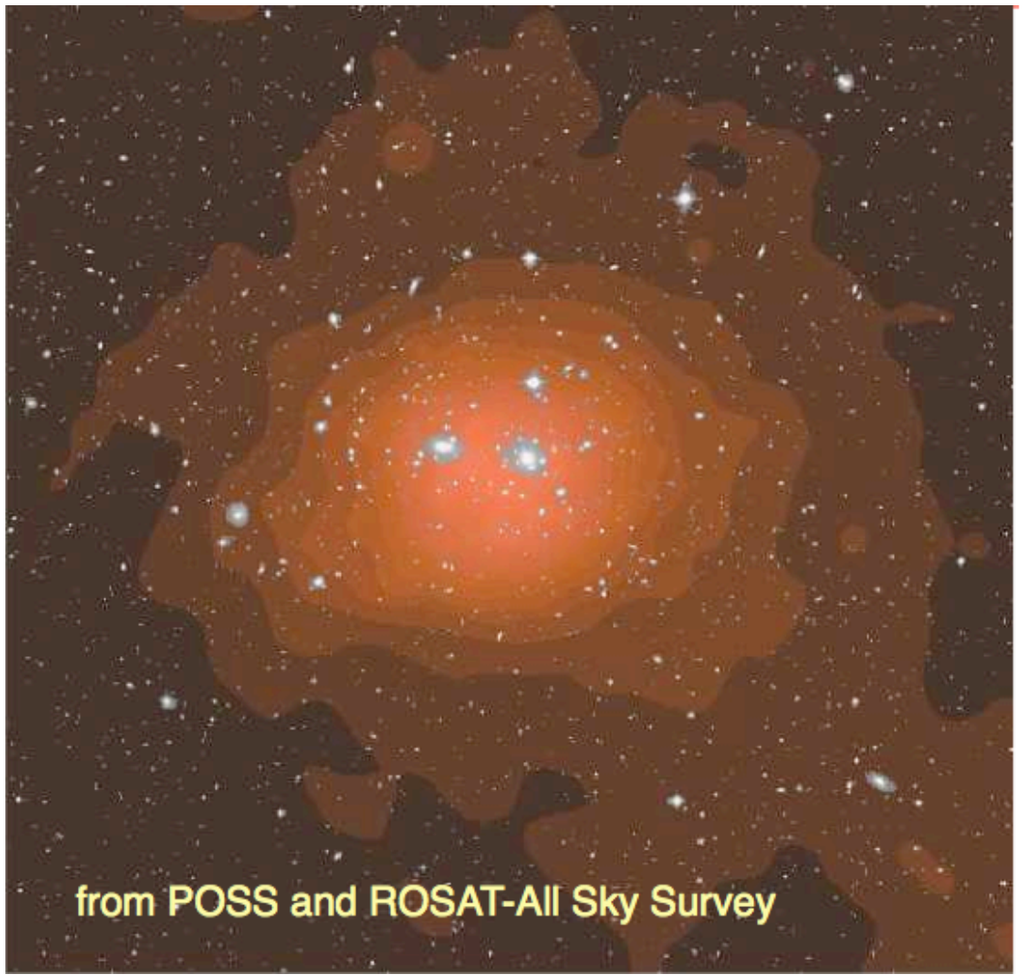

The composition of galaxy clusters:

- **78 – 87% = Dark Matter**
- **11 – 14% = hot gas**
- **2 - 6% = galaxies (in total)**

for $H_0 = 70$

White et al. (1993)

Table 1.1. *Mass Hierarchy in the Coma Cluster*

Component	$M(< 1.5\,h^{-1}$ Mpc) $(M_\odot)$	$M/M_{\rm vis}$
Total[a]	$1.3 \pm 0.3 \times 10^{15}\ h_{70}^{-1}$	9.0 ± 2.5
Intracluster gas	$1.3 \pm 0.2 \times 10^{14}\ h_{70}^{-5/2}$	0.90 ± 0.02
Galaxies	$1.4 \pm 0.3 \times 10^{13}\ h_{70}^{-1}$	0.10 ± 0.03

[a]Estimated from gas dynamic simulations.

Discovery of Dark Matter

Fritz Zwicky (1898 - 1974)

Fritz Zwicky noted in 1933 that outlying galaxies in Coma cluster moving much faster than mass calculated for the visible galaxies would indicate

Virial Theorem: $2\langle T\rangle = -\langle V\rangle$

$$\frac{1}{2}m(3\sigma^2) \rightarrow \mathrm{KE_{avg}} = -\frac{1}{2}\ \mathrm{GPE_{avg}} \leftarrow G\frac{M_{tot}(r)m}{r}$$

$$M \sim \frac{3R\sigma_v^2}{G} = 10^{15}\,h^{-1}\,\mathrm{Mpc}\left(\frac{R}{1.5\,h^{-1}\,\mathrm{Mpc}}\right)\left(\frac{\sigma_v}{1000\,\mathrm{km\,s^{-1}}}\right)^2$$

Virial theorem

The virial theorem (for gravitational force) states that, for a stable, self-gravitating, spherical distribution of equal mass objects (stars, galaxies, etc), the total kinetic energy of the objects is equal to minus 1/2 times the total gravitational potential energy.

Suppose that we have a gravitationally bound system that consists of N individual objects (stars, galaxies, globular clusters, etc.) that have the same mass m and some average velocity v. The overall system has a mass $M_{tot} = N \cdot m$ and a radius R_{tot}.

The kinetic energy of each object is K.E.(object) = 1/2 m v^2

while the kinetic energy of the total system is K.E.(system) = 1/2 m N v^2 = 1/2 M_{tot} v^2

$$P.E.(system) \simeq -\frac{1}{2} G \frac{N^2 m^2}{R_{tot}} = -\frac{1}{2} G \frac{M_{tot}^2}{R_{tot}}$$

$$\frac{1}{2} M_{tot} v^2 = +\frac{1}{4} G \frac{M_{tot}^2}{R_{tot}}$$

$$M_{tot} \simeq 2 \frac{R_{tot} v^2}{G}$$

Virial theorem and hydrostatic equilibrium condition

The virial theorem is more restrictive than the hydrostatic equilibrium condition, because it assumes the self-gravitating system has reached *equipartition between its kinetic energy and potential energy!*

The application of hydrostatic equilibrium, on the other hand, only requires us to assume the net acceleration of the gas at any point (resulting from the sum of gravitational and hydrostatic forces) is zero.

$$\frac{dv}{dt} = -\frac{\nabla P}{\rho} + g + F$$

$$\frac{dv}{dt}; F \to 0 \quad (equilibrium)$$

$$-\frac{\nabla P}{\rho} \to -\frac{1}{\rho}\frac{\partial P}{\partial r} \quad (spherical\ symmetry)$$

$$\Rightarrow \frac{\partial P}{\partial r} = -\frac{Gm\rho}{r^2}$$

The virial theorem is then derived from the HE equation under suitable boundary conditions.

Discovery of Dark Matter

Fritz Zwicky (1898 - 1974)

F. Zwicky, Astrophysical Journal, vol. 86, p.217 (1937)

$$\mathcal{M} > 9 \times 10^{46} \text{gr} . \qquad (35)$$

The Coma cluster contains about one thousand nebulae. The average mass of one of these nebulae is therefore

$$\overline{M} > 9 \times 10^{43} \text{ gr} = 4.5 \times 10^{10} M_{\odot} . \qquad (36)$$

the average mass of nebulae in the Coma cluster. This result is somewhat unexpected, in view of the fact that the luminosity of an average nebula is equal to that of about 8.5×10^7 suns. According

The mass of a self-gravitating system in equilibrium:

$$M = R\, v^2 / G$$

This assumes velocities in equilibrium. But two-body relaxation process with galaxies is extremely slow. How do galaxy clusters (and so to speak, also galaxies containing stars) attain equilibrium?

Violent relaxation

The thermalization of the molecules e.g. in this lecture room is achieved by two-body collisions moderated by short range forces. For stars in galaxies and galaxies, and Dark Matter particles in clusters of galaxies, we have to deal with long range forces. Here calculations show that two-body interactions are very ineffective. The thermalization of stars in galaxies would take many Hubble times.

How do equilibrium configurations form even when relaxation is so slow ? How is an approximately Maxwellian velocity distribution achieved, if two-body relaxation is so slow?

Answer: „Violent Relaxation“ – mixing of phase space in the strong fluctuating gravitational potential when the cluster forms (theory by Lynden-Bell) – the fine grained phase space density is preserved but the coarse grained phase space density is mixed.

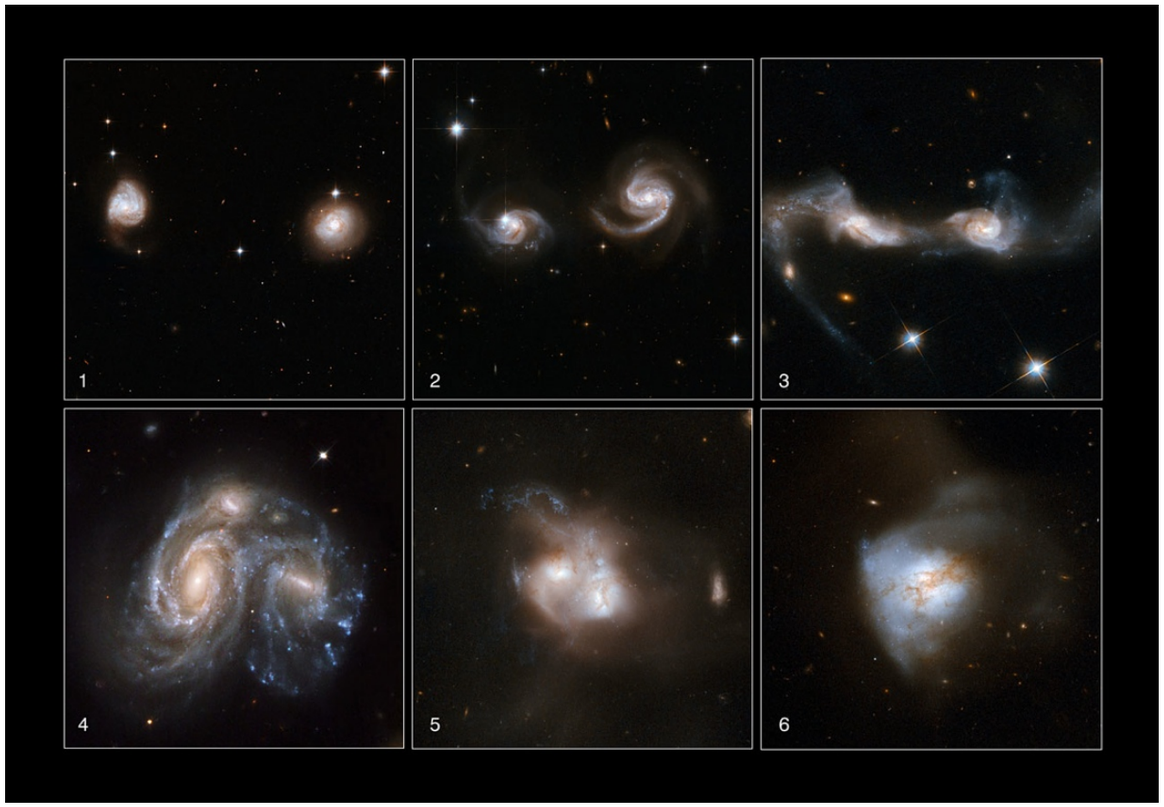

arXiv: astro-ph/9602021

Violent relaxation

Difference of two-body and violent relaxation:

Two-body : (collisional) $$v^2 \propto \frac{kT}{m} \quad \Rightarrow \quad v \propto \sqrt{m}$$

Violent relaxation : v independent of m (m mass of particle)

Toward the late stages of the merger the shape of the gravitational potential begins changing so quickly that galaxy orbits are greatly affected, and lose any memory of their previous orbit.

Proof: no velocity segregation in clusters

TABLE IV. Velocity dispersion vs magnitude.

$(m_1 < m \leqslant m_2, r < 30')$			
m_1	m_2	n	σ
	$\leqslant 15.0$	21	1085
15.0	15.5	31	1081
15.5	16.0	37	984
16.0	16.5	24	1176
16.5$\leqslant$		32	1250

Dark matter with galaxy clusters

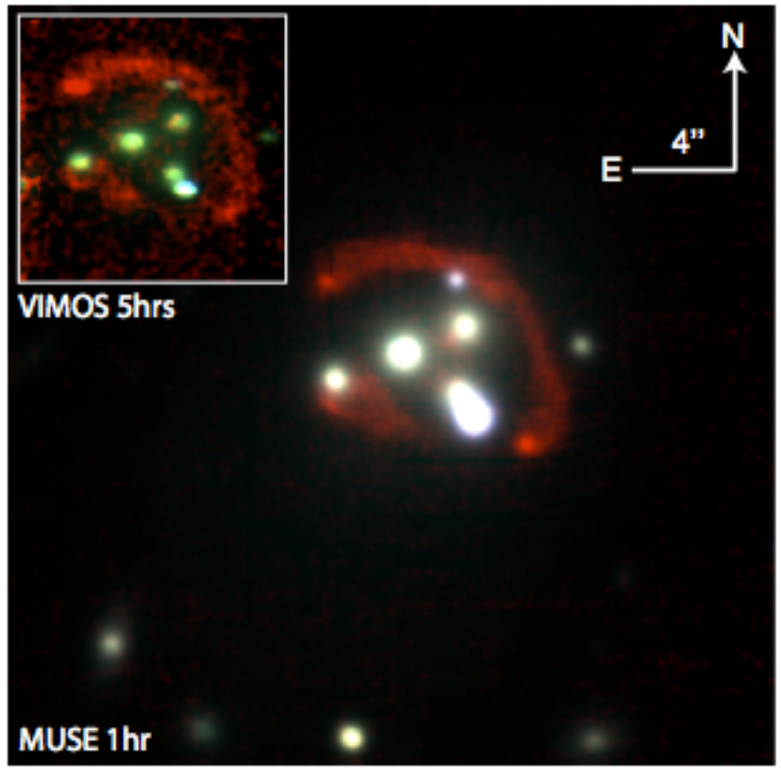

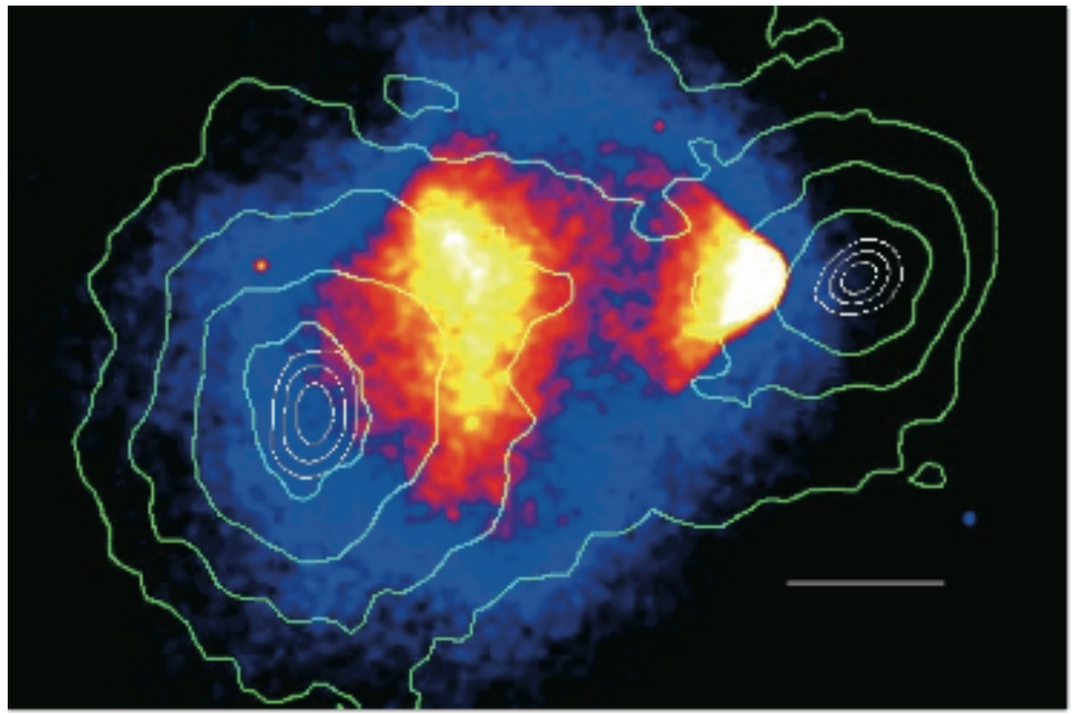

Clowe et al. 2006

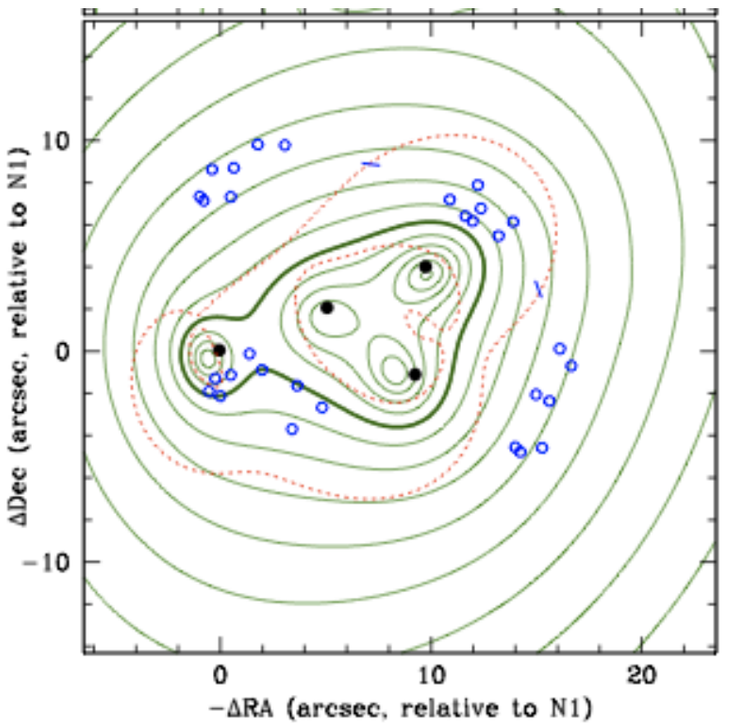

Abell 3827 (Massey et al. 2015)

Cluster radii

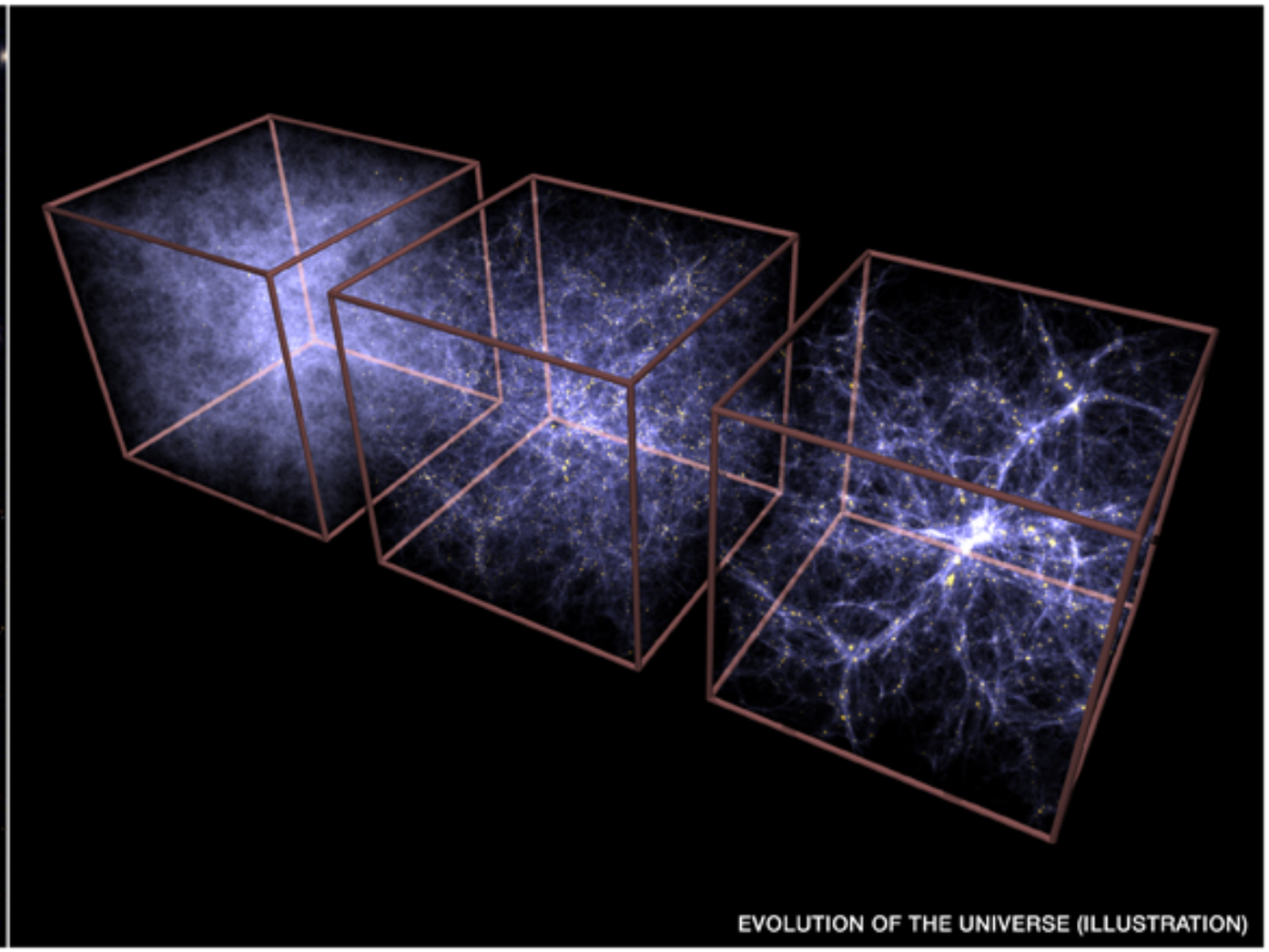

Where are the boundaries of a cluster?

Overdensity radii

- ⋆ A radius within which the mean density is Δ times the critical density (ρ_c) at the cluster's redshift
- ⋆ Clusters are centrally concentrated so larger Δ correspond to smaller radii
- ⋆ Write radii as R_Δ
  - e.g. R_{200} means Δ=200

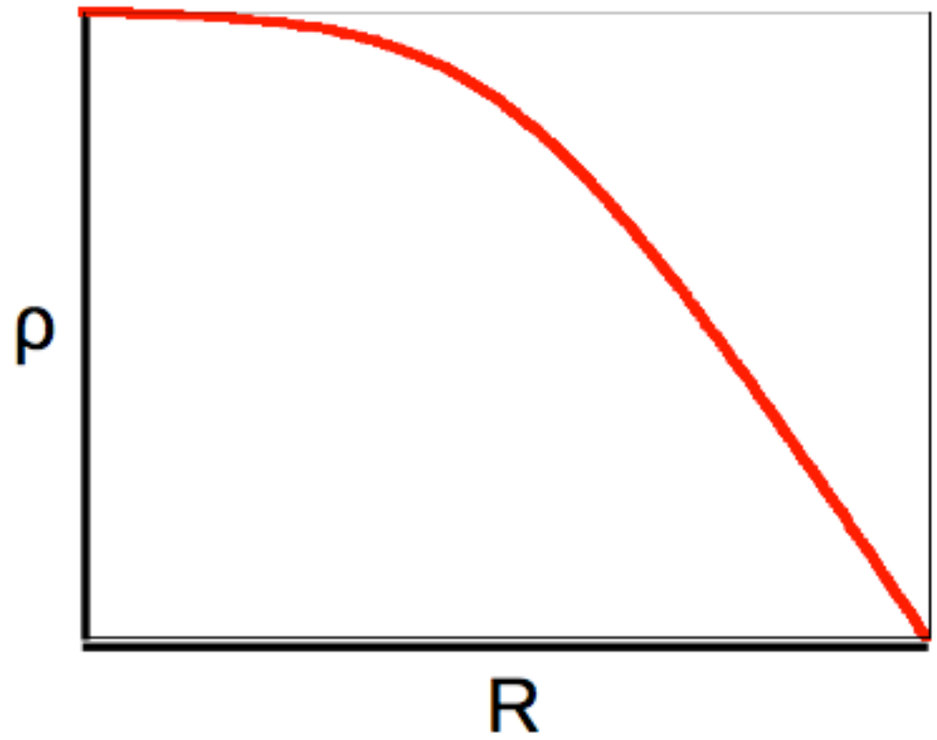

N.B. here ρ is the total mass density (not just gas)

Overdensity radii allow fair comparison of properties of clusters of different sizes, key part of self-similar model

Cluster virial radius

Beware: r_{200} is not the same thing as virial radius
but simulations show r_{200} to be a fair approximation

In a spherical collapse model, the behavior of a mass shell follows the equation:

$$\ddot{r}_{\rm sh} = -\frac{GM_{\rm sh}}{r_{\rm sh}^2} - \frac{1+3w}{2}\Omega_\Lambda H_0^2 (1+z)^{3(1+w)} r_{\rm sh},$$

Under simplistic assumption ("top-hat model", which means cluster is assumed to be of constant density), the mean density of perturbations that lead to collapse is $18\pi^2 \approx 178$ for flat, EdS cosmology.

For ΛCDM the solution is:

$$\Delta_{\rm v} = 18\pi^2 + 82[\Omega_{\rm M}(z) - 1] - 39[\Omega_{\rm M}(z) - 1]^2$$

Thus for z=0, the "virial radius" should be ~ r_{100}

Radii comparison

X-ray
strong lensing

X-ray
SZE
weak lensing

SZE
weak lensing

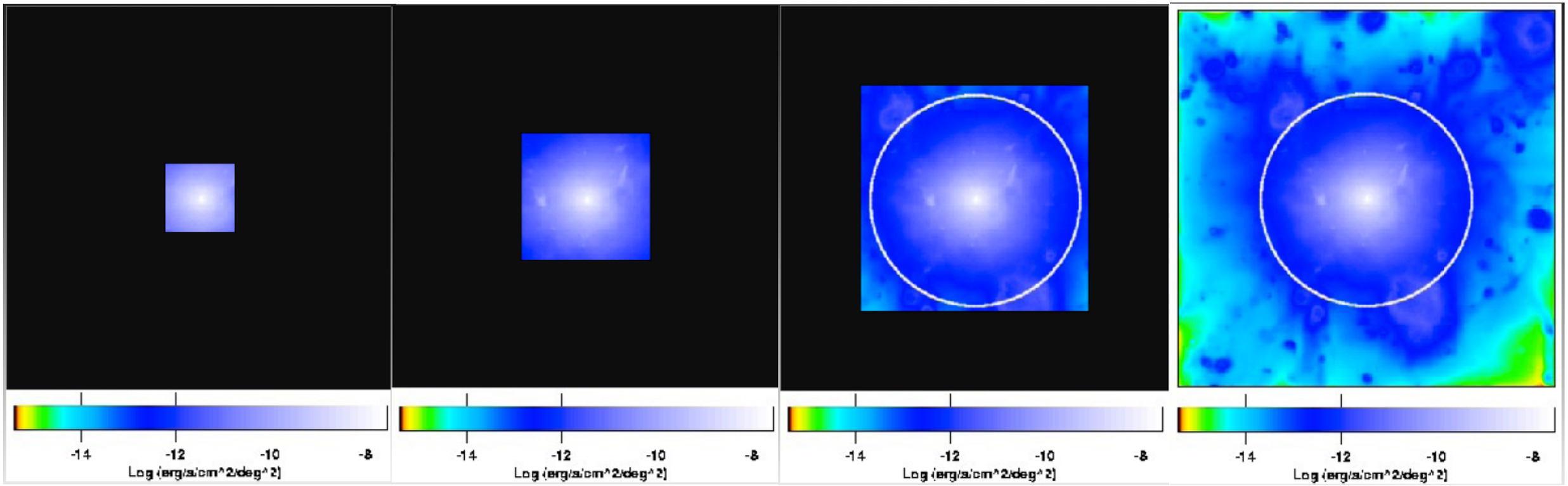

Roncarelli, Ettori et al. 2006

R_{2500}
~ 0.3 R_{200}
~ 0.5 Mpc

R_{500}
~ 0.7 R_{200}
~ 1 Mpc

R_{200}
~ 1.5 Mpc

The intra-cluster medium (ICM), its detection & modeling

The Intra-Cluster Medium (ICM)

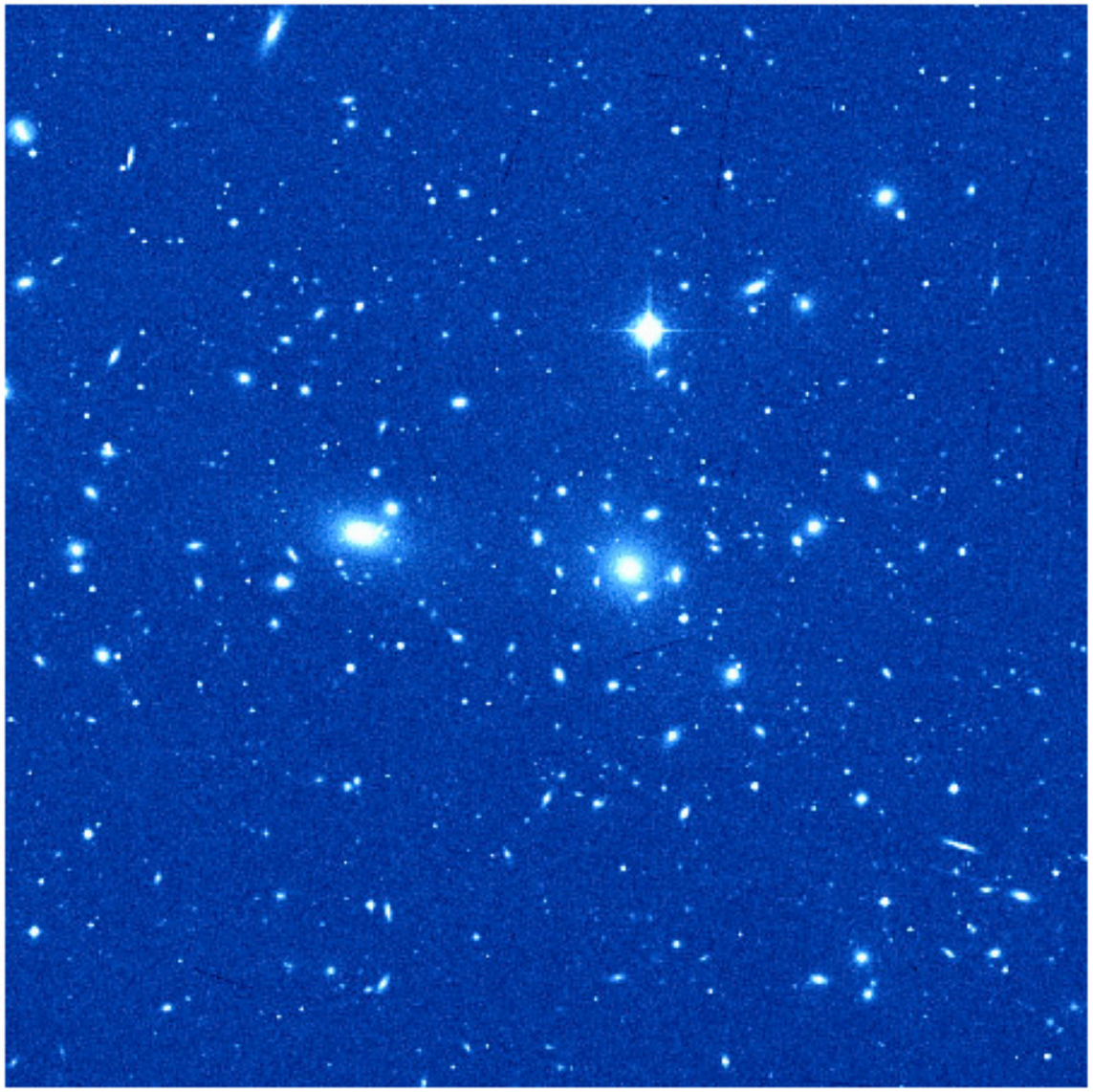

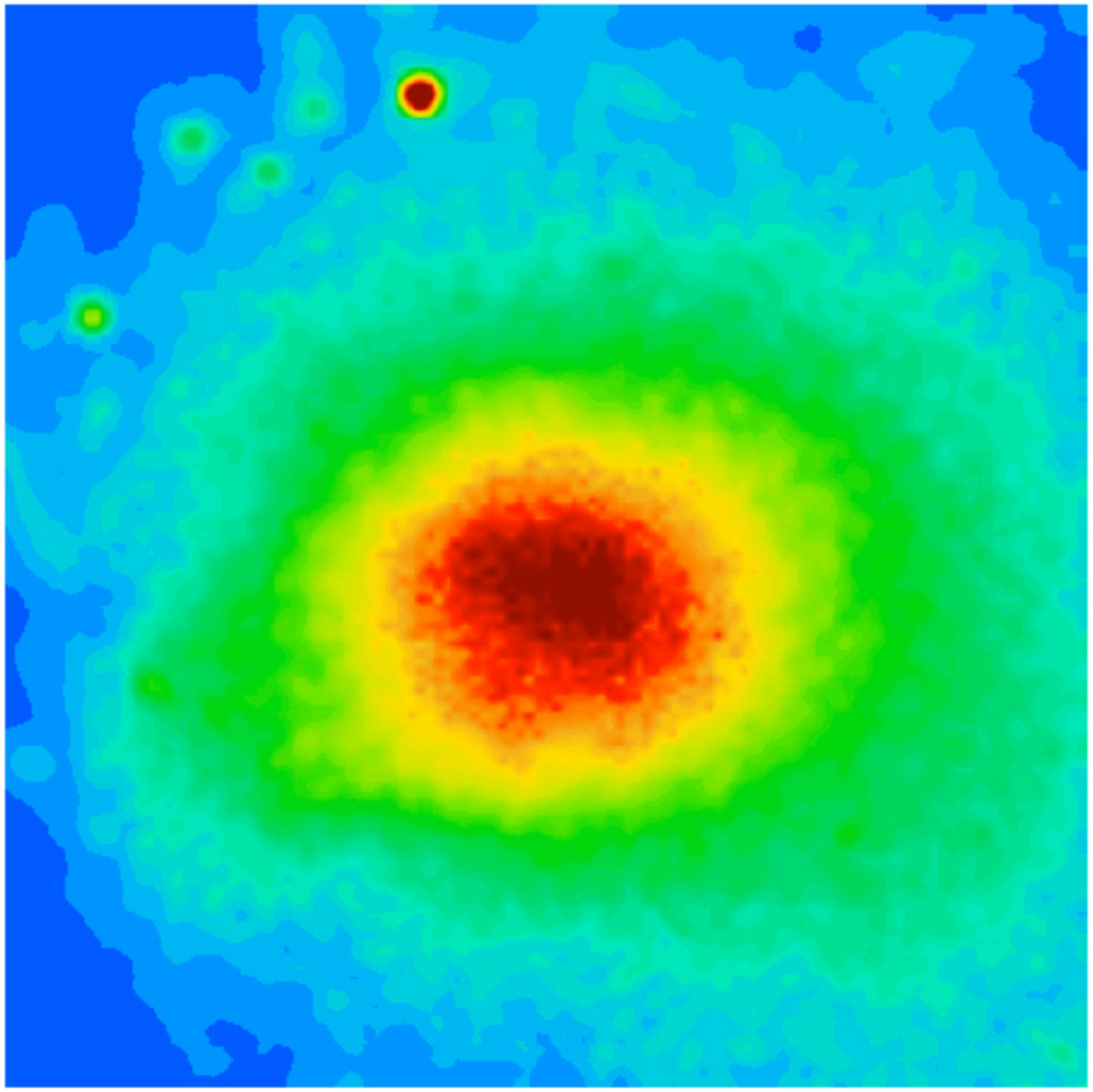

Coma cluster in optical and X-rays

Surprise from X-ray astronomy: the inter-galactic space is not empty!

The Intra-Cluster Medium (ICM)

- Majority of observable cluster mass (majority of baryons) is hot gas
- Temperature $T \sim 10^8$ K ~ 10 keV (heated by gravitational potential)
- Electron number density $n_e \sim 10^{-3}$ cm^{-3}
- Mainly H, He, but with heavy elements (O, Fe, ..)
- Mainly emits X-rays (but also radio and gamma rays)
- $L_X \sim 10^{45}$ erg/s, most luminous extended X-ray sources in Universe
- Causes the Sunyaev-Zel'dovich effect (SZE) by inverse Compton scattering the background CMB photons

Why the ICM is so hot?

A cluster's temperature directly relates to the depth of its potential well.

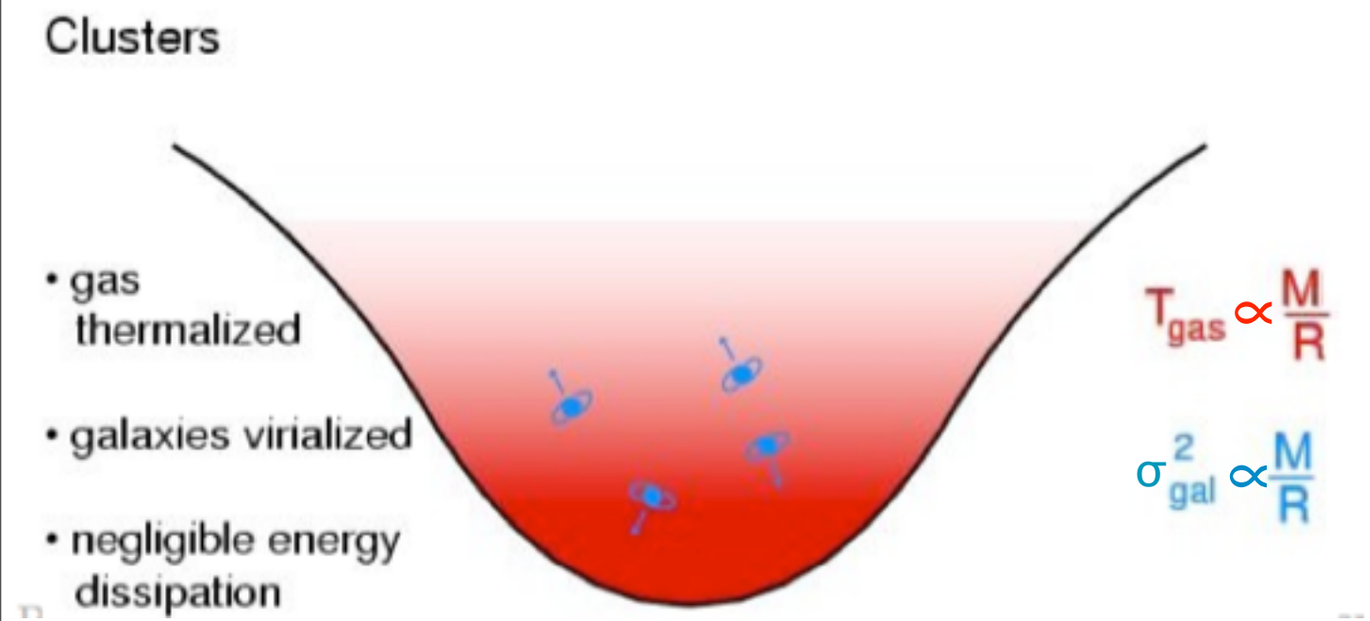

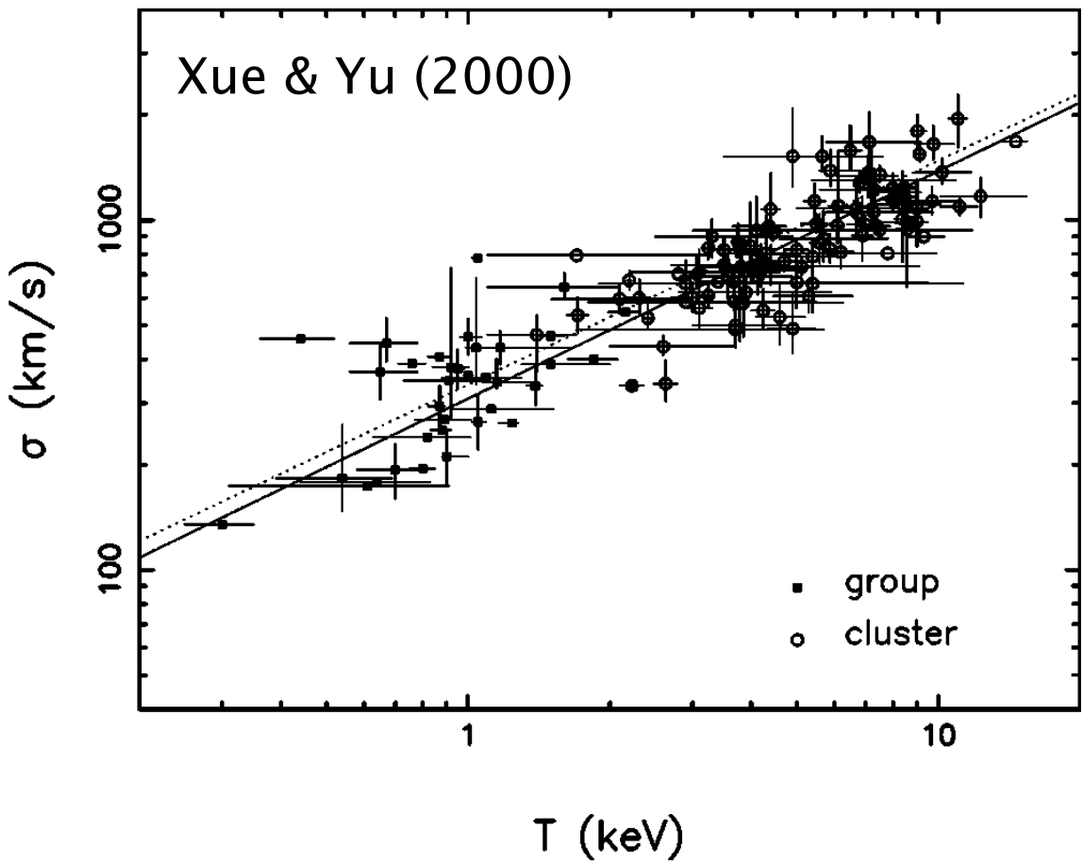

Velocity dispersion is the optical analog of X-ray temperature.

Observationally, $\sigma^2 = (1.0 \pm 0.1)\, k_B\, T_X / \mu\, m_p$ (see figure)

X-ray emission from galaxy clusters

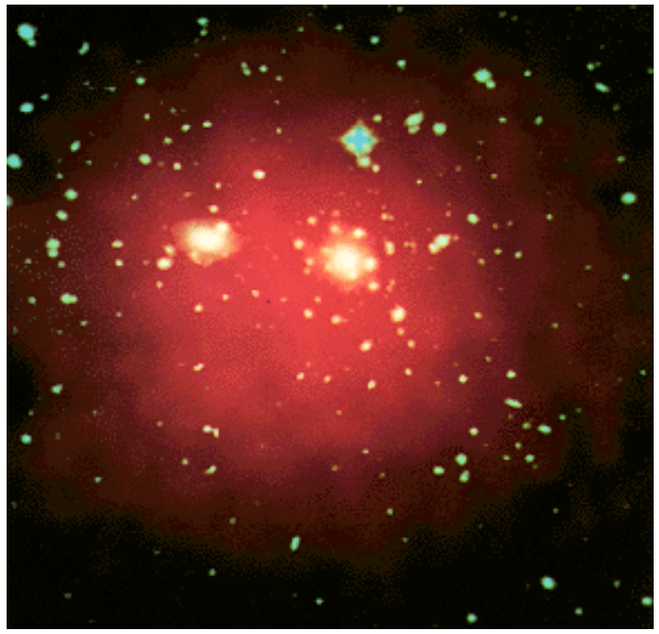

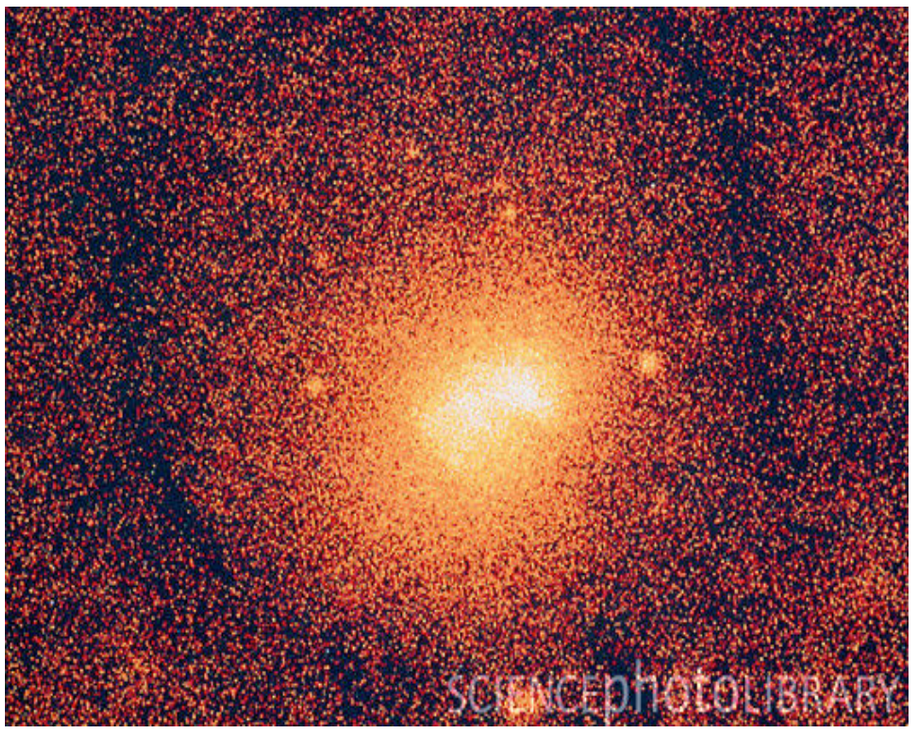

- Most luminous extended X-ray sources in the extragalactic fields are galaxy clusters

- Clusters can be identified based on an extent criterion that distinguishes them from AGN, which are 10 times more abundant. This allows a very efficient and clean selection in extragalactic fields (|b|>20deg)

- In deep XMM exposures (>3h) clusters are visible out to z>1

- X-ray selection has a high contrast (n_e^2), allows accurate mass measurements, and search volumes can be quantified

- Additional optical cluster confirmation of a galaxy overdensity is needed

- distance measurements mostly with optical spectroscopy of cluster galaxies

First X-ray images of clusters

From the *Uhuru satellite* (1970–73), with two sets of proportional counters and roughly 5° imaging resolution

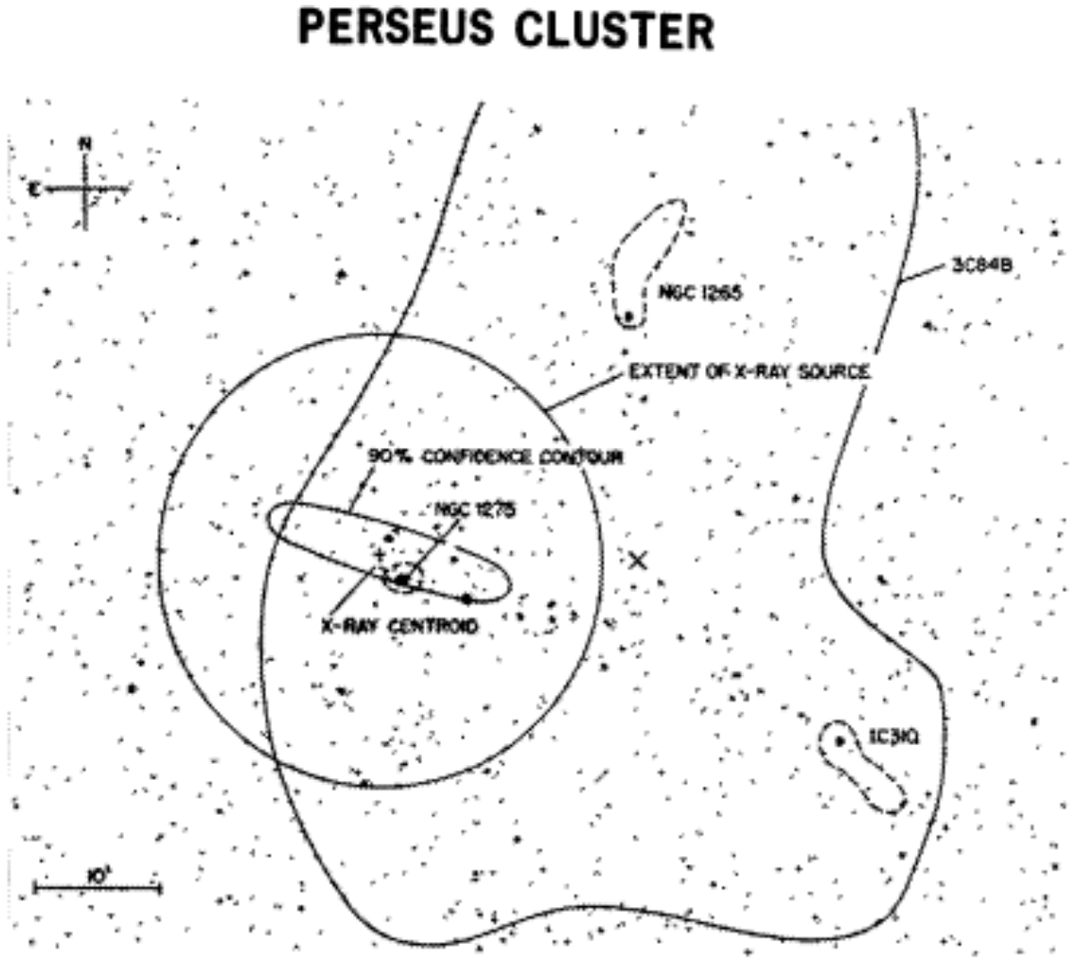

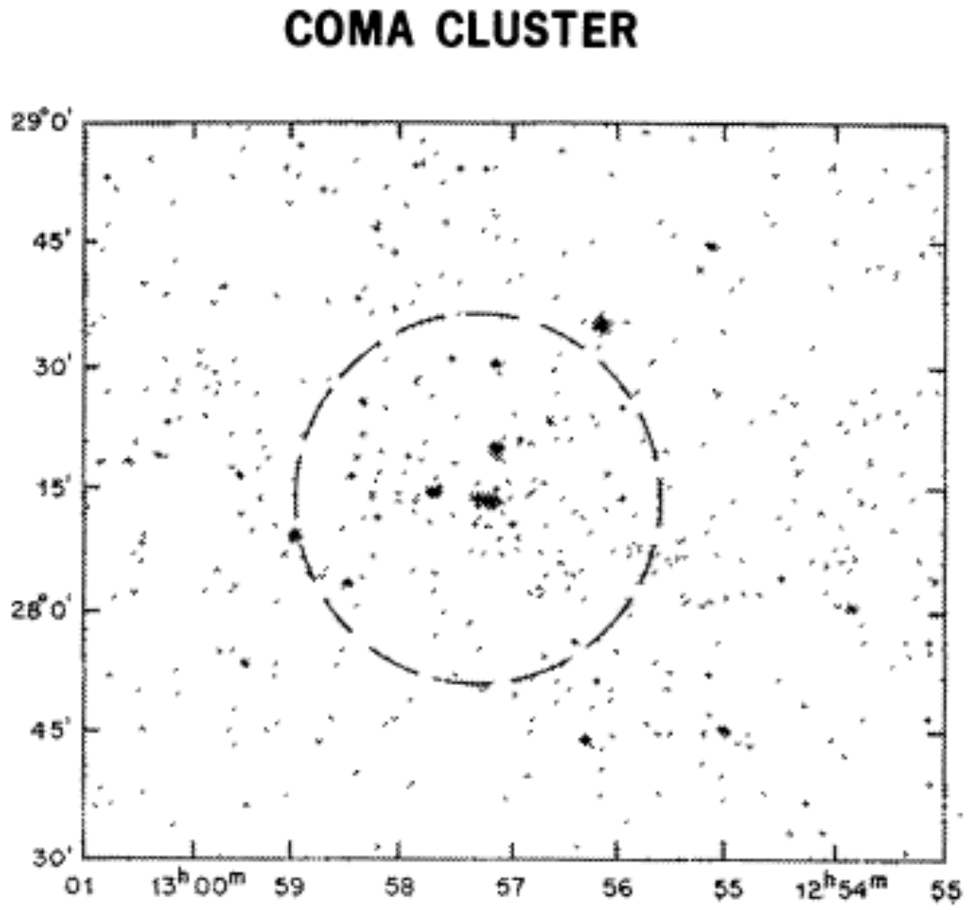

(From Kellogg 1973)

ROSAT (1990-98) image of Coma

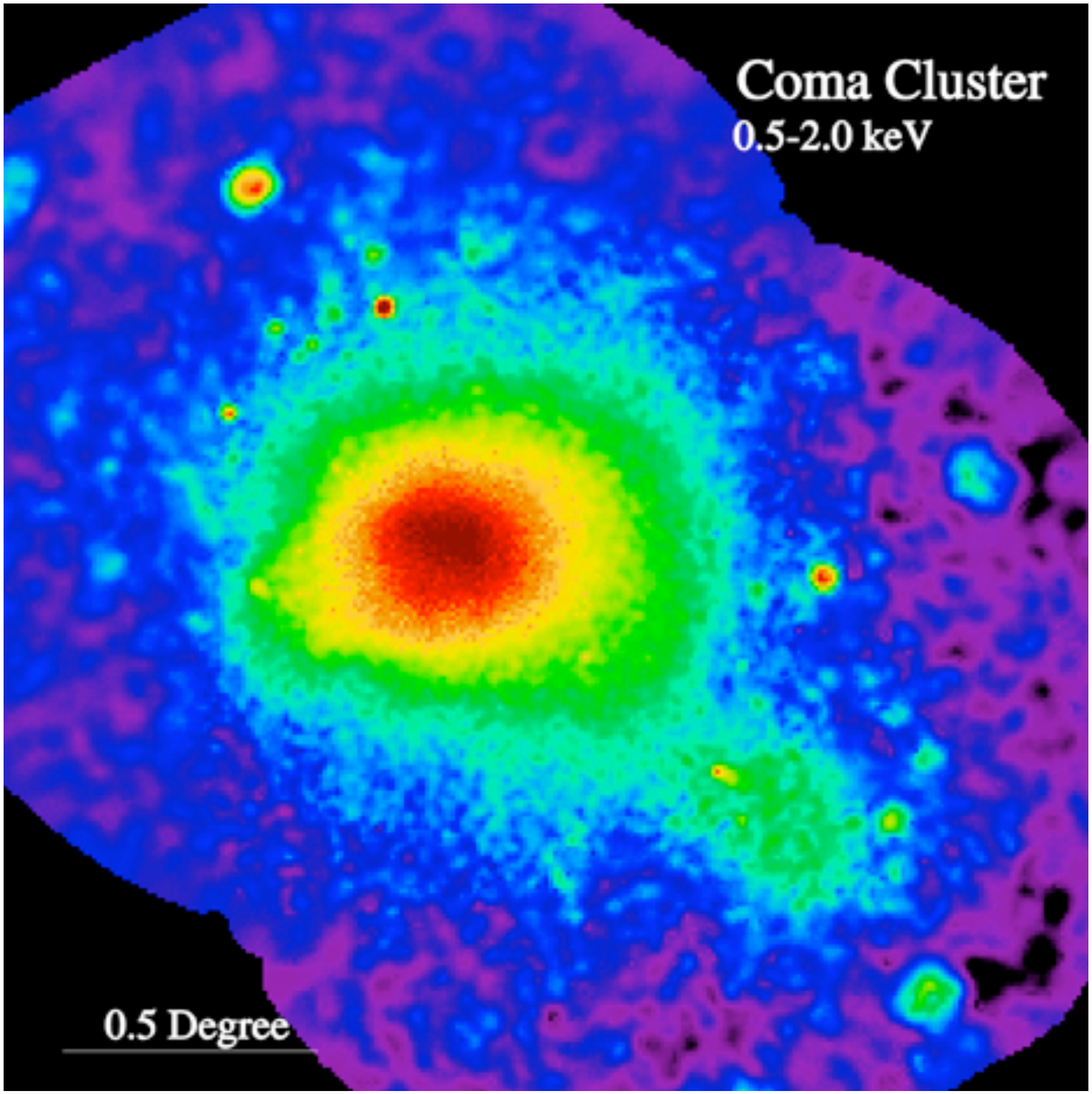

NORAS-II/REFLEX-II

Redshift 0.0<z<0.5

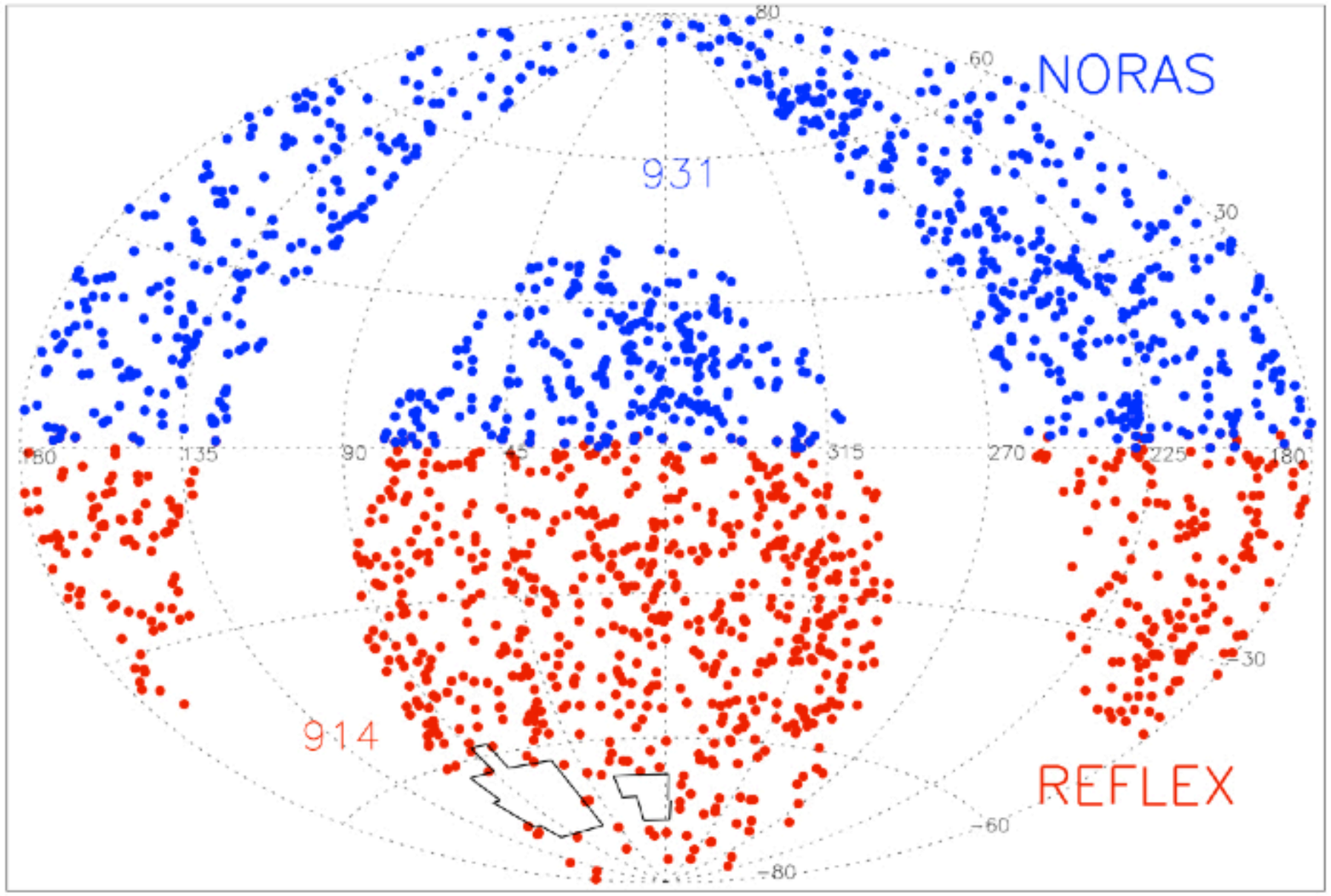

European X-ray observatories

ROSAT

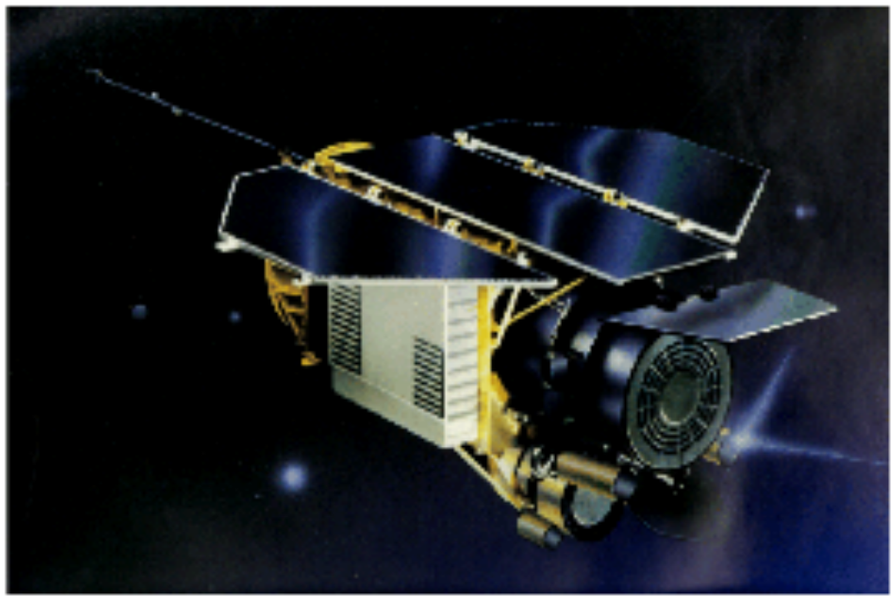

- German Survey-Satellite
- 1990-1998
- first All-Sky X-ray survey
- detection of ~2000 clusters
- census of the local cluster population (REFLEX+NORAS)
- 5 GC at z>1

XMM-Newton

- European X-ray Observatory
- 1999-201x
- 5"-10" resolution
- dozens of clusters z>1 (ongoing)

eROSITA

- German survey-instrument (MPE)
- start ~2012
- ~20" resolution
- all-Sky Survey
- goal: ~100,000 clusters

Thermal Bremsstrahlung

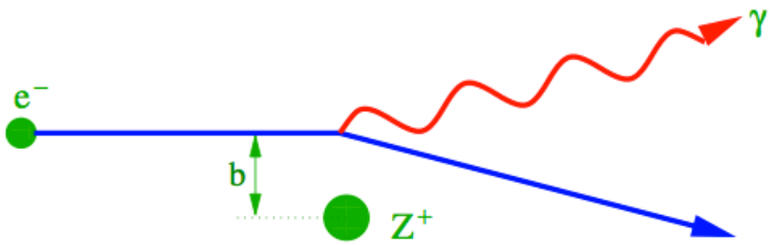

Emission from a single electron:

$$I = \frac{8\,Z^2\,e^6}{3\,pc^3\,m_e{}^2\,v^2\,b^2.}$$

Emission from a thermal plasma:

$$\epsilon_\nu^{ff} = 6.8\times10^{-52}\,T^{-1/2}\,Z^2\,n_e\,n_i\,\exp[-h\nu/(k_BT)]\,\bar{g}_{ff}(\nu)$$

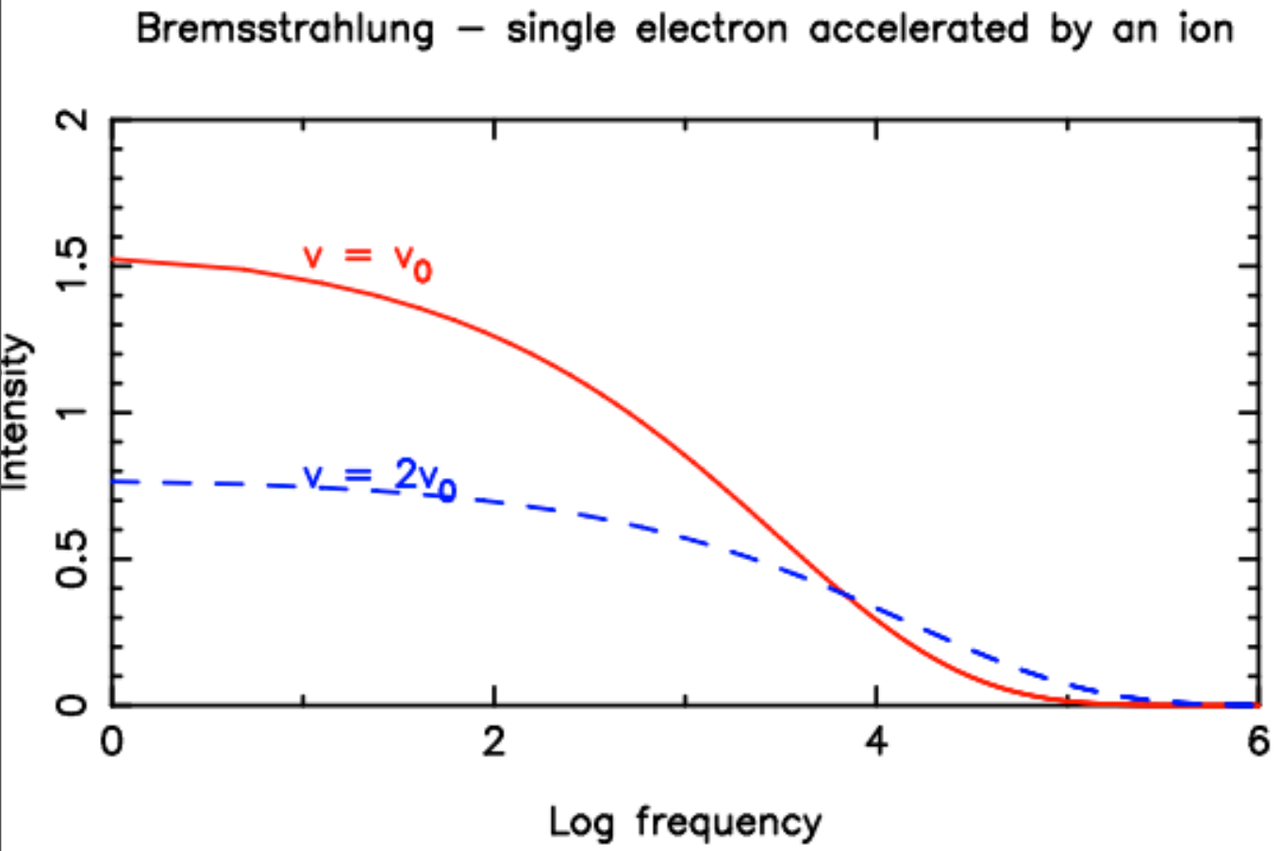

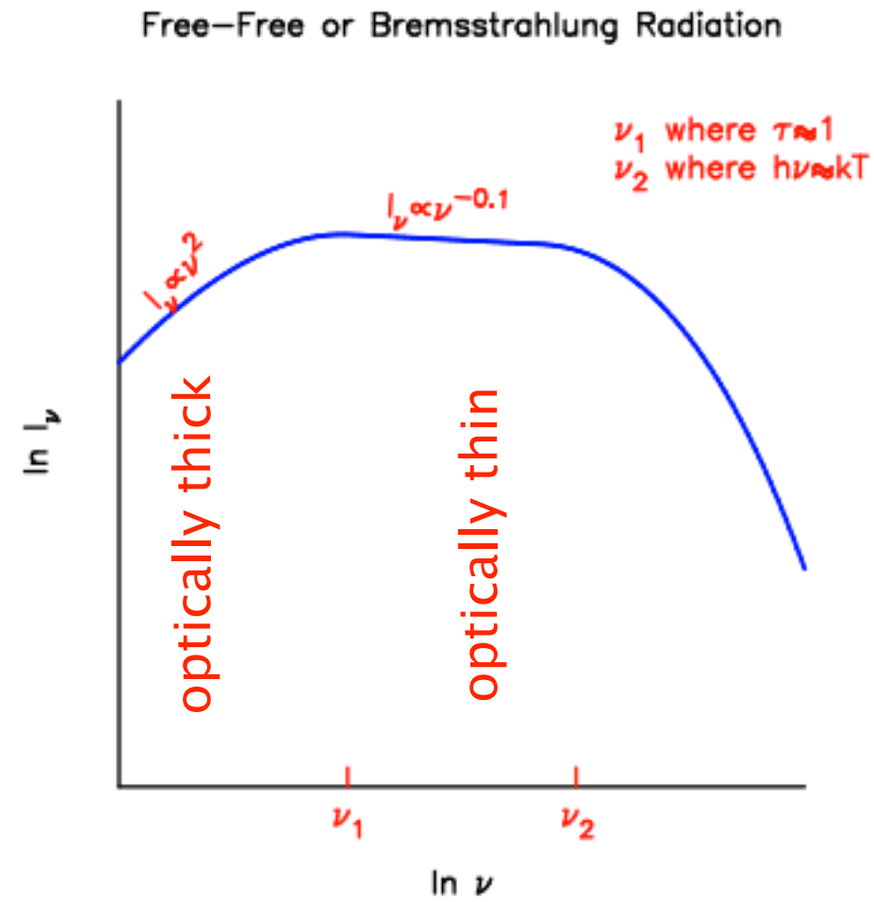

Bremsstrahlung summary

Because the plasma is optically thin, the total emitted specific intensity is proportional to the emissivity integrated along the line of sight.

$$I_\nu \propto \int n_e^2 T^{-1/2} \, dl$$

This is proportional to n^2 as we would expect for a collisonal process.

The integral $\int n_e^2 \, dl$ is called the *emission measure*, and is often written in units of $\mathrm{cm}^{-6}\,\mathrm{pc}$.

Total Emissivity

Integrate over frequency to get the *total emissivity*:

$$\epsilon^{ff} = 1.4 \times 10^{-28} T^{1/2} \, Z^2 \, n_e \, n_i \, \bar{g}_B$$

This has units of $\mathrm{W\,m}^{-3}$.

- Gas in clusters of galaxies at temperatures of $T_e \approx 10^8$ K ($\equiv$ 8.6 keV). Therefore Bremsstrahlung emission extends into X-rays.
- Very low gas density, $n_e \approx 10^4\ \mathrm{m}^{-3}$, so emission optically thin. Cluster core radius $r_c \approx 200$ kpc.
- Estimate T_e from location of "knee" in spectrum.
- X-ray flux density $F_X \propto \int n_e^2 T_e^{-1/2} dl$.
- Bolometric (total) X-ray luminosity $L_X \propto \int n_e^2 T_e^{1/2} dl$.

X-ray emission from clusters

Thermal Bremsstahlung

$$\epsilon(\nu) = \frac{16\, e^6}{3\, m_e\, c^2}\left(\frac{2\pi}{3 m_e\, k_B T_X}\right)^{1/2} n_e n_i\, Z^2\, g_{ff}(Z, T_X, \nu)\, \exp\left(\frac{-h\nu}{k_B T_X}\right),$$

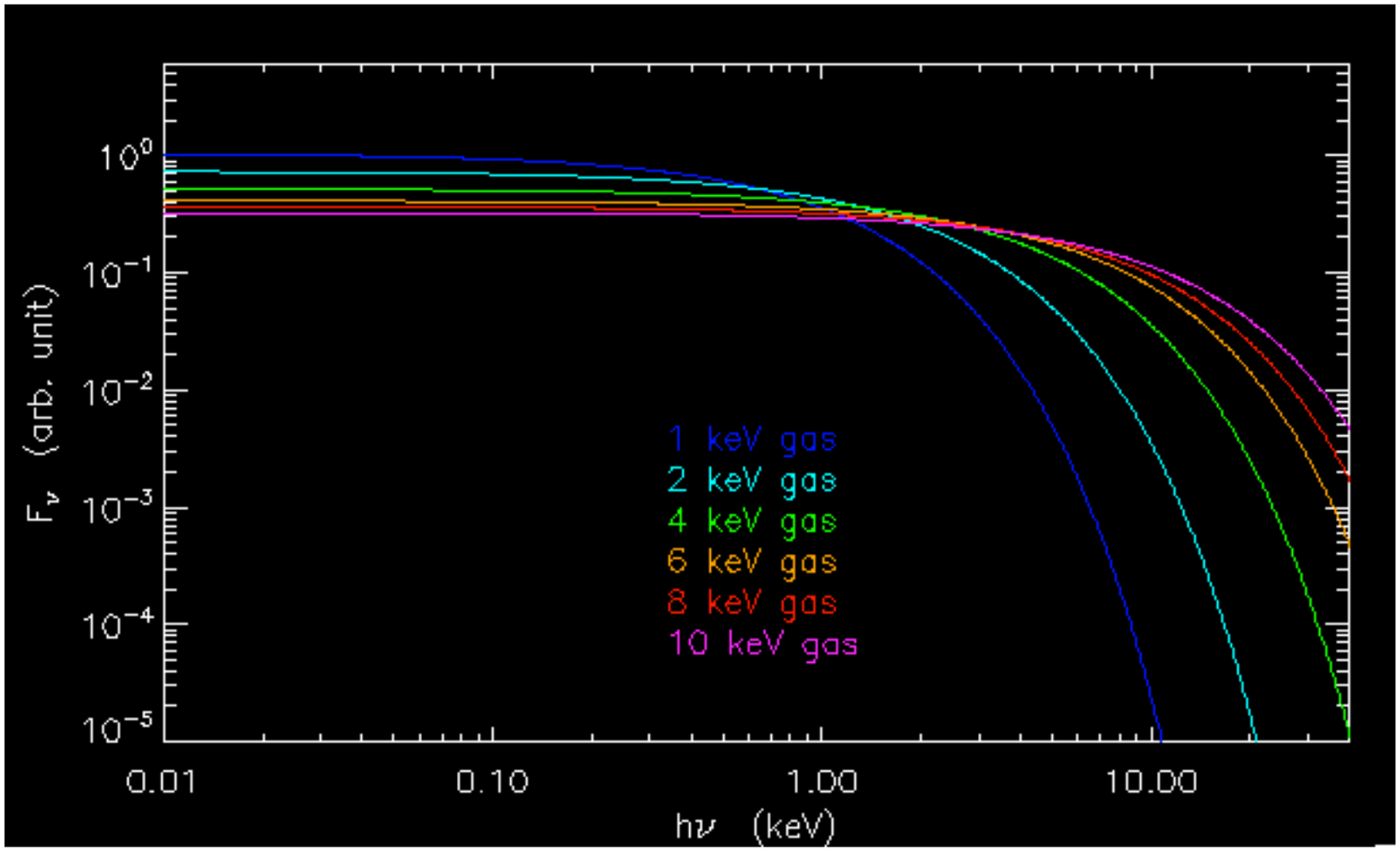

X-ray emission from clusters

Thermal Bremsstahlung

$$\epsilon(\nu) = \frac{16\, e^6}{3\, m_e\, c^2}\left(\frac{2\pi}{3 m_e\, k_B T_X}\right)^{1/2} n_e n_i\, Z^2\, g_{ff}(Z, T_X, \nu)\, \exp\left(\frac{-h\nu}{k_B T_X}\right),$$

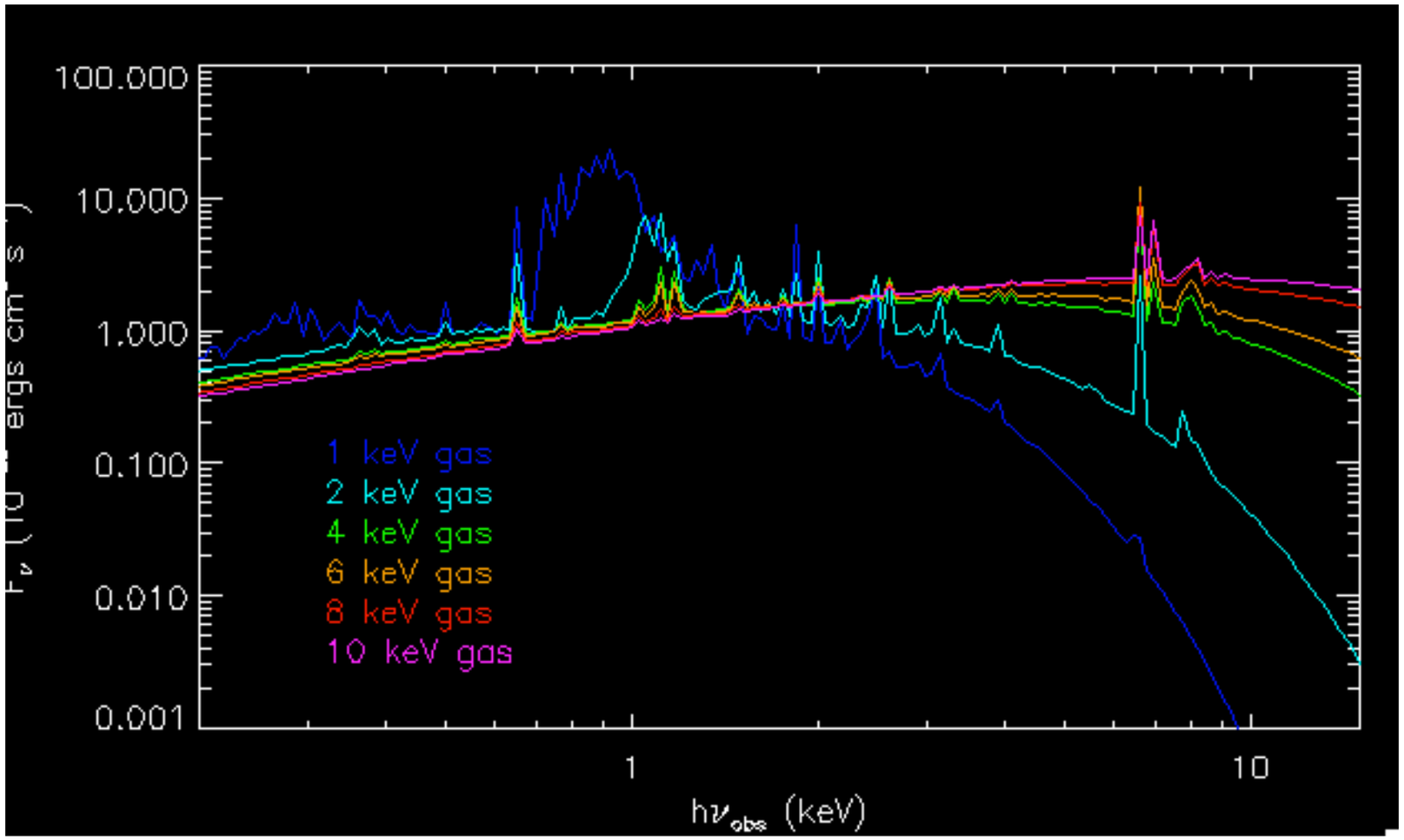

X-ray spectra

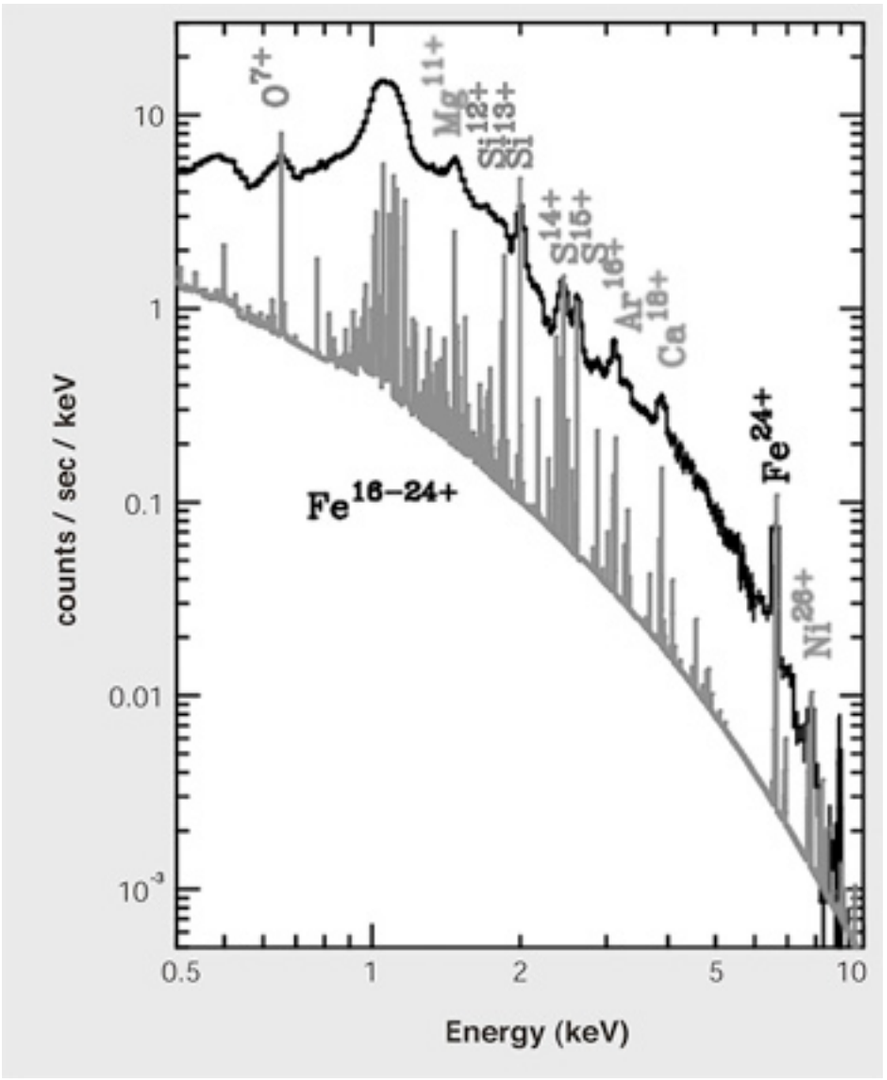

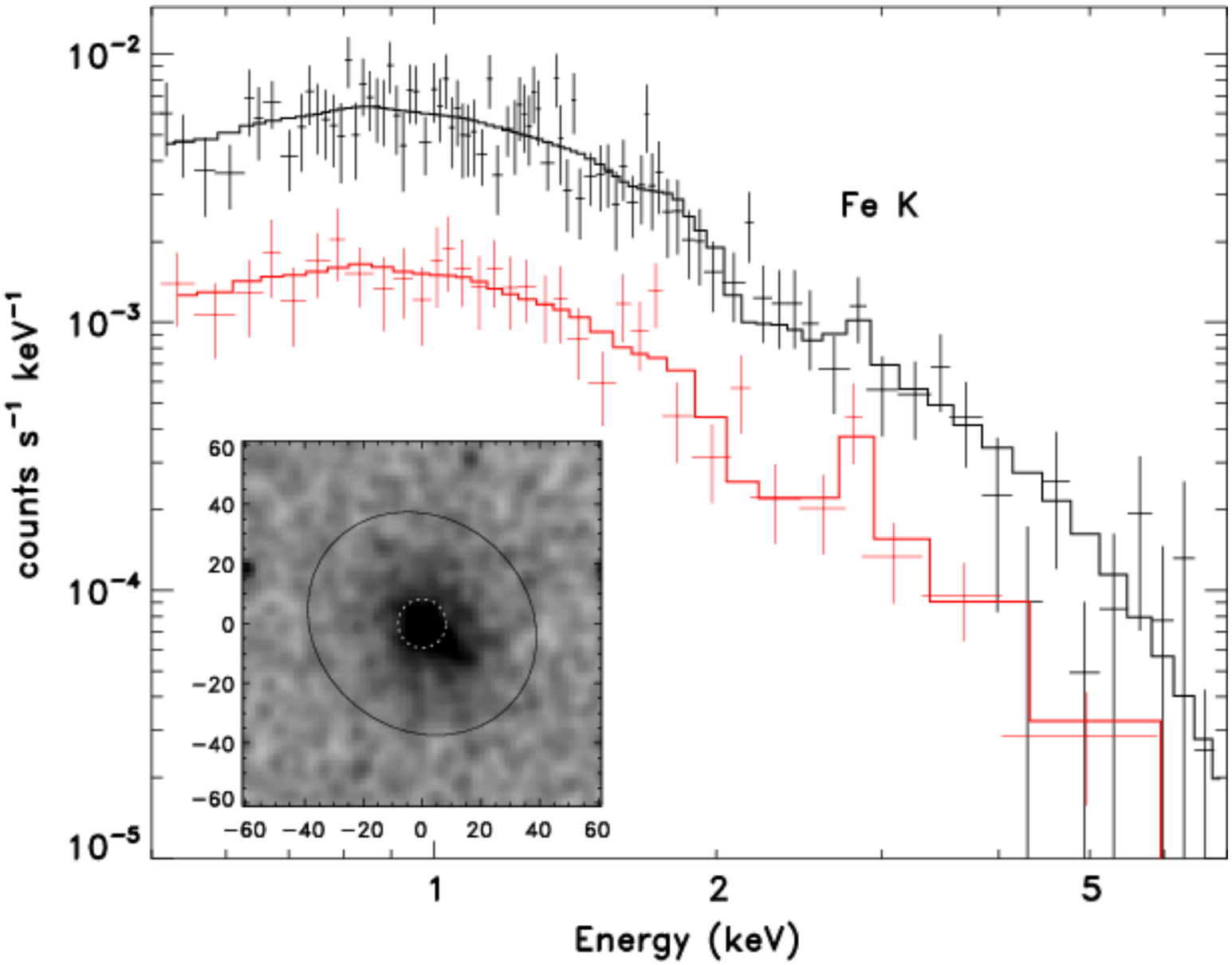

X-ray spectroscopy offers the only viable method of measuring the metal abundance in the ICM

Projected (2D) → deprojected (3D) profiles

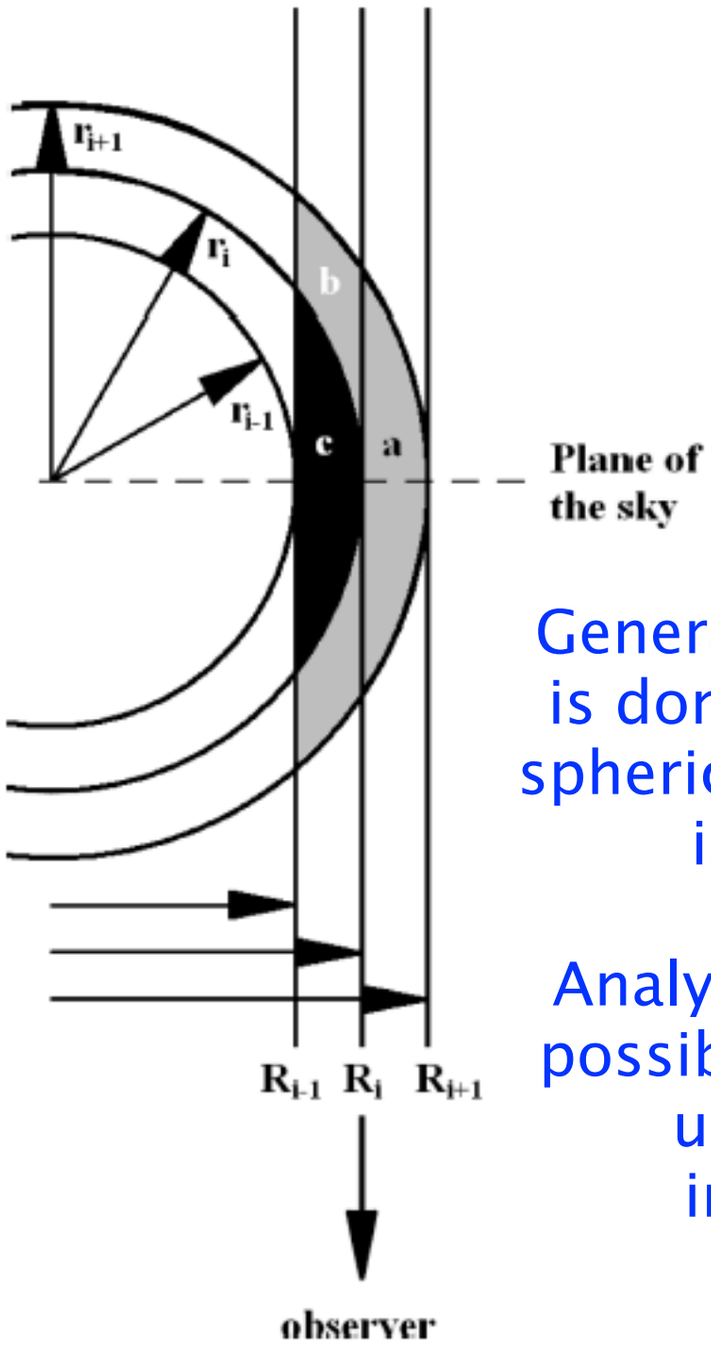

$$S_X(R) \propto 2 \int_R^\infty n_e^2(r)\, T_e(r)^{1/2}\, \frac{r\,dr}{\sqrt{r^2 - R^2}}$$

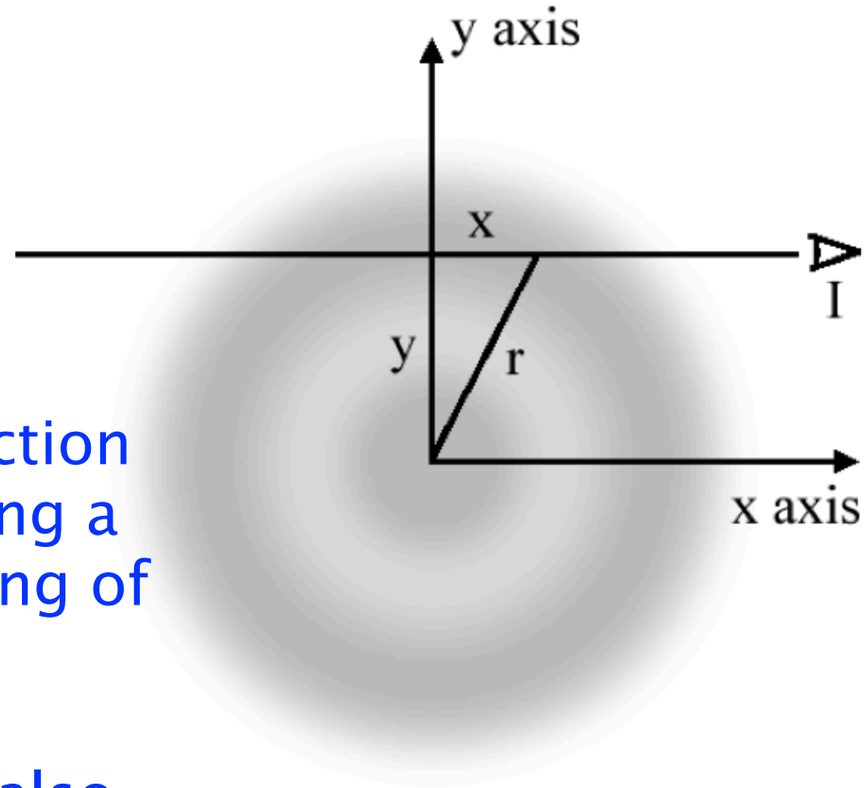

Generally, the de-projection is done numerically using a spherical model consisting of isothermal shells.

Analytic de-projection also possible for very good data, using Abel integral inversion method.

$$F(y) = 2 \int_y^\infty \frac{f(r) r\, dr}{\sqrt{r^2 - y^2}}.$$

$$f(r) = -\frac{1}{\pi} \int_r^\infty \frac{dF}{dy} \frac{dy}{\sqrt{y^2 - r^2}}.$$

X-ray density & temperature profiles

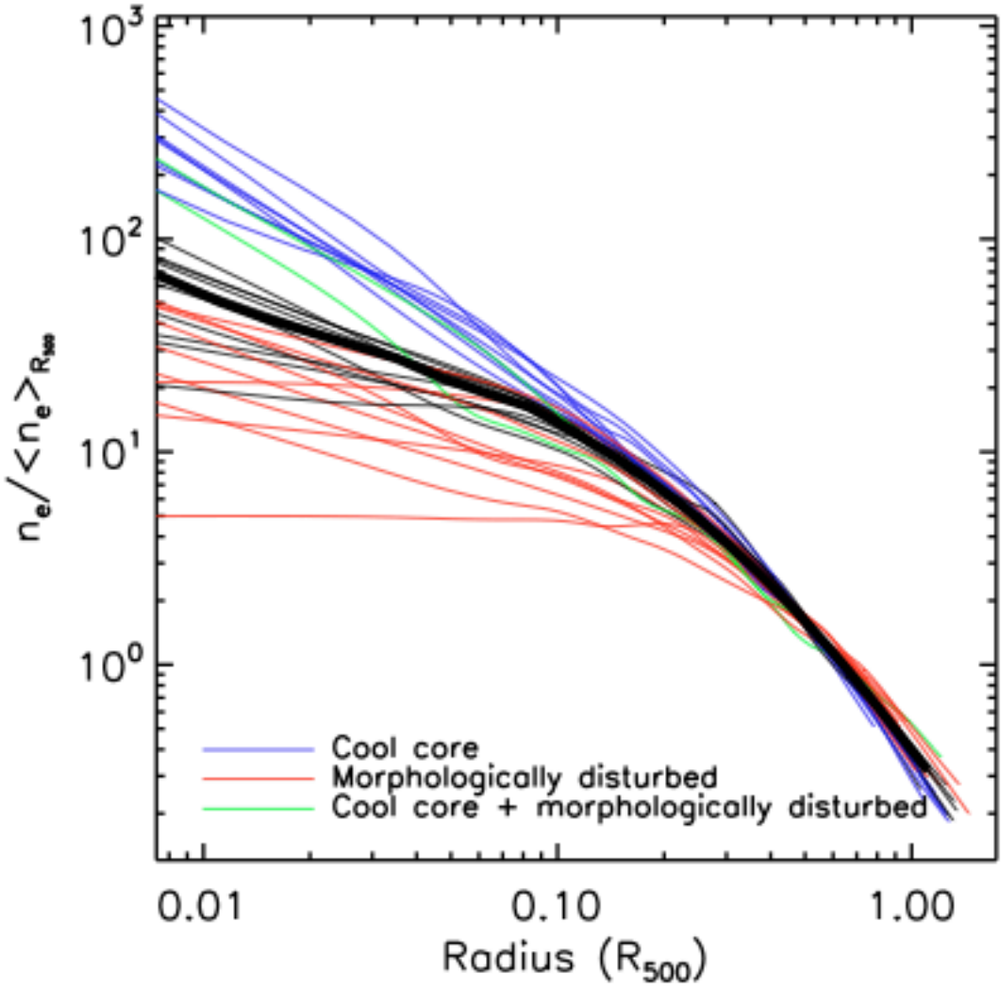

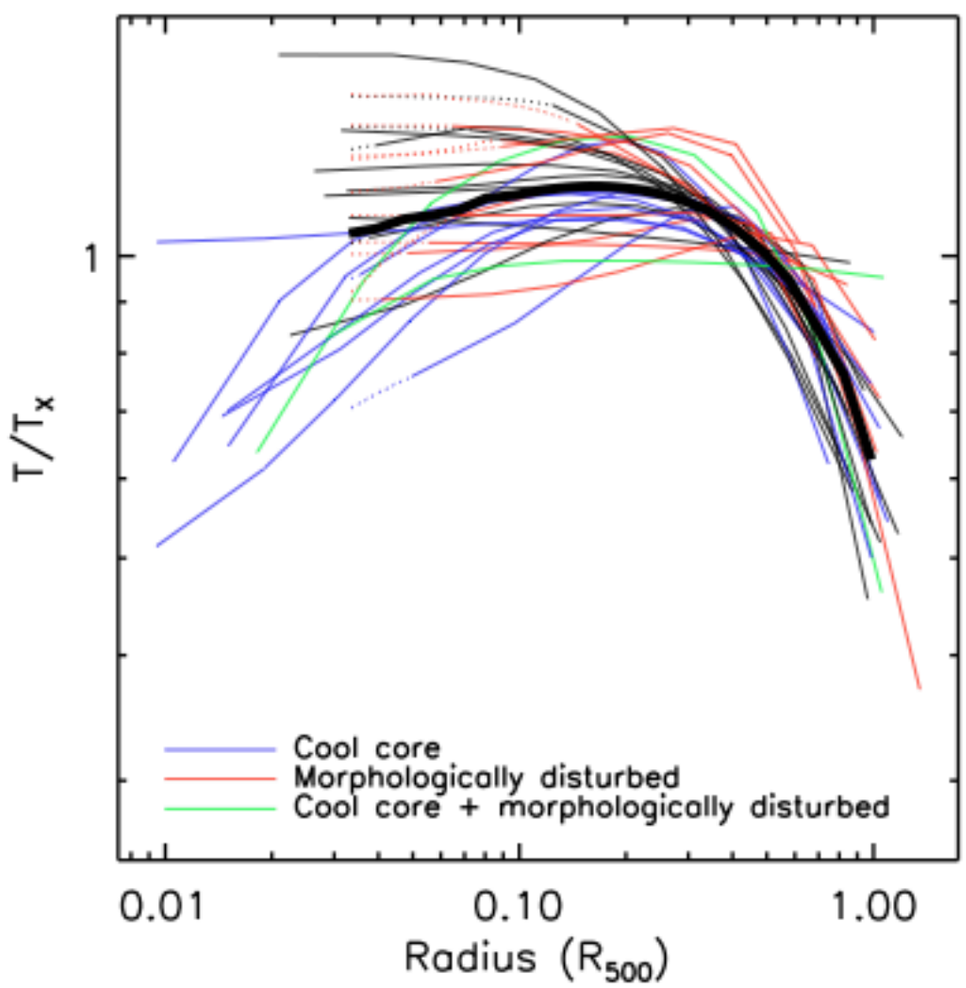

From a representative sample of massive, nearby galaxy clusters (Arnaud et al. 2010)

More: pressure & entropy profiles

Derived from the fundamental thermodynamic quantities n_e and T_e

$P_e = n_e T_e$

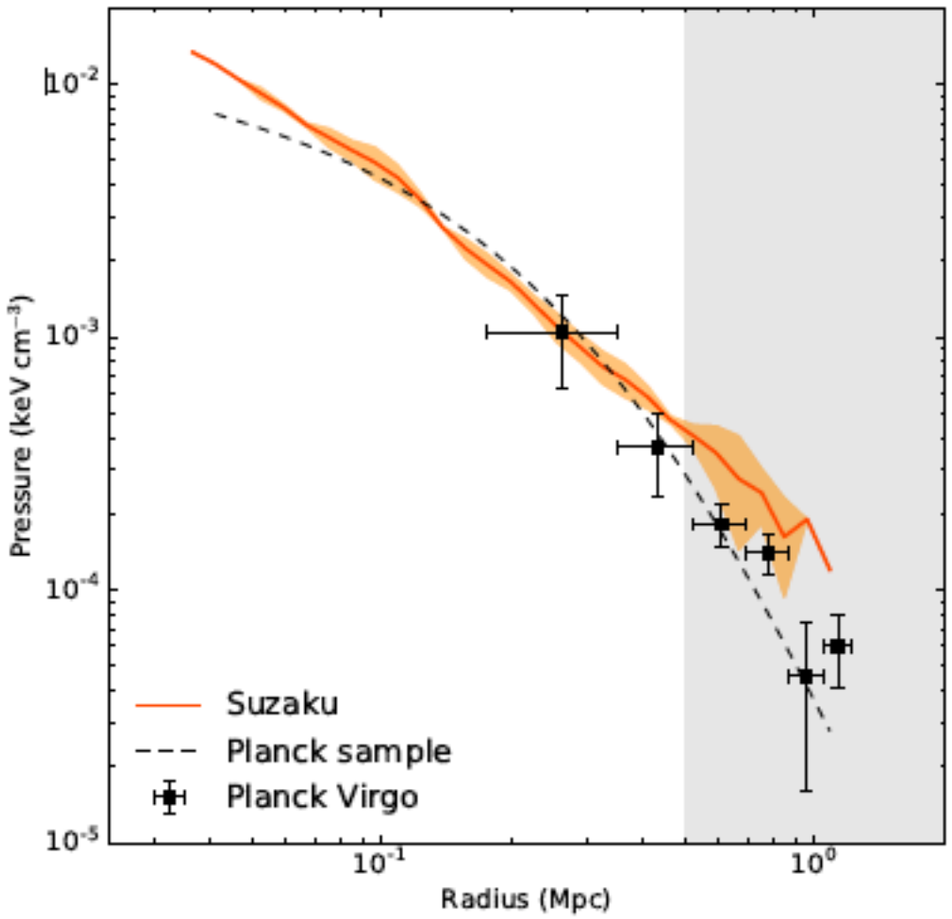

$S_e = T_e / n_e^{2/3}$

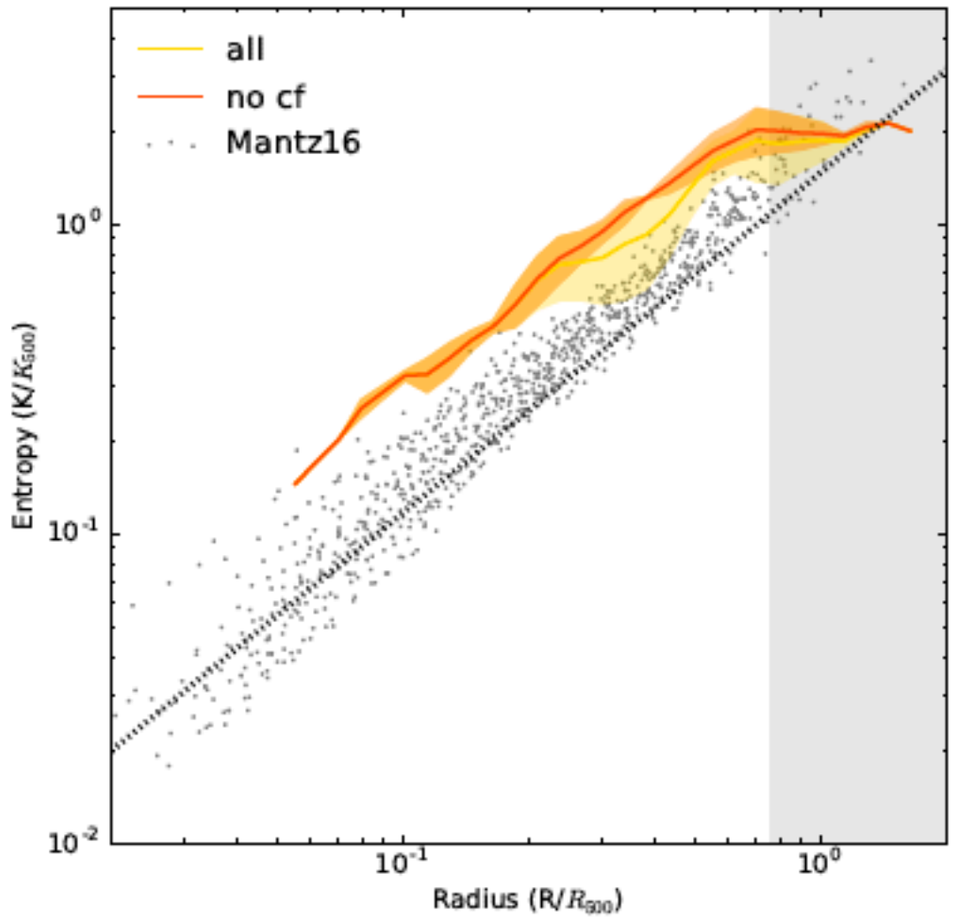

Results for the Virgo cluster, Simionescu et al. (2017)

Hydrostatic equilibrium – I.

Once the gas density has been determined by either model fitting or deprojection, the gas mass can be derived simply as

$$M_{\rm gas}(r) = 4\pi \int_0^r \rho(r')(r')^2 \, {\rm d}r' \ .$$

Here, $M_{\rm gas}(r)$ is the gas mass interior to the radius r.

Unless it is disturbed in some way, one would expect the gas in a cluster to relax into hydrostatic equilibrium on roughly the sound crossing time of the cluster,

$$t_s \equiv \frac{D}{c_s} \approx 6.6 \times 10^8 \, {\rm yr} \left(\frac{T}{10^8 \, {\rm K}} \right)^{-1/2} \left(\frac{D}{1 \, {\rm Mpc}} \right) \ .$$

Here, D is the diameter of the cluster, and c_s is the sound speed. Since this time scale is shorter than the age of a typical cluster, which is a fraction of the Hubble time, the gas in many clusters should be close to hydrostatic equilibrium. Exceptions would include clusters which are undergoing or have recently undergone a major merger, and regions of a cluster where an AGN has injected energy recently.

In hydrostatic equilibrium, the pressure forces balance gravity:

$$\boldsymbol{\nabla} P = -\rho \boldsymbol{\nabla} \Phi \ , \qquad \frac{1}{\rho} \frac{{\rm d}P}{{\rm d}r} = -\frac{GM(r)}{r^2} \ ,$$

Hydrostatic equilibrium – II.

The total gravitational mass can be derived from the condition of hydrostatic equilibrium (22), which can be written as

$$M(r) = -\frac{r^2}{G\rho(r)} \frac{\mathrm{d}P}{\mathrm{d}r} \,,$$

where $M(r)$ is the total mass interior to r. This equation can also be written as

$$M(r) = -\frac{kT(r)r}{\mu m_p G} \left[\frac{\mathrm{d}\ln\rho(r)}{\mathrm{d}\ln r} + \frac{\mathrm{d}\ln T(r)}{\mathrm{d}\ln r} \right] \,.$$

The gas mass fraction $f_{\rm gas}(r)$ and baryon fraction $f_{\rm b}(r)$ are then

$$f_{\rm gas}(r) = \frac{M_{\rm gas}(r)}{M(r)} \,, \qquad f_{\rm bary}(r) = \frac{M_{\rm gas}(r) + M_{\rm gal}(r)}{M(r)} \,.$$

X-ray total mass from H.E.

A) X-ray Image

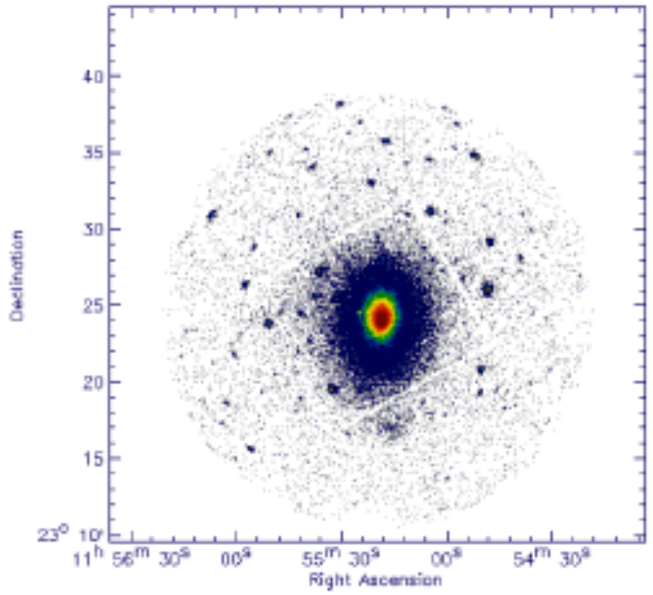

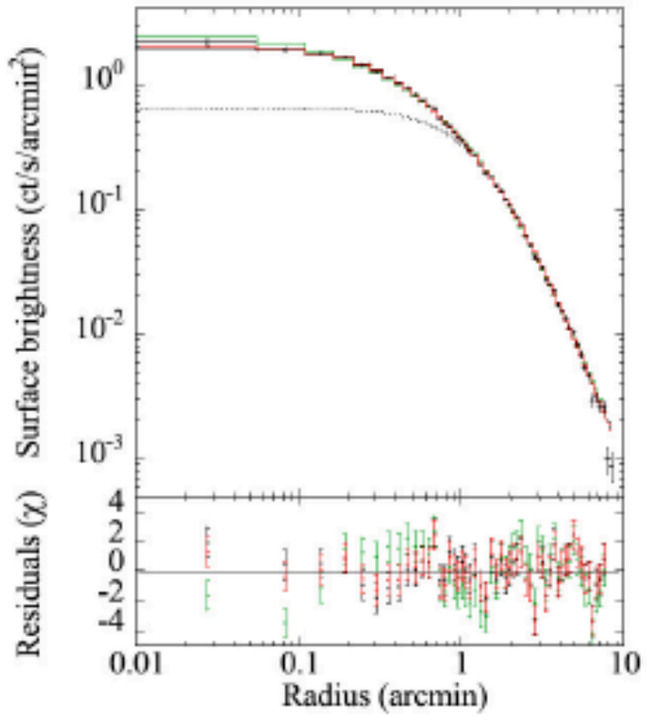

B) Surface Brightness Profile

β -model profile

C) Temperature Profile

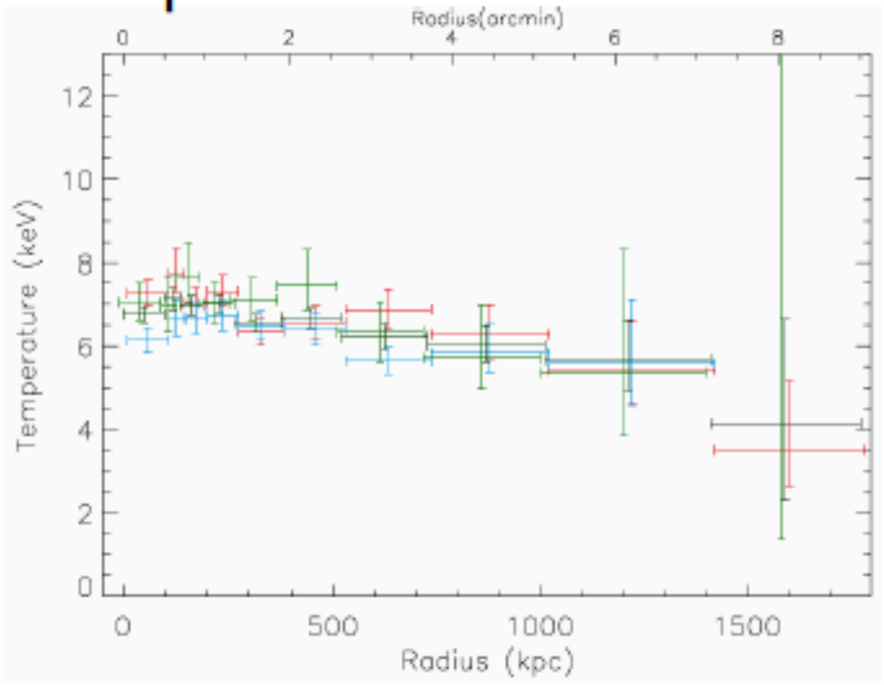

Source: Pratt & Arnaud 2002

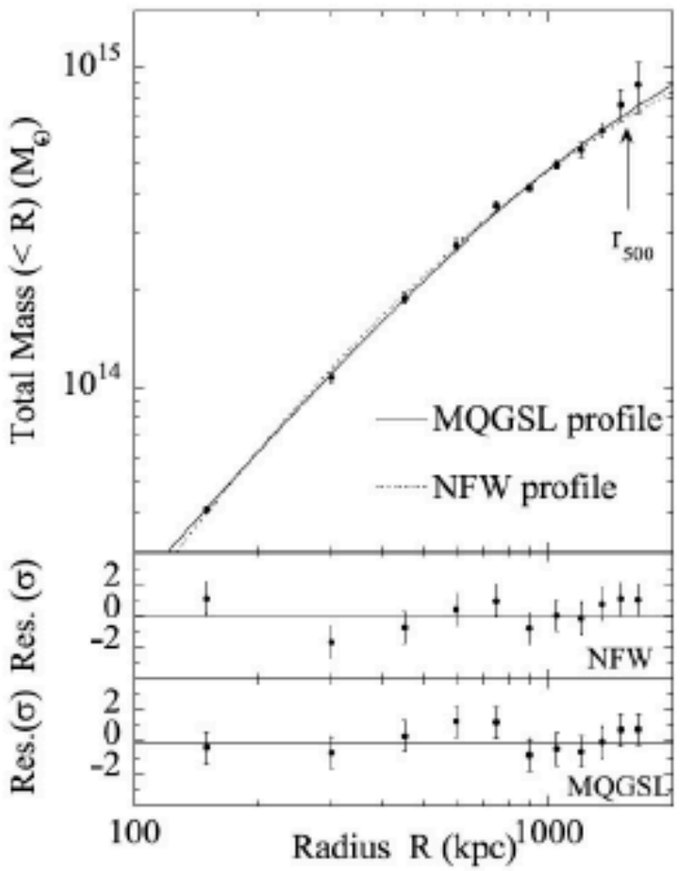

D) Mass Profile

NFW profile

$M_{200}=6.5\times10^{14}\ M_{sun}$

Gas mass fraction

Since galaxy clusters collapse from a scale of ~10 Mpc, they are expected to contain a fair sample of the baryonic content of the universe (mass segregation is not believed to occur at such large scales).

The gas mass fraction, f_{gas}, is therefore a reasonable estimate of the baryonic mass fraction of the cluster. It should also be reasonable approximation to the universal baryon mass fraction, $f_B = \Omega_B / \Omega_m$

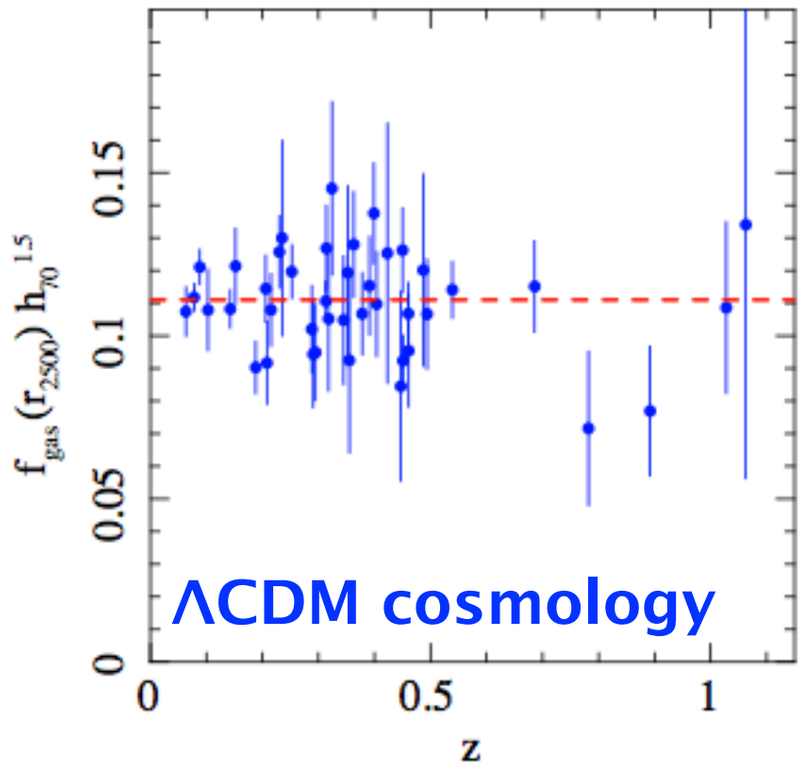

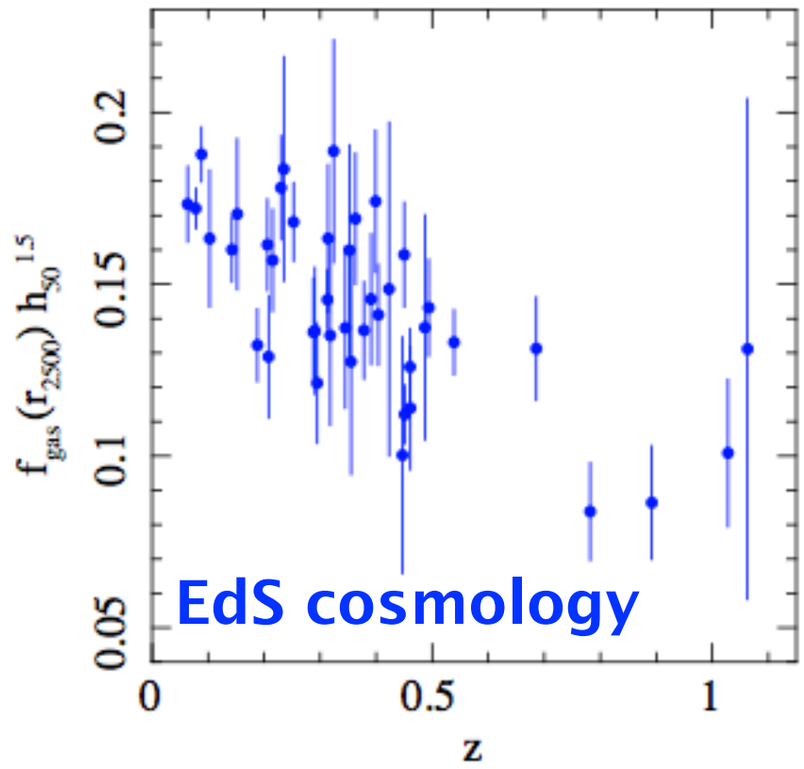

Allen et al. 2008

Gas mass fraction

Since galaxy clusters collapse from a scale of ~10 Mpc, they are expected to contain a fair sample of the baryonic content of the universe (mass segregation is not believed to occur at such large scales).

The gas mass fraction, f_{gas}, is therefore a reasonable estimate of the baryonic mass fraction of the cluster. It should also be reasonable approximation to the universal baryon mass fraction, $f_B = \Omega_B / \Omega_m$

Mantz, Allen et al.

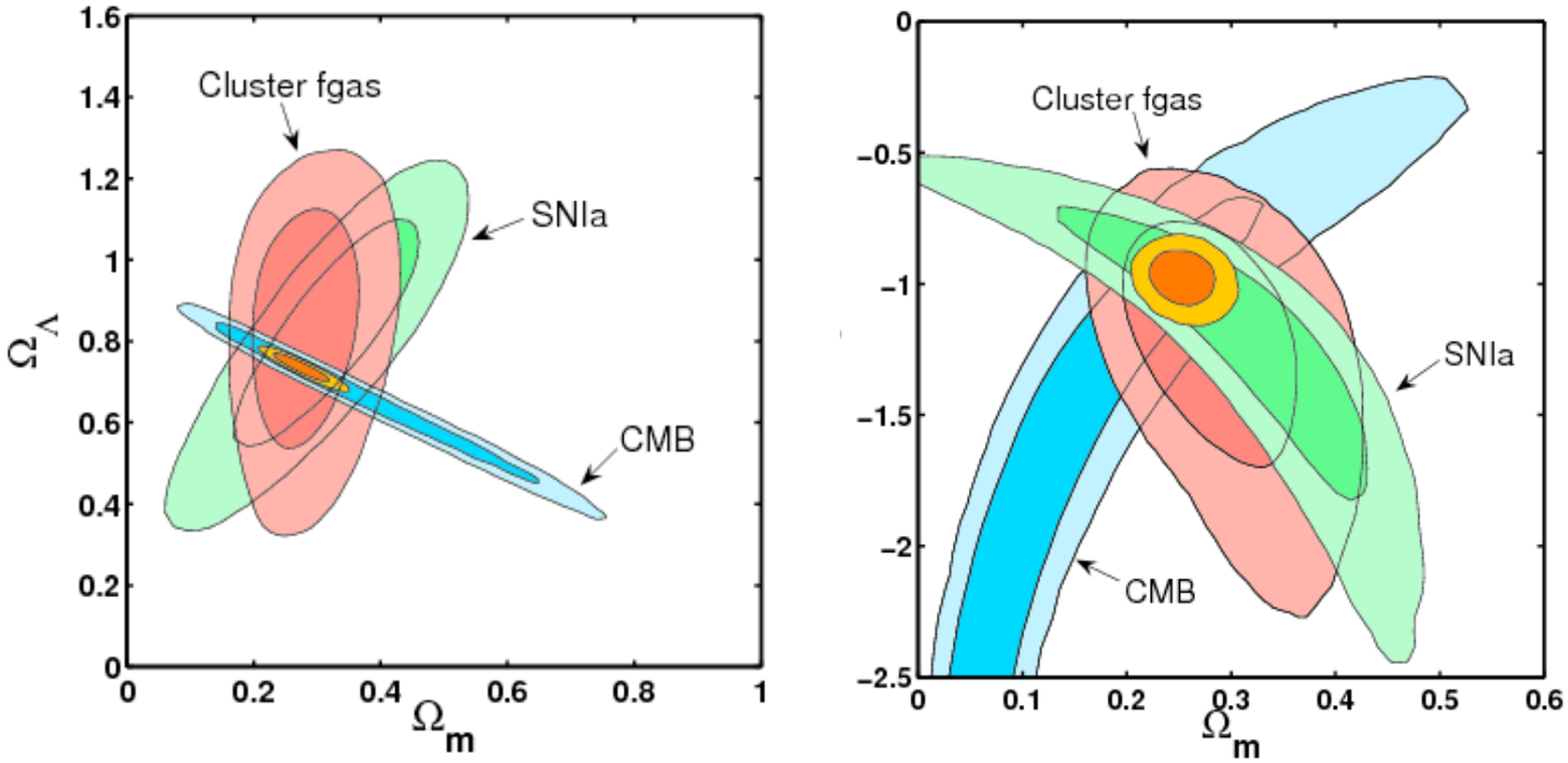

Results for cluster cosmology

Table 2: Recent cosmological results from galaxy clusters[a,b]

Reference[c]	Data	σ_8	$\Omega_{\rm m}$	$\Omega_{\rm DE}$	w	h
Local abundance and evolution[d]						
M10	X-ray	0.82 ± 0.05	0.23 ± 0.04	$1 - \Omega_{\rm m}$	-1.01 ± 0.20	
V09	X-ray	0.81 ± 0.04	0.26 ± 0.08	$1 - \Omega_{\rm m}$	-1.14 ± 0.21	
Local abundance only						
R10	optical	0.80 ± 0.07	0.28 ± 0.07	$1 - \Omega_{\rm m}$	-1	
H09	X-ray	0.88 ± 0.04	0.3	$1 - \Omega_{\rm m}$	-1	
Local abundance and clustering						
S03	X-ray	$0.71^{+0.13}_{-0.16}$	$0.34^{+0.09}_{-0.08}$	$1 - \Omega_{\rm m}$	-1	
Gas-mass fraction						
A08	X-ray		0.27 ± 0.06	0.86 ± 0.19	-1	
A08	X-ray		0.28 ± 0.06	$1 - \Omega_{\rm m}$	$-1.14^{+0.27}_{-0.35}$	
E09	X-ray		0.32 ± 0.05	$1 - \Omega_{\rm m}$	$-1.1^{+0.7}_{-0.6}$	
L06	X-ray+SZ		$0.40^{+0.28}_{-0.20}$	$1 - \Omega_{\rm m}$	-1	
XSZ distances						
B06	X-ray+SZ		0.3	$1 - \Omega_{\rm m}$	-1	$0.77^{+0.11}_{-0.09}$
S04	X-ray+SZ		0.3	$1 - \Omega_{\rm m}$	-1	0.69 ± 0.08

Allen, Evrard & Mantz 2011

The Sunyaev-Zel'dovich (SZ) effect

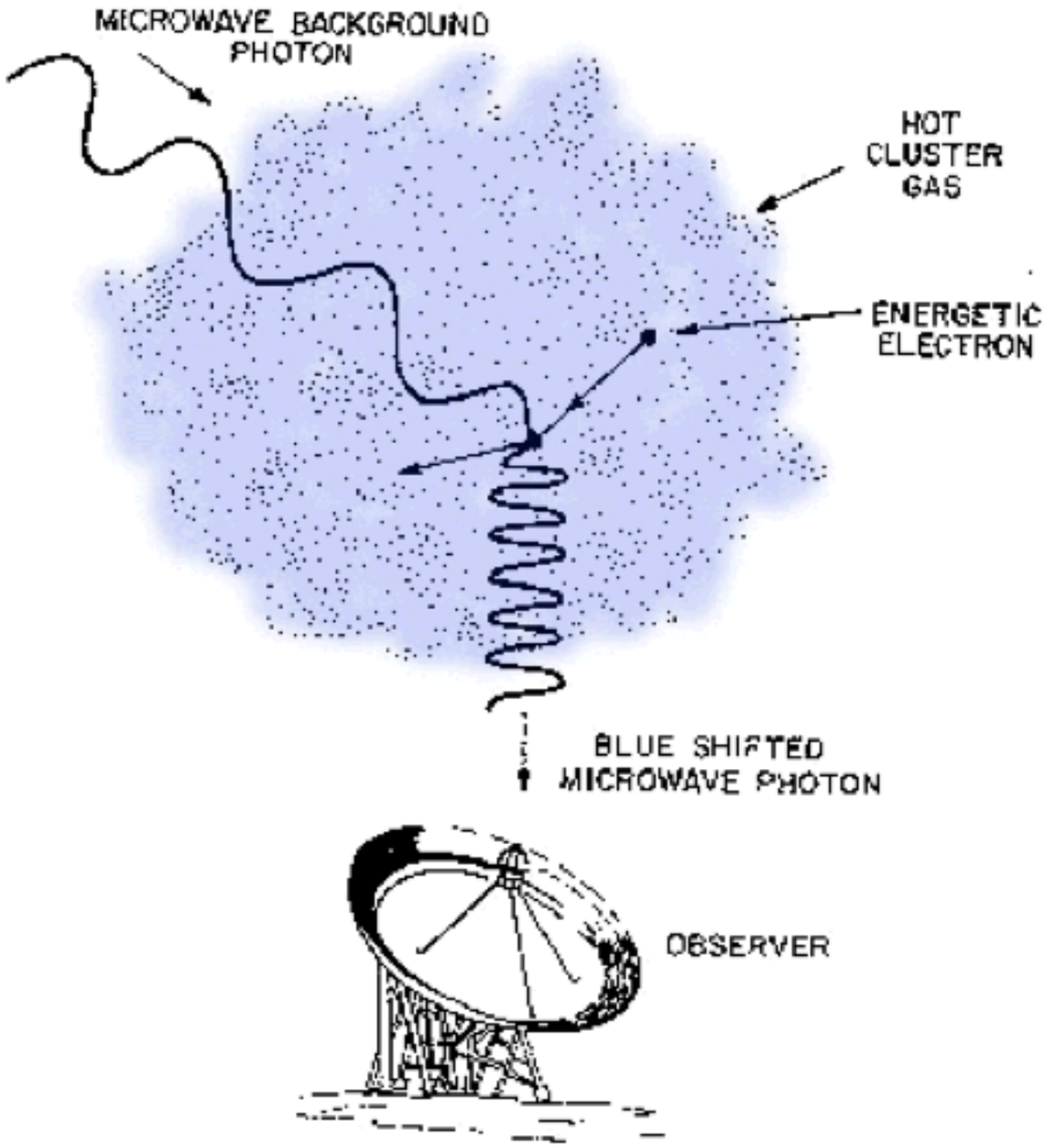

Source: http://astro.uchicago.edu/sza/primer.html

The Sunyaev-Zel'dovich (SZ) effect

Thermal X-ray Emission

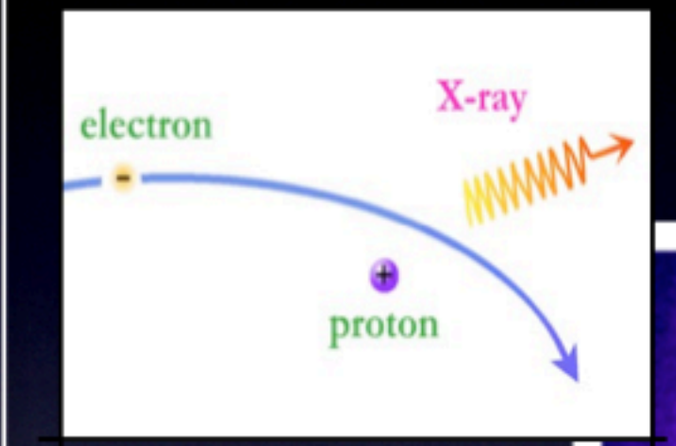

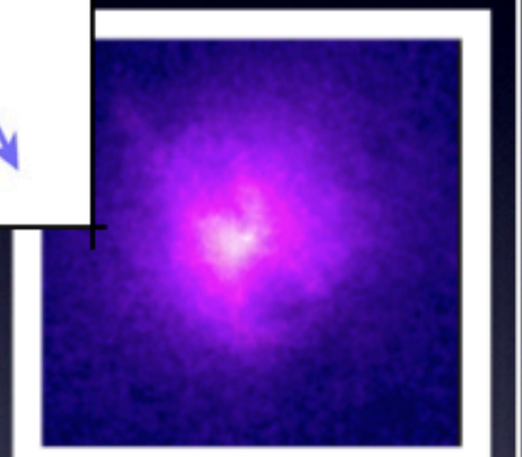

X-ray $\sim n_e^2 \, \Lambda(T_e)$

The hot, ionized ICM emits in the X-rays due to thermal bremsstrahlung. X-ray surface brightness scales as gas density squared, and has a weak temperature dependence in the 0.5−2 keV band.

Sunyaev-Zel'dovich (SZ) Effect

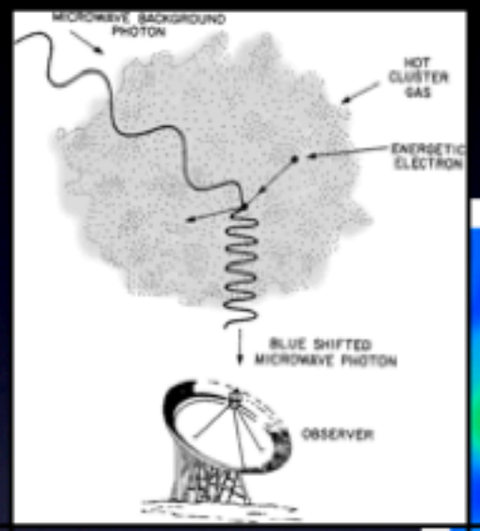

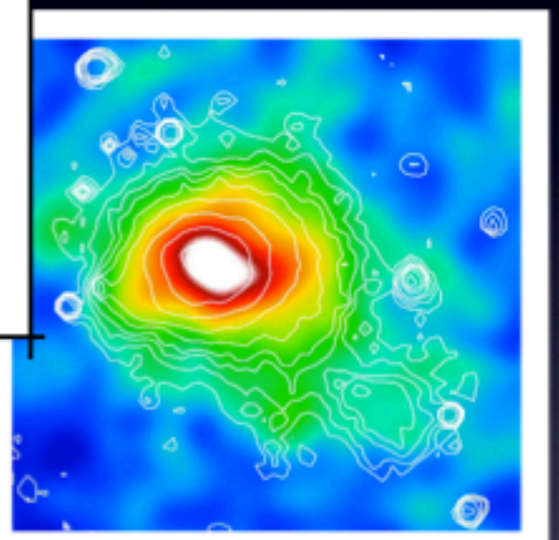

SZE $\sim n_e \, T_e$

The same electrons in the ICM causes (inverse) Compton scattering of the background CMB photons, known as the Sunyaev-Zel'dovich effect. Signal is proportional to the gas pressure.

Spectrum of the SZ effect

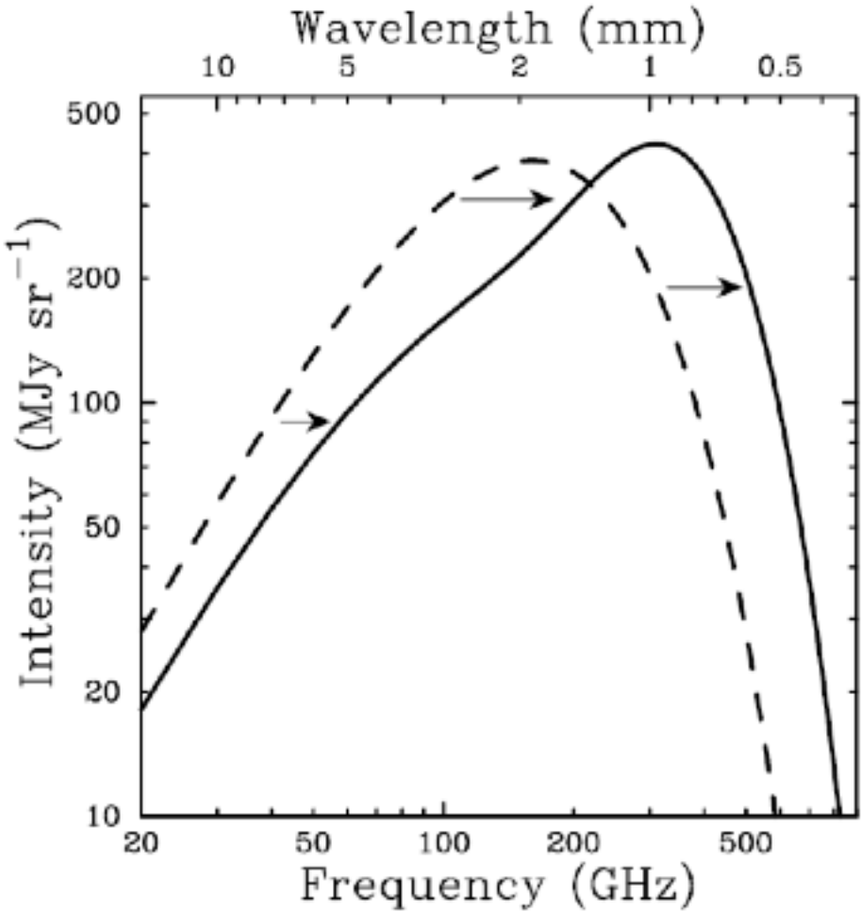

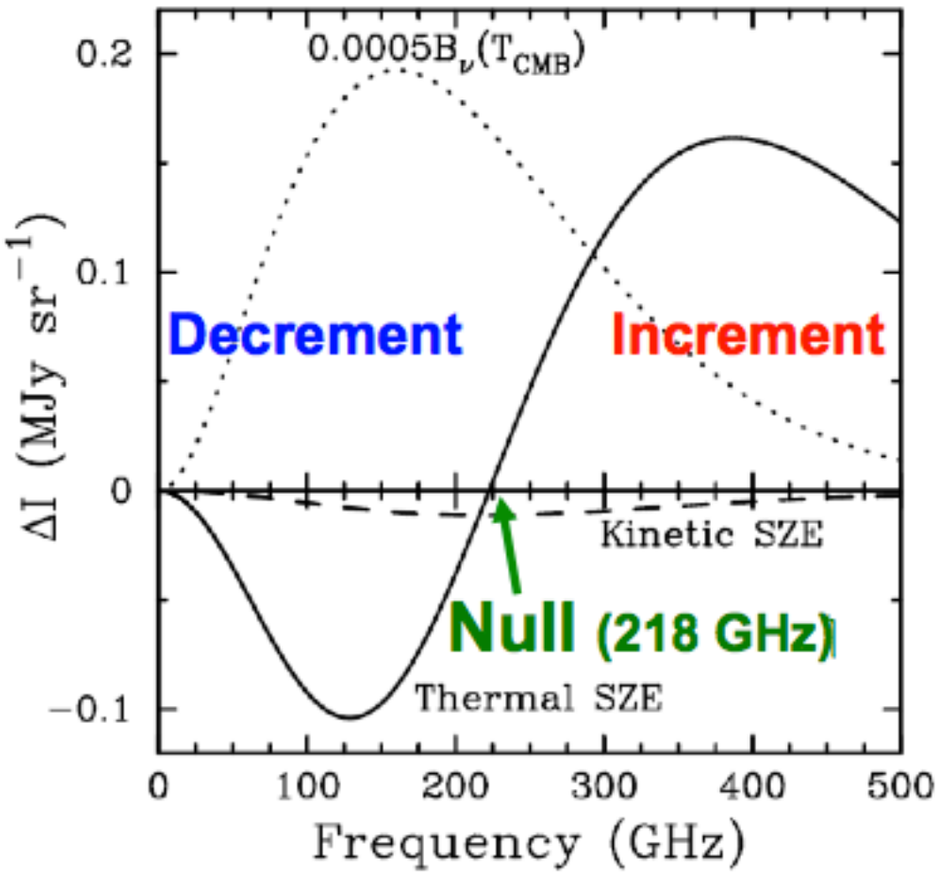

decrement in Rayleigh-Jeans part: $\Delta I(\nu) = -2\,y\,I(\nu)$

Compton-y parameter: $y \equiv \frac{\sigma_{\rm T}\,k_{\rm B}}{m_{\rm e}\,c^2} \int T_{\rm e}\,n_{\rm e}\,dl$

integrated effect: $Y = \int y\,dA \propto n_{\rm e}\,T\,dV \propto E_{\rm thermal}$

Source: Carlstrom et al., 2002

Spectrum of the SZ effect

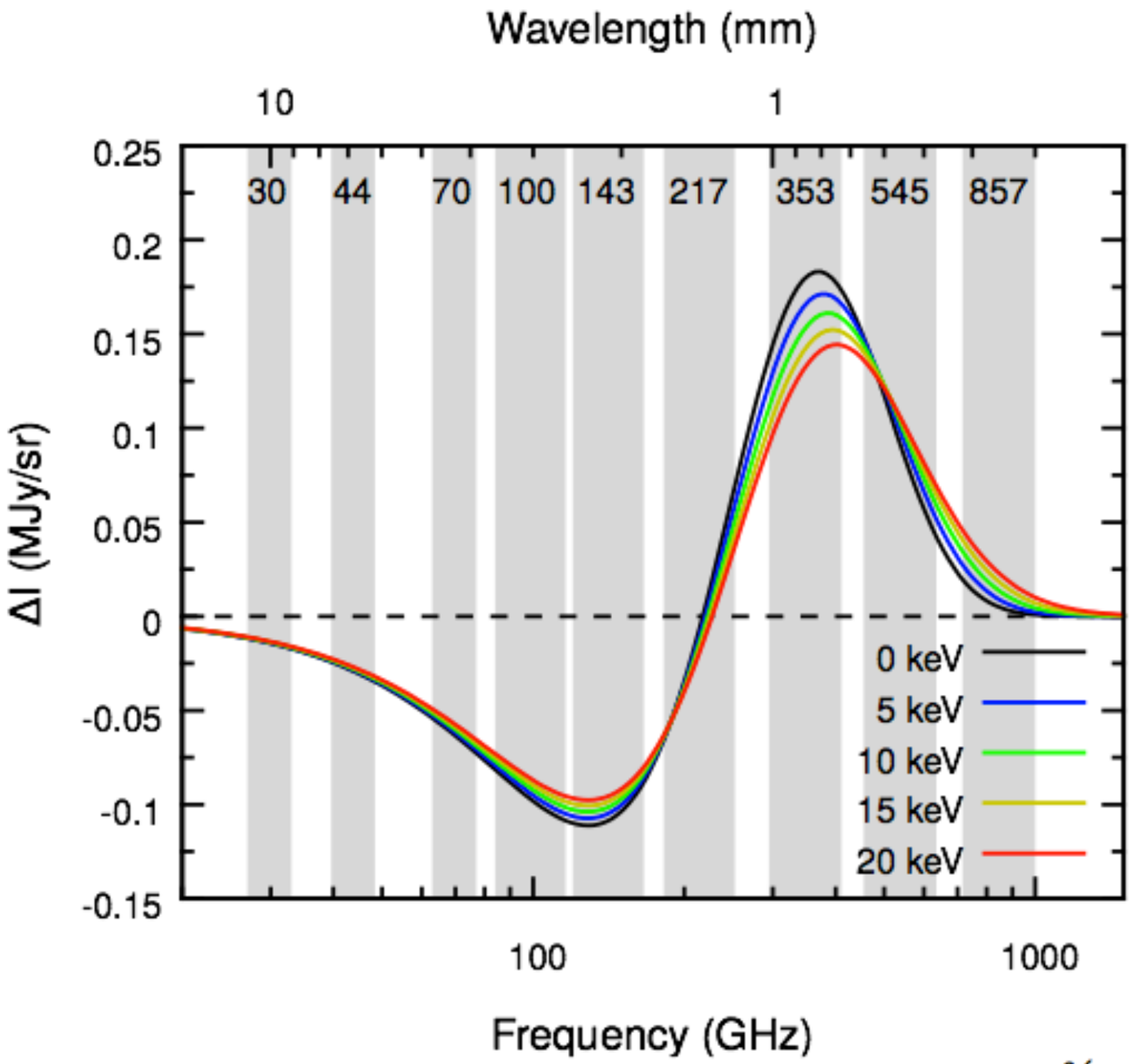

$$\frac{\Delta I_{\rm SZ}}{I_0} = h(x)\left[\underbrace{f(x,T_{\rm e})\,y}_{\rm tSZ} - \underbrace{\tau_{\rm e}\left(\frac{v_{\rm pec}}{c}\right)}_{\rm kSZ}\right]$$

The y-parameter is the line-of-sight integral of pressure:

$$y = \frac{\sigma_{\rm T}}{m_{\rm e}c^2}\int_{\rm l.o.s.} n_{\rm e}k_{\rm B}T_{\rm e}\,{\rm d}l,$$

The following definitions are used:

$$x \equiv h\nu/(k_{\rm B}T_{\rm CMB})$$

$$I_0 = 2(k_{\rm B}T_{\rm CMB})^3/(hc)^2,$$

$$h(x) = x^4\exp(x)/(\exp(x)-1)^2$$

and

$$f(x,T_{\rm e}) = \left(x\frac{\exp(x)+1}{\exp(x)-1} - 4\right)(1+\delta_{\rm SZE}(x,T_{\rm e}))$$

Different types of SZ effect

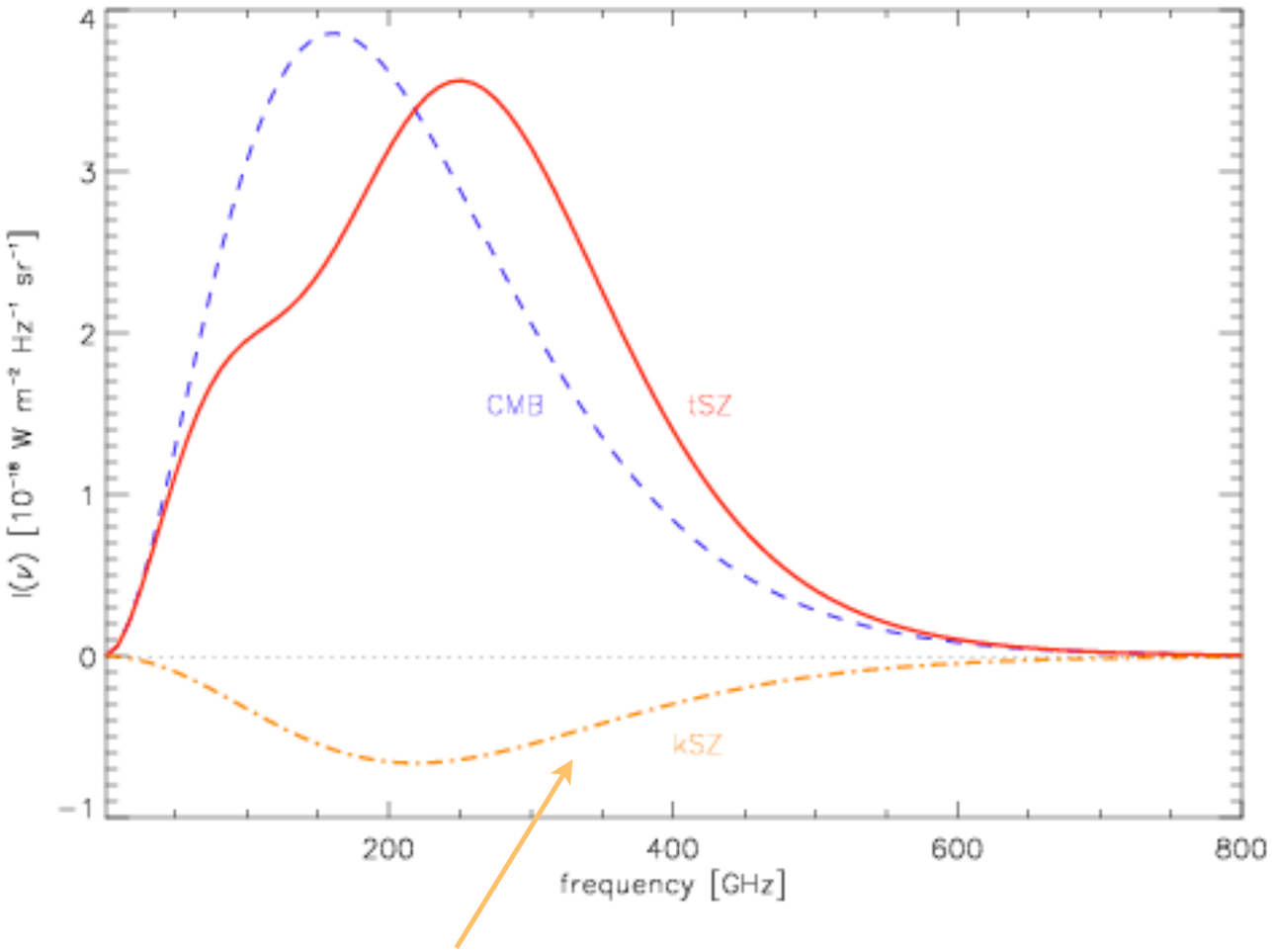

tSZ

kSZ

rSZ

pSZ

ntSZ

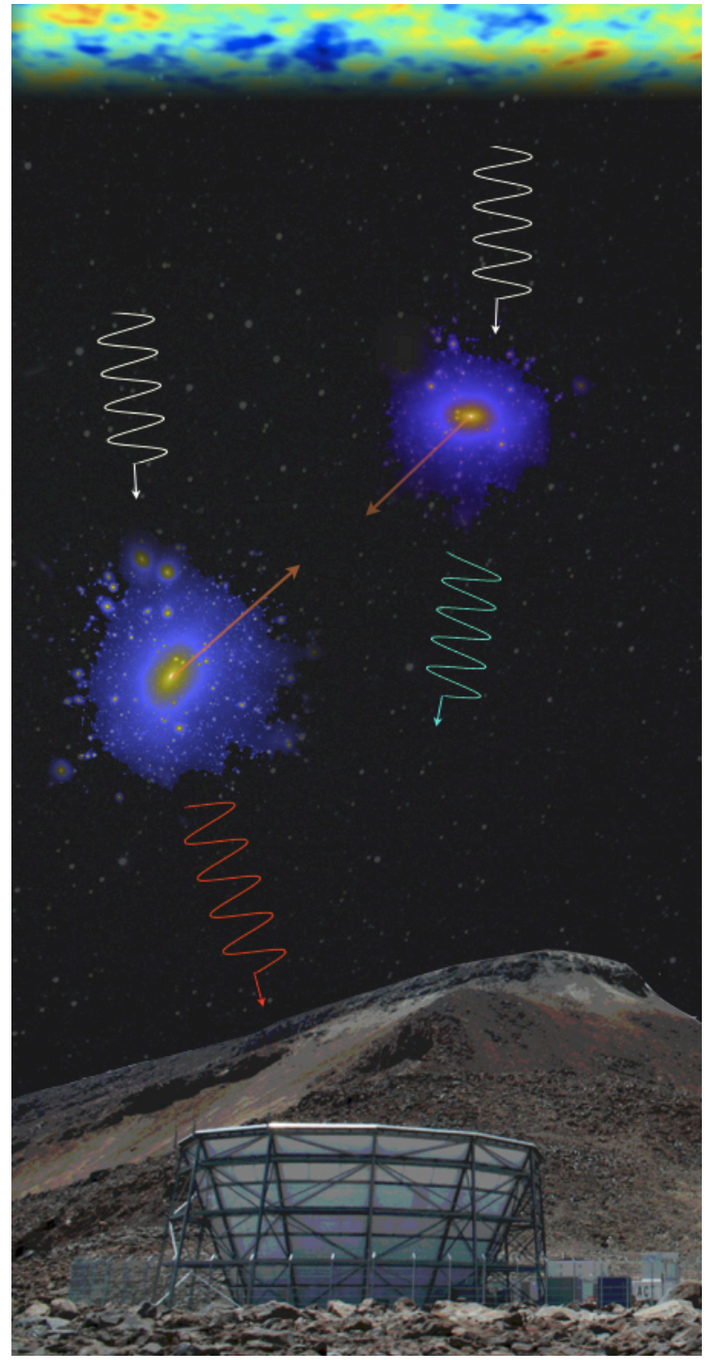

Credit: Hand et al.
ACT collaboration

The kinetic SZ (kSZ) effect is caused by the motion of the scattering electrons as a whole (bulk motion), which causes a Doppler shift in the energy.

$$\frac{\Delta T}{T} = -\frac{\mathbf{v_r}}{c}\tau \equiv -\frac{\mathbf{v_r}}{c}\int \sigma_T n dl$$

A polarized SZ (pSZ) effect can arise from scattering of the quadrupole radiation in the cluster frame, both primordial and due to cluster's motion.

Properties of the (thermal) SZ effect

Thermal SZE is a small (<1 mK) distortion in the CMB caused by inverse Compton scattering of the CMB photons

$$\frac{\Delta T}{T_{\rm CMB}} = f(x, T_e) \int n_e(l) \, \frac{k_{\rm B} T_e(l)}{m_e c^2} \, dl$$

Total cluster flux density is independent of redshift!

$$\Delta S_\nu = \int \Delta I_\nu \, d\Omega \propto \frac{\int n_e T_e \, dV}{D_{\rm A}^2} \propto \frac{f_{\rm gas} M_{\rm tot} T_e}{D_{\rm A}^2}$$

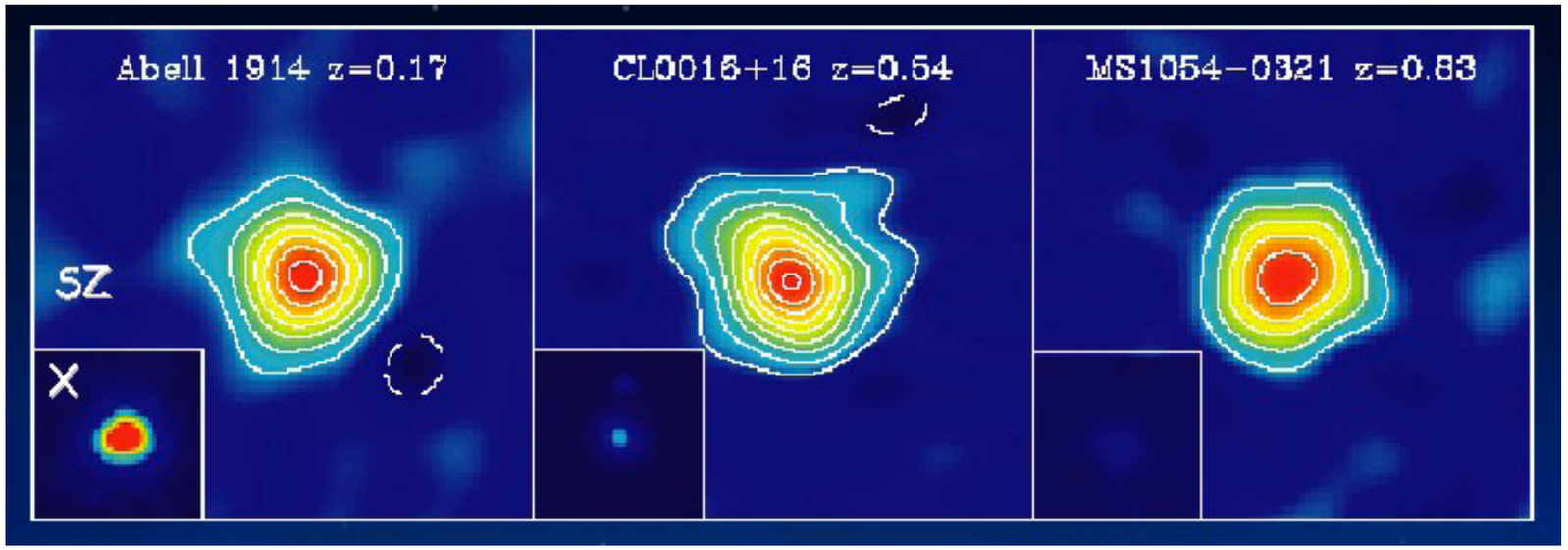

The first four SZE discovered galaxy clusters

unfiltered map (with CMB)

filtered detection maps

null maps

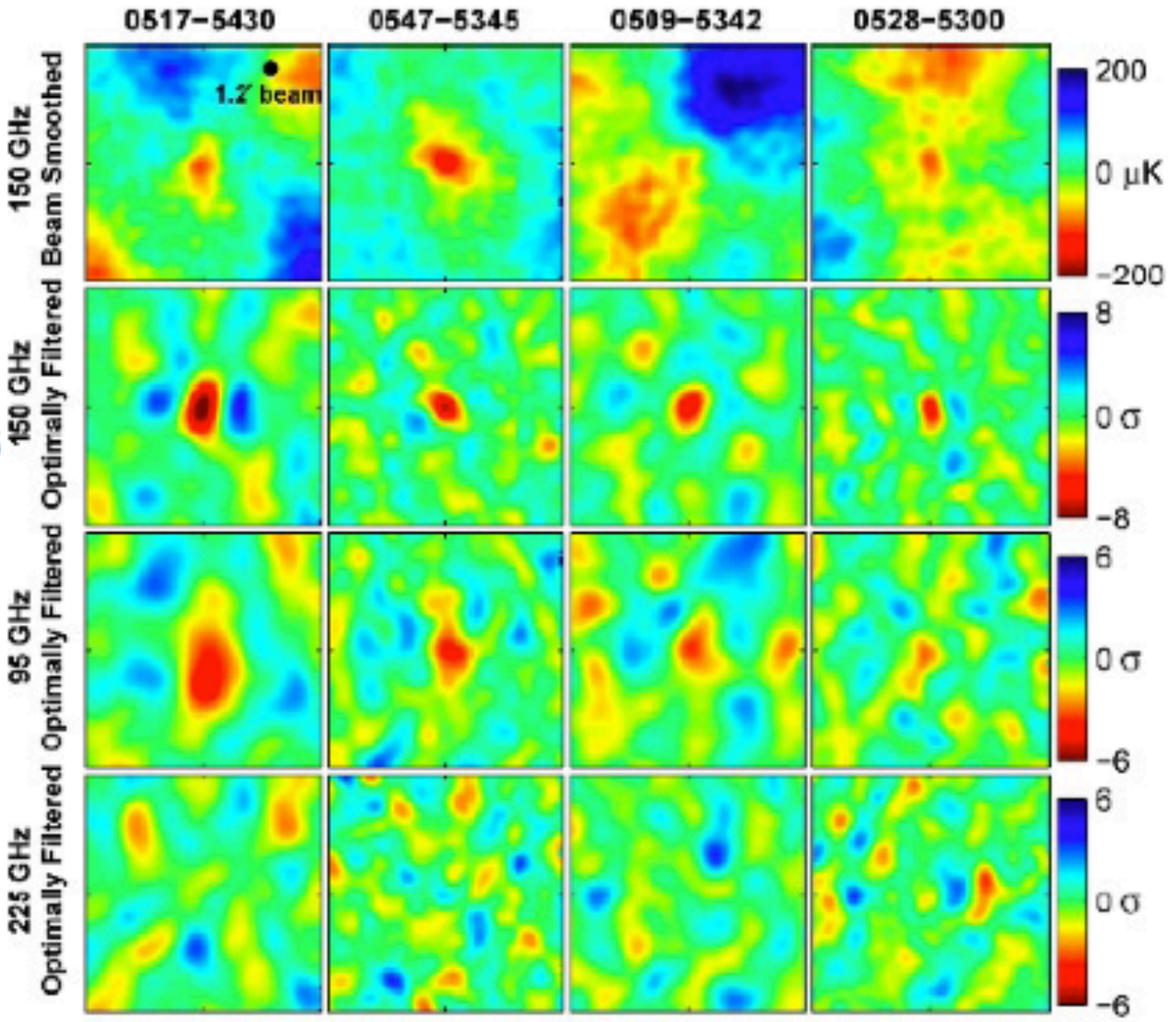

20’x20’ field-of-view

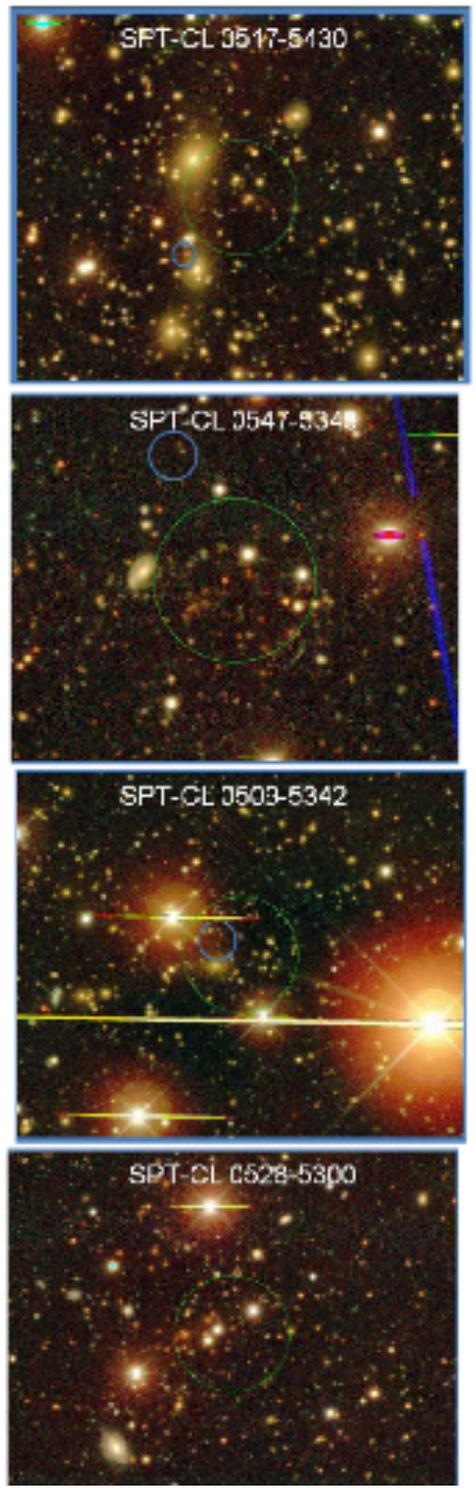

Source: Staniszewski et al. 2009

SZ cluster surveys

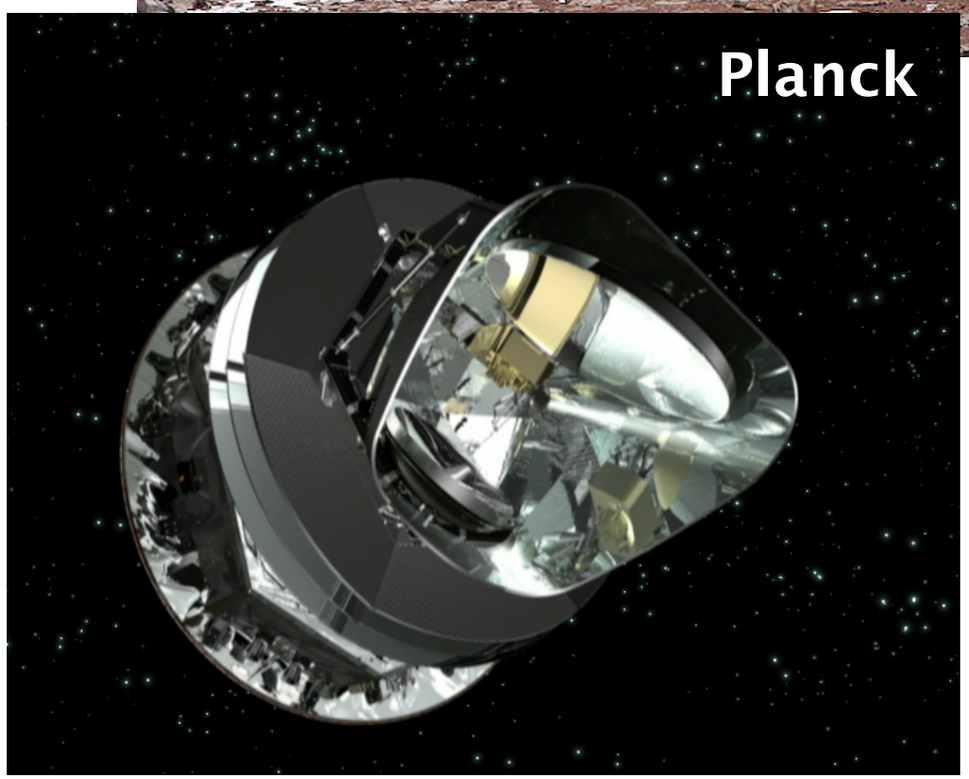

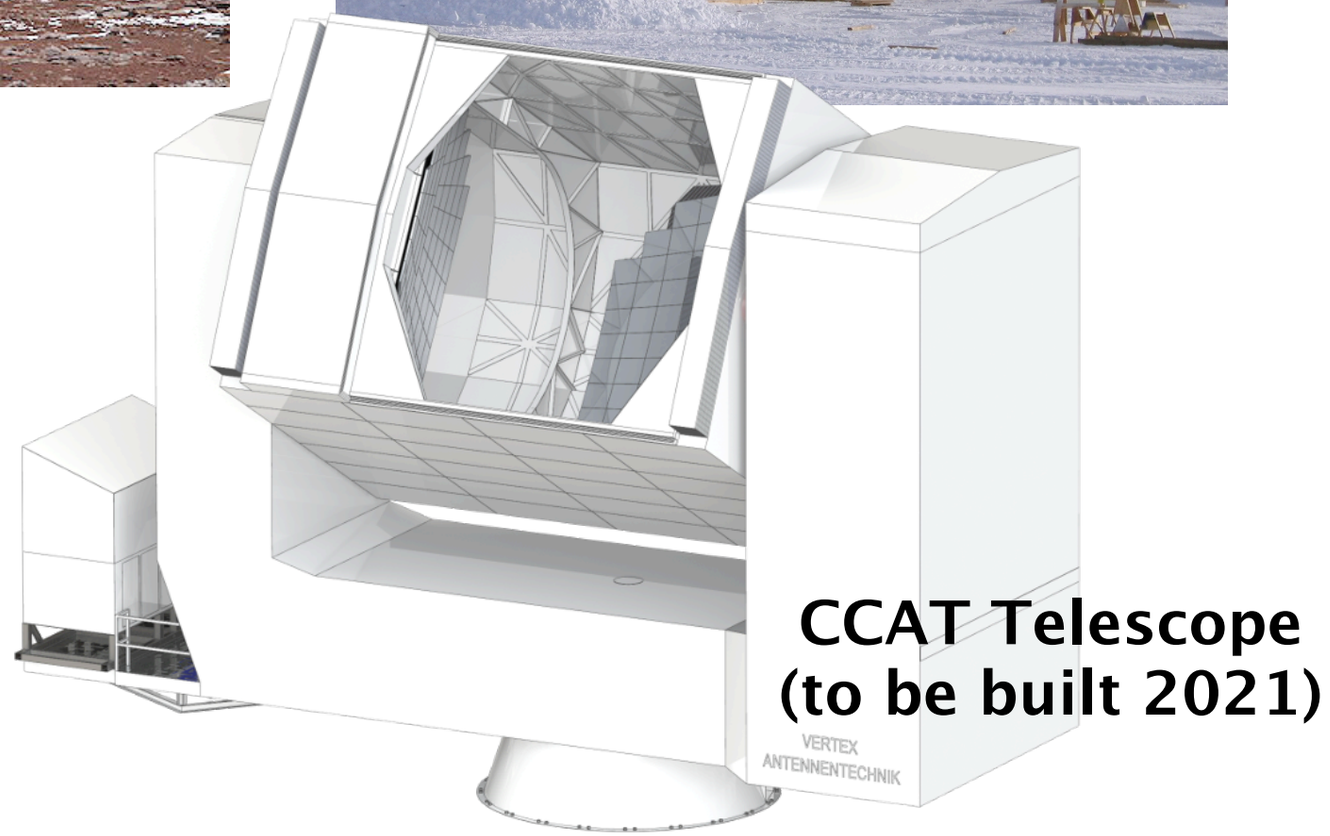

APEX telescope

- 12-m on-axis ALMA prototype
- Located at the Chilean altiplano, elevation 5100 m
- 1 arcmin reolution @ 150 GHz, 0.4 deg FoV
- Surface accuracy 18 μm

Clusters detected by APEX-SZ

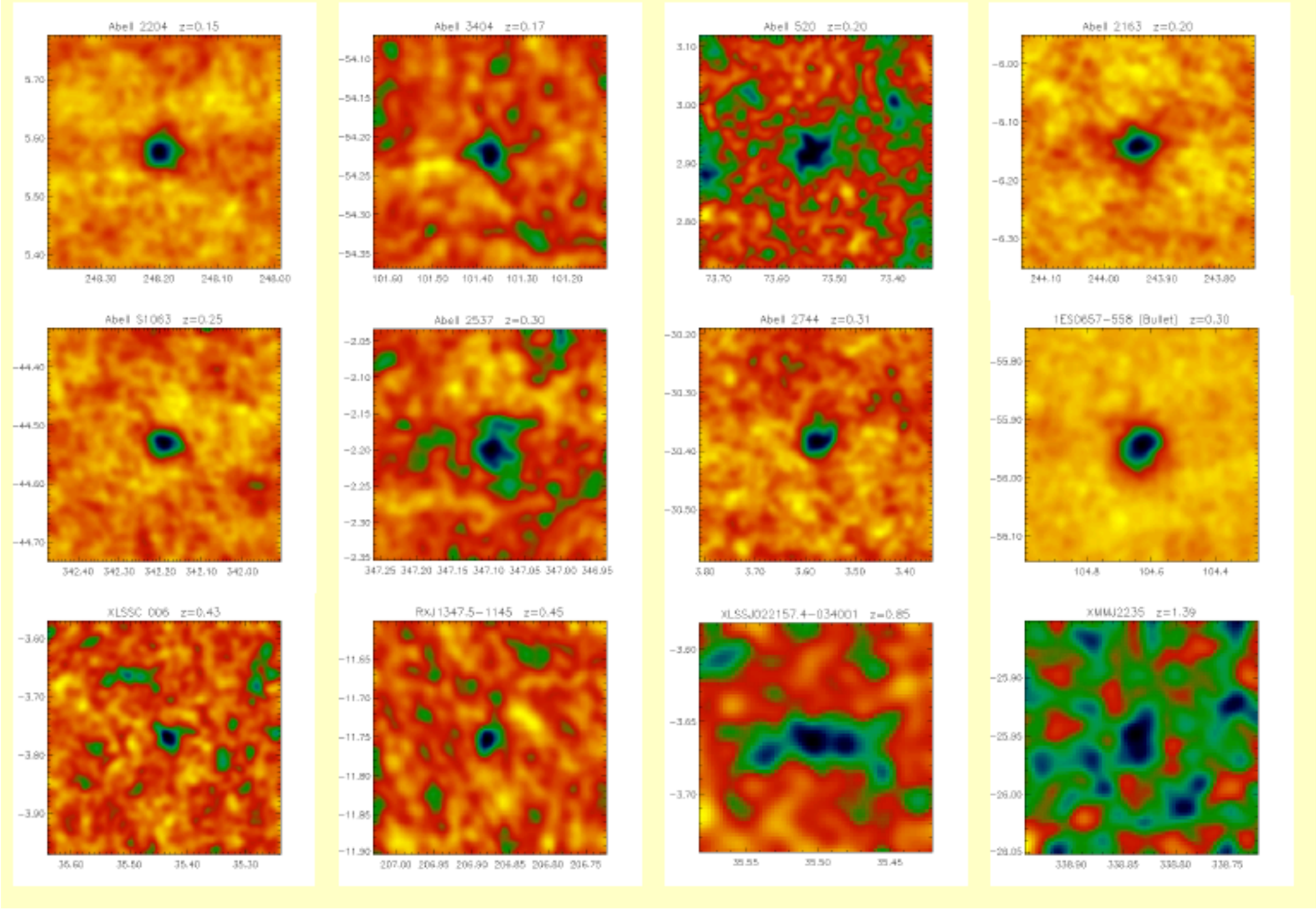

Modeling the ICM

Parametric models for the ICM

A consistently good empirical fit!

$$n_e(r) = n_{e0}\left(1+\frac{r^2}{r_c^2}\right)^{-3\beta/2}$$

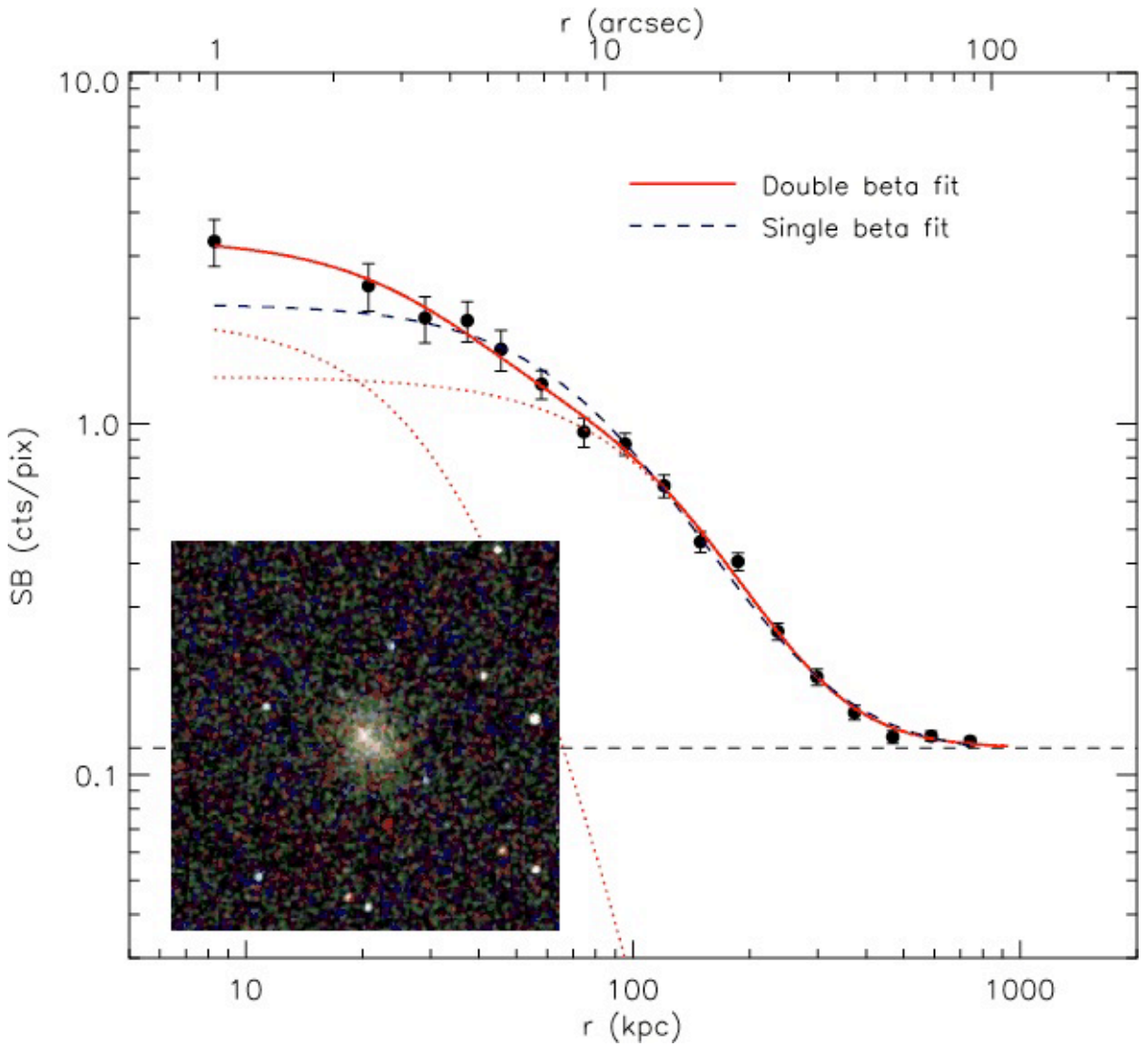

For cool core cluster a better fit for density is double β-model

$$n_e(r) = n_{e0}\left[f\left(1+\frac{r^2}{r_{c1}^2}\right)^{-3\beta/2} + (1-f)\left(1+\frac{r^2}{r_{c2}^2}\right)^{-3\beta/2}\right]$$

ICM and galaxy density profile

- the ICM obeys the baryonic gas physics, so that the ICM density profile $\rho_{gas}(r)$ could be different from that of the DM parent halo
- the easiest physically motivated density distribution is the one for a **self-gravitating sphere of an isothermal gas** with T(r)=T=const
- particles of an isothermal gas have a Maxwellian (MW) velocity distribution

- $\rho_{gas}(r)$ can be derived from:
  1. hydrostatic equation + ideal gas equation (as before)

$$-\rho_{\rm gas}(r)\frac{G\,M_{\rm tot}(<r)}{r^2} = \frac{k_{\rm B}}{\mu\, m_{\rm P}}\frac{d[\rho_{\rm gas}(r)\,T_{\rm X}(r)]}{dr}$$

  2. plug in T=const, $M(<r) = 4\pi\int r^2\rho(r)dr$, and $k_B T = (\mu m_P)\cdot\sigma_r^2 = const$ which follows from: $\overline{E}_{kin} = \frac{3}{2}k_B T = \frac{1}{2}\langle m\rangle\langle v^2\rangle = \frac{1}{2}\cdot(\mu m_P)\cdot 3\sigma_r^2$
  3. rearrange and differentiate both sides to arrive at the differential equation:

$$\sigma_r^2\cdot\frac{d}{dr}\left(\frac{r^2}{\rho(r)}\frac{d\rho(r)}{dr}\right)+4\pi G r^2\rho(r)=0$$

ICM and galaxy density profile

Singular Isothermal Sphere (SIS) model:

the **Singular Isothermal Sphere (SIS)** is an analytic solution to this differential equation:

$$\rho_{iso}(r) = \frac{\sigma^2}{2\pi G} r^{-2}$$

Properties:

1. singularity for r→0
2. M(r) grows linearly with r → divergent total mass

Reason: MW distribution has a tail with particles at very high velocities; the required gravitationally binding of these particles requires a divergent mass M(r)

ICM and galaxy density profile

King model:

the King Model (King 1966) solves the problem of the divergent total mass

by means of a truncation of the Maxwellian distribution at high velocities, the total mass is only 'logarithmically divergent' (as NFW) and has a flat core:

$$\rho_{King}(r) = \rho_0 \left(1 + \frac{r^2}{r_c^2}\right)^{-\frac{3}{2}}$$

$\mathbf{r_c}$ is the **core radius**, i.e. the characteristic length scale within which the density profile flattens out

$$\rho_{King}(r << r_c) = \rho_0 = const$$

$$\rho_{King}(r >> r_c) \propto r^{-3}$$

ICM and galaxy density profile

The β model:

generalization of the isothermal King models for the approximate description of the X-ray ICM density profile by introducing an additional parameter β :

3d gas profile: $$\rho_{\rm gas}(r) = \frac{\rho_{\rm gas,0}}{\left[1+\left(\frac{r}{r_{\rm c}}\right)^2\right]^{\frac{3\beta}{2}}}$$

β is the ratio of the kinetic energies of tracers of the gravitational potential (galaxies) and the mean thermal energies of ICM gas particles:

$$\beta = \mu\, m_{\rm p}\, \sigma_{\rm r}^2/(k_{\rm B} T_{\rm gas})$$

$$\sigma^2_{\rm gal} = \beta\, \sigma^2_{\rm gas}$$

We should expect β = 1.
But clusters are not in perfect hydrostatic equilibrium, neither the mass profile is a King profile.
Hence $\beta_{\rm fit} < 1$ (usually $\beta_{\rm fit} \approx 2/3$)

X-ray and SZ in β-model

The most convenient feature of isothermal β-model is that X-ray surface brightness and SZE decrement **in projection** takes simple analytical forms

$$S_x = S_{x0}\left(1+\frac{\theta^2}{\theta_c^2}\right)^{(1-6\beta)/2},$$

$$\Delta T = \Delta T_0\left(1+\frac{\theta^2}{\theta_c^2}\right)^{(1-3\beta)/2},$$

These two equations are the results of the following two integrals:

$$\Delta T = f_{(x,T_e)} T_{\rm CMB} D_{\rm A} \int d\zeta\, \sigma_{\rm T} n_e \frac{k_{\rm B} T_e}{m_e c^2}$$

$$S_{\rm X} = \frac{1}{4\pi(1+z)^4} D_{\rm A} \int d\zeta\, n_e n_{\rm H} \Lambda_{e{\rm H}}$$

integration is along the line of sight $dl = D_A\, d\zeta$

Solving for $n_e(0)$ with β-model

$$n_{e0} = \left\{ \frac{S_{x0} 4\pi (1+z)^4 \mu_H}{\Lambda_{eH} \mu_e} \left[D_A \int \left(1 + \frac{\theta^2}{\theta_c^2} \right)^{-3\beta/2} d\theta \right]^{-1} \right\}^{1/2}$$

$$n_{e0} = \frac{\Delta T_0}{f_{(x,T_e)} T_{\mathrm{CMB}}} \frac{m_e c^2}{\sigma_T k_B T_e} \left[D_A \int \left(1 + \frac{\theta^2}{\theta_c^2} \right)^{-3\beta/2} d\theta \right]^{-1}$$

Integrating over density distribution gives total gas mass:

$$M_{\mathrm{gas}}(r_0) = 4\pi \mu_e n_{e0} m_p \int_0^{r_0} \left(1 + \frac{r^2}{r_c^2} \right)^{-3\beta/2} r^2 dr$$

Solving for d_A

From Reese et al. (2002)

One can solve for the angular diameter distance by eliminating n_{e0} (noting that $n_{\rm H} = n_e \mu_e / \mu_{\rm H}$, where $n_j \equiv \rho / \mu_j m_p$ for species j), yielding

$$D_{\rm A} = \frac{(\Delta T_0)^2}{S_{\rm X0}} \left(\frac{m_e c^2}{k_{\rm B} T_{e0}} \right)^2 \frac{\Lambda_{e{\rm H}0} \mu_e / \mu_{\rm H}}{4\pi^{3/2} f^2_{(x,T_e)} T^2_{\rm CMB} \sigma^2_{\rm T} (1+z)^4} \frac{1}{\theta_c}$$

$$\times \left[\frac{\Gamma(3\beta/2)}{\Gamma(3\beta/2 - 1/2)} \right]^2 \frac{\Gamma(3\beta - 1/2)}{\Gamma(3\beta)} \, ,$$

where $\Gamma(x)$ is the gamma function. Similarly, one can eliminate $D_{\rm A}$ instead and solve for the central density n_{e0}.

More generally, the angular diameter distance is

$$D_{\rm A} = \frac{(\Delta T_0)^2}{S_{\rm X0}} \left(\frac{m_e c^2}{k_{\rm B} T_{e0}} \right)^2 \frac{\Lambda_{e{\rm H}0} \mu_e / \mu_{\rm H}}{4\pi f^2_{(x,T_e)} T^2_{\rm CMB} \sigma^2_{\rm T} (1+z)^4}$$

$$\times \frac{1}{\theta_c} \frac{\int (n_e/n_{e0})^2 (\Lambda_{e{\rm H}} / \Lambda_{e{\rm H}0}) d\eta|_{R=0}}{\left[\int (n_e/n_{e0})(T_e/T_{e0}) d\eta|_{R=0} \right]^2} \, ,$$

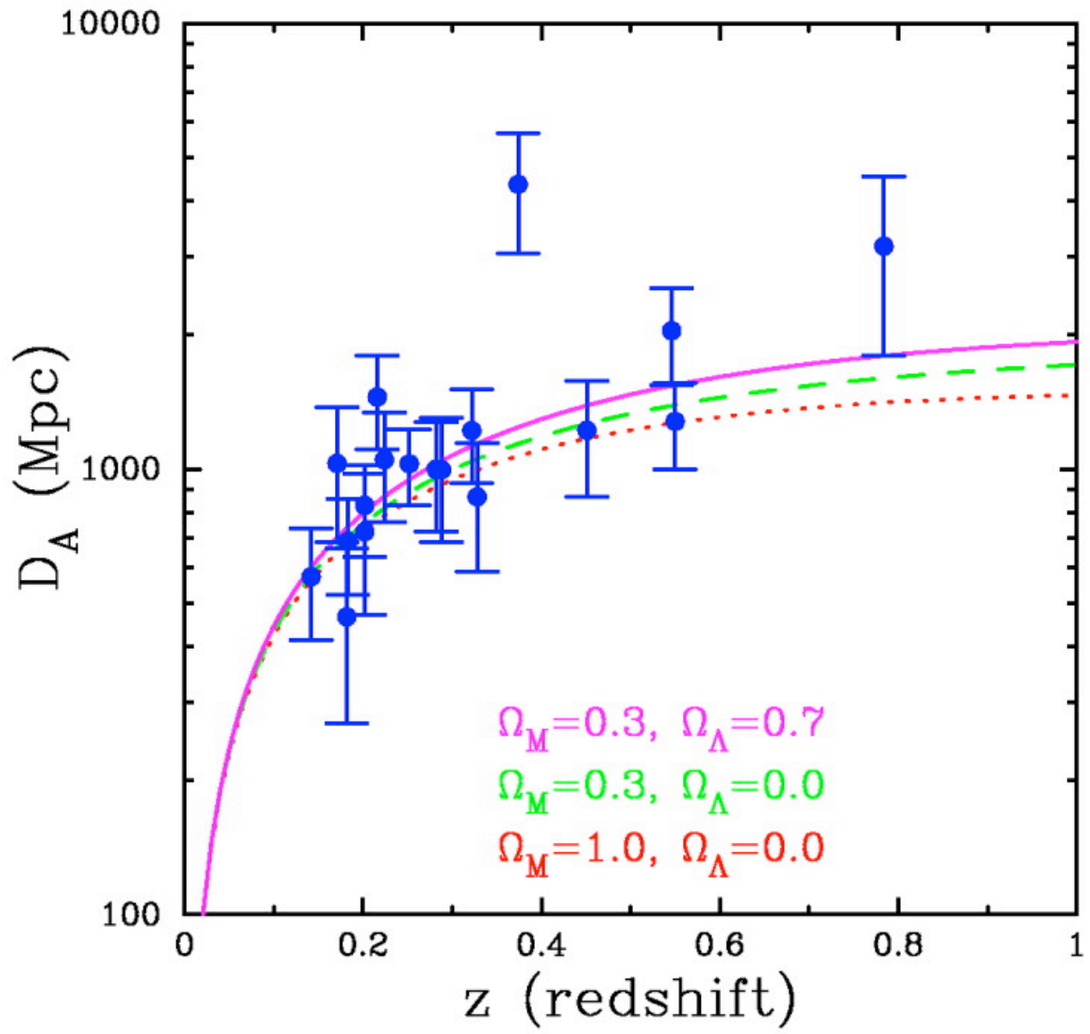

H_0 from SZ/X-ray measurements

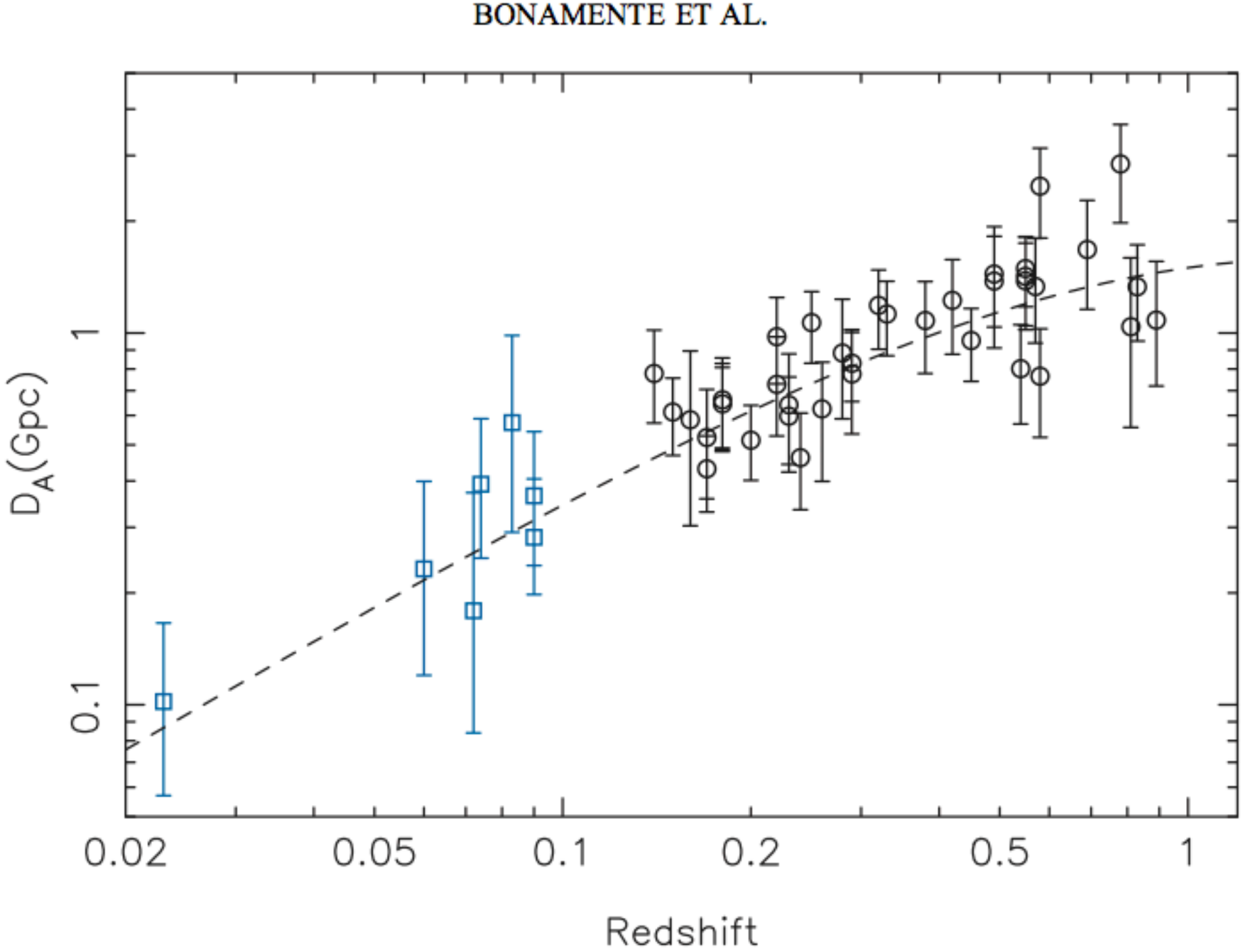

Universal temperature model

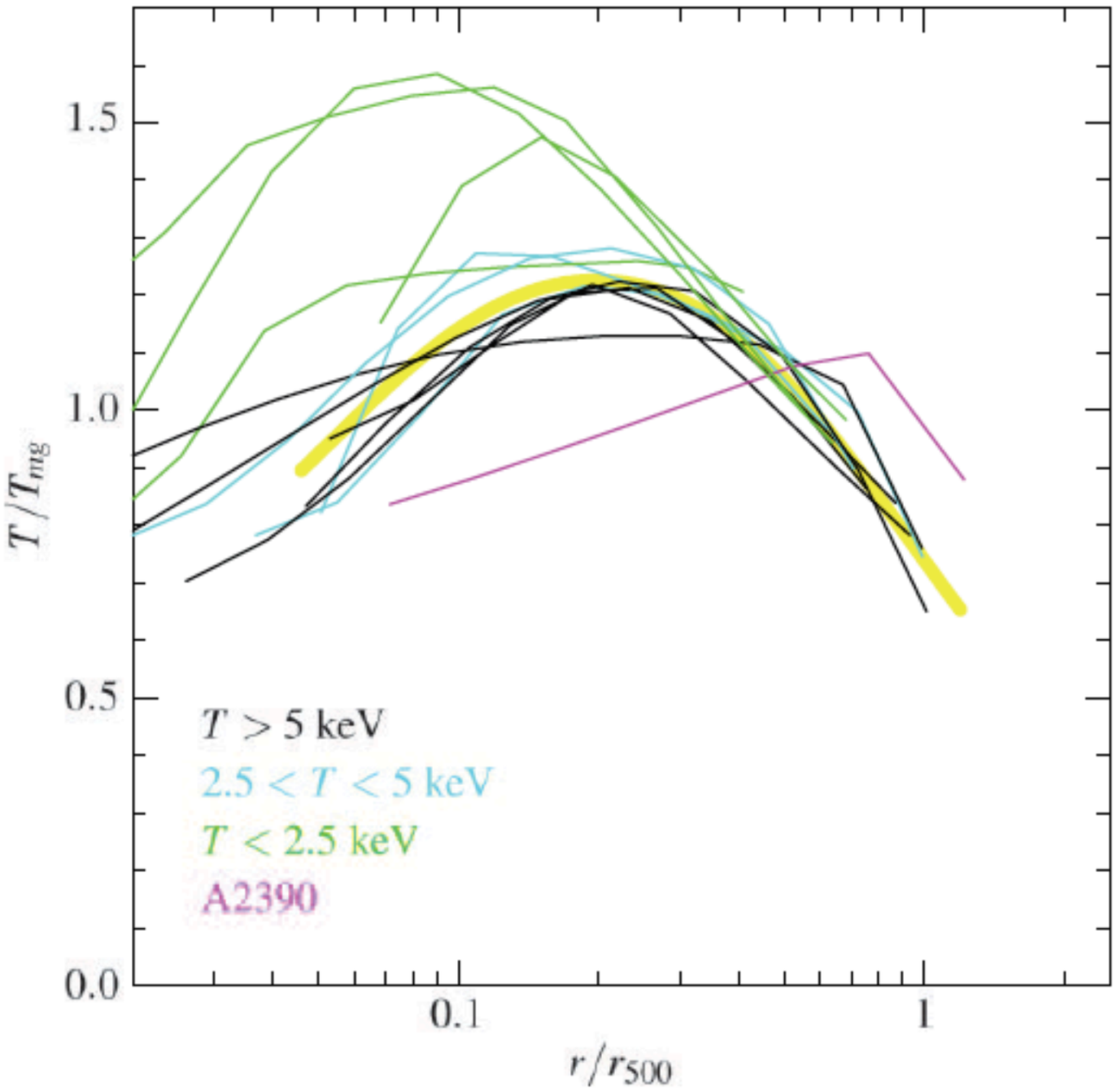

(Vikhlinin et al. 2006)

$$t(r) = \frac{(r/r_t)^{-a}}{\left[1 + (r/r_t)^b\right]^{c/b}}$$

$$t_{\rm cool}(r) = \frac{(x + T_{\rm min}/T_0)}{(x+1)}, \quad x = \left(\frac{r}{r_{\rm cool}}\right)^{a_{\rm cool}}$$

$$T_{\rm 3D}(r) = T_0 t_{\rm cool}(r) t(r).$$

Universal pressure model

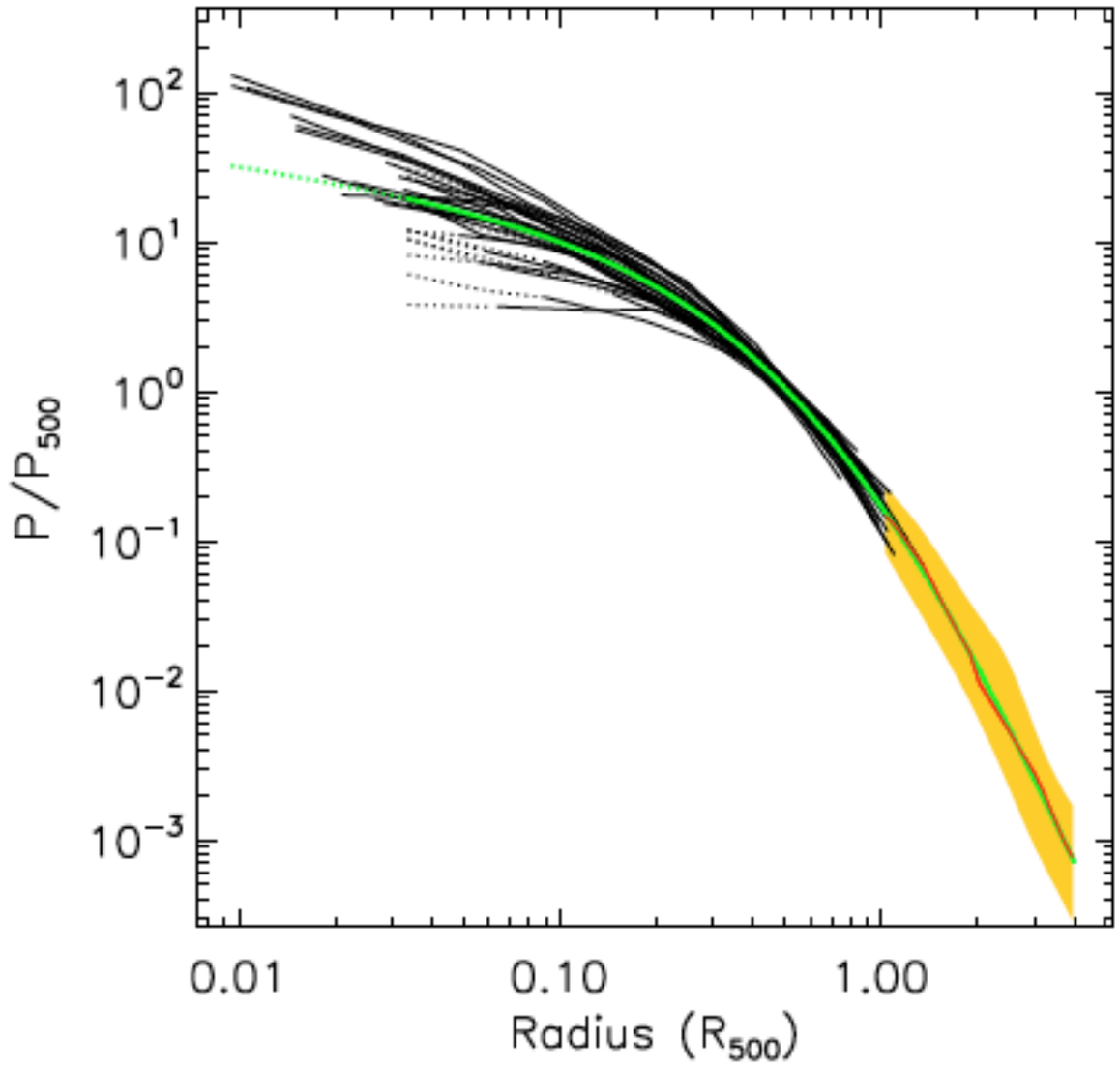

Fig. 8. GNFW model of the universal pressure profile (green line). It is derived by fitting the observed average scaled profile in the radial range [0.03–1] R_{500}, combined with the average simulation profile beyond R_{500} (red line). Black lines: REXCESS profiles. Orange area: dispersion around the average simulation profile.

(Arnaud et al. 2010)

Generalized NFW (GNFW) model first proposed by Nagai et al. (2007)

$$\mathbb{p}(x) = \frac{P_0}{(c_{500}x)^\gamma \left[1 + (c_{500}x)^\alpha\right]^{(\beta-\gamma)/\alpha}}$$

$$P(r) = P_{500}\left[\frac{M_{500}}{3\times 10^{14}\, h_{70}^{-1}\, M_\odot}\right]^{\alpha_\mathrm{p}+\alpha'_\mathrm{p}(x)} \mathbb{p}\,(x)$$

Integrated SZ signal is easily obtained by integrating the pressure

$$Y_{\mathrm{sph}}(R) = \frac{\sigma_\mathrm{T}}{m_\mathrm{e}c^2}\int_0^R 4\pi P(r) r^2 \mathrm{d}r$$

Cluster selection and scaling relations

Cluster scaling relations

The problem:

From the theory's point of view, clusters are solely characterized by their mass.

However:

- we cannot observe the mass directly in a (ICM based) survey
- The cluster selection depends on other obervables

The solution: Galaxy cluster scaling relations

As the gas mostly responds to the cluster's gravitational potential, there exists tight correlations between the gas observables and the total mass

Scaling relation from Bayesian PoV

Bayes' theorem makes clear that identifying the most likely cosmology (C) is dependent on knowing how likely the observations (R) are within that cosmological model:

$$P(C|R) \sim P(R|C)\, P_{prior}(C)$$

For galaxy clusters, nonlinear dynamics and astrophysical uncertainties (e.g. uncertain baryonic physics) complicate the computation of the observable likelihood $P(R \mid C)$.

The question of computing the likelihood can be split into two parts:

- How many clusters of mass M exist in this cosmology at redshift z?

- What is the likelihood that a cluster of mass M at redshift z will have temperature T_X (or some other observable)

Scaling relations

Prediction in terms of mass

Detection via X-ray flux,
SZ flux, optical richness

$$dN / dz\, dM \quad \rightarrow \quad dN / dz\, dF$$

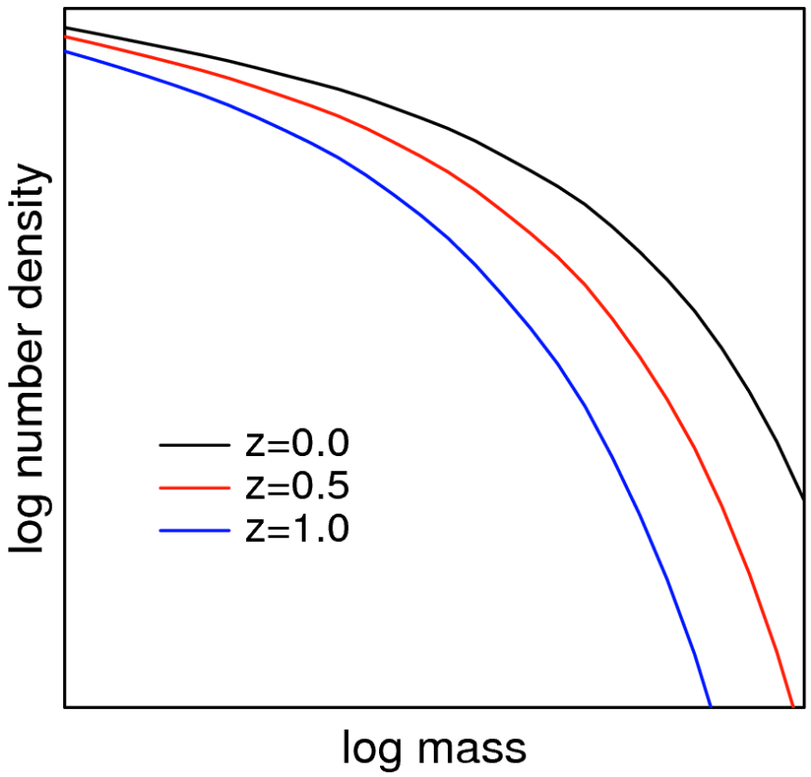

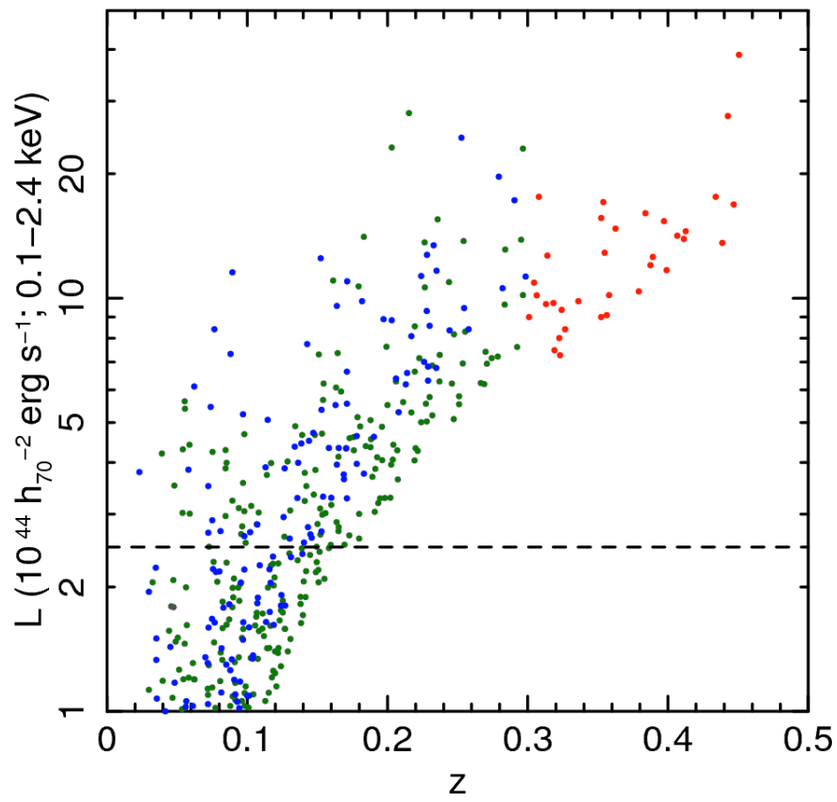

Scaling relations

Prediction in terms of mass

Detection via X-ray flux,
SZ flux, optical richness

$dN / dz\, dM \rightarrow dN / dz\, dF$

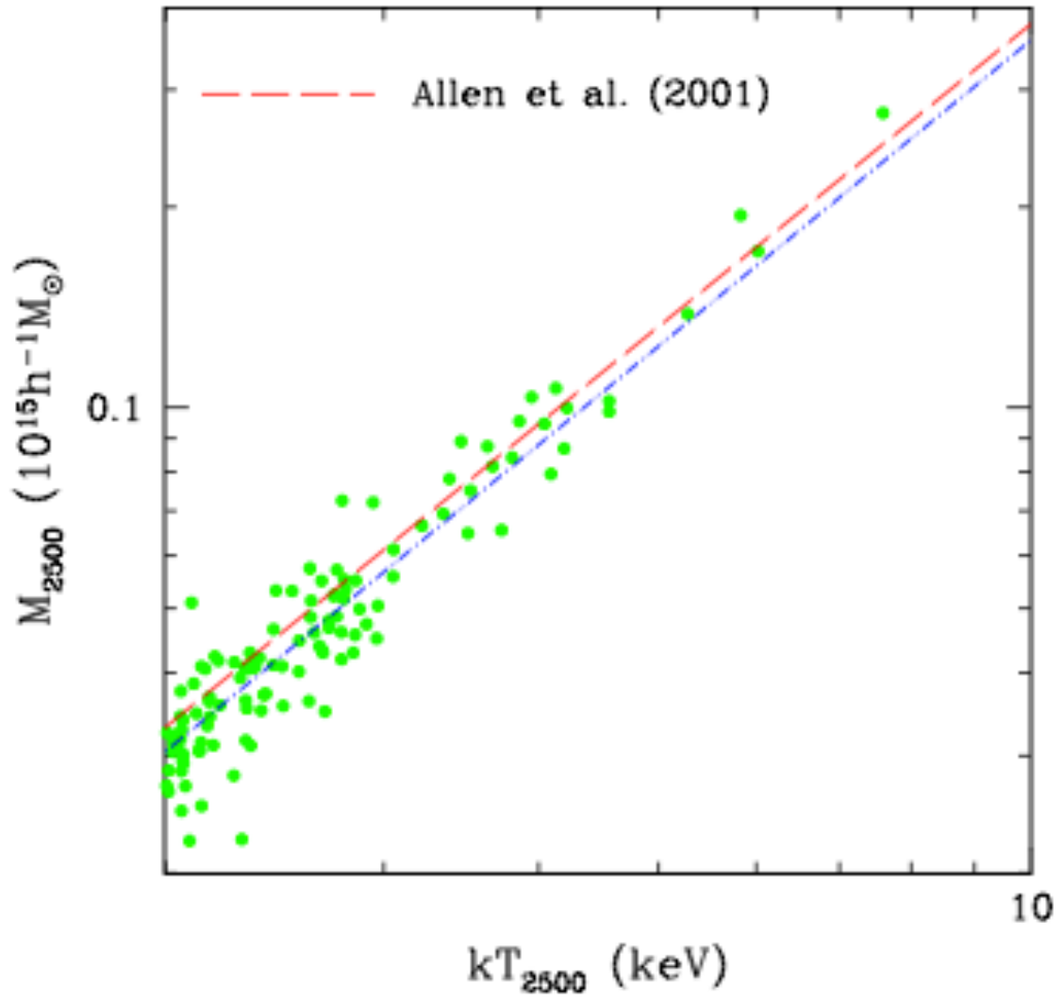

Self-similar scaling

The simplest model to explain cluster physics is based on the assumption that *only gravity determines its properties*.

This makes clusters just scaled version of each other!

Self-similar scaling

The simplest model to explain cluster physics is based on the assumption that *only gravity determines its properties*.

This makes clusters just scaled version of each other!

X-ray temperature specifies the thermal energy per gas particle.

For Virial equilibrium: $T \propto \frac{M}{r}$

$$M_{200} = \frac{4\pi}{3} \Delta_c \rho_{\rm crit} r_{200}^3$$

$$T \propto= \frac{M_{200}}{r_{200}} \propto r_{200}^2 \propto M^{2/3}$$

M-T scaling relation

$$T \propto= \frac{M_{200}}{r_{200}} \propto r_{200}^2 \propto M^{2/3}$$

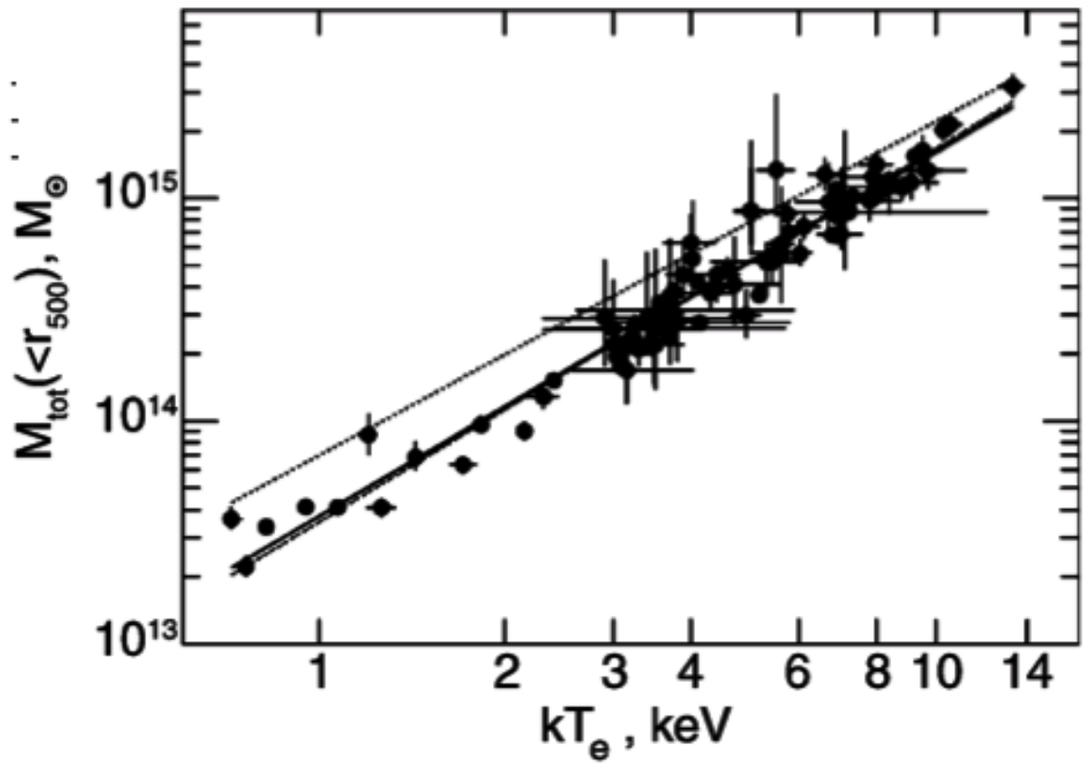

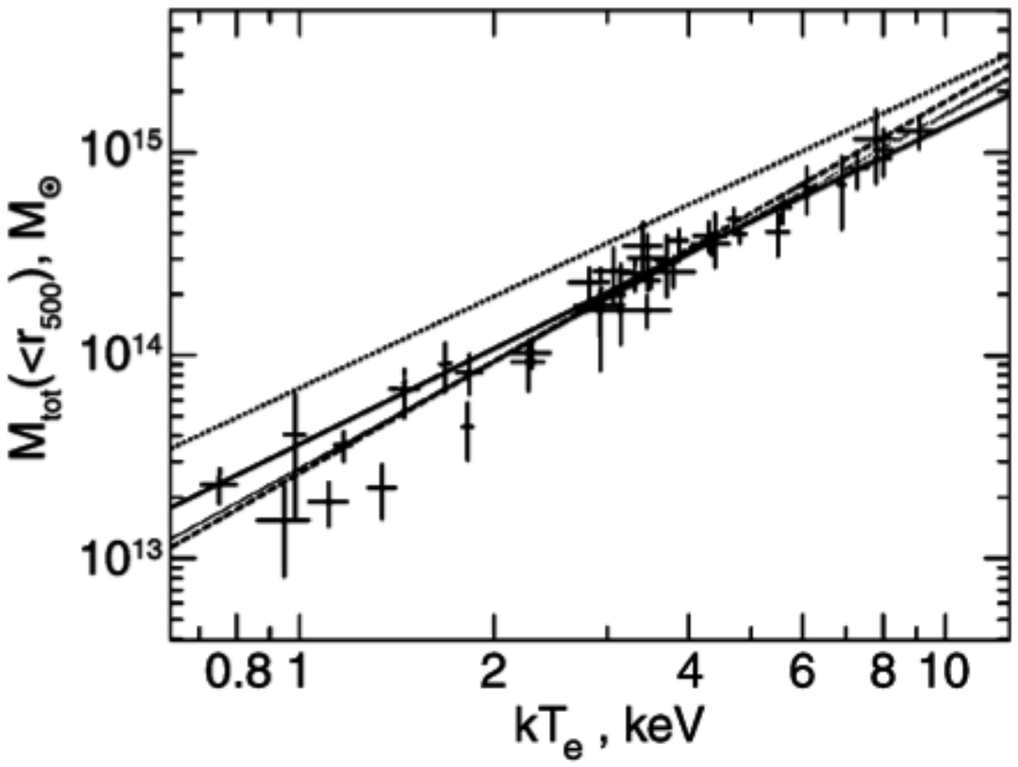

$$M_{500} = 3.57 \times 10^{13}\, M_\odot \left(\frac{kT}{1\,keV}\right)^{1.58}$$

X-ray temperature is good measure of virial mass (better than velocity dispersion).

M–L and L–T relations

$$T \propto= \frac{M_{200}}{r_{200}} \propto r_{200}^2 \propto M^{2/3}$$

From Bremmstrahlung radiation, we have:

$$L_X \propto \rho_g^2 T^{1/2} r_{\rm vir}^3 \propto \rho_g^2 T^{1/2} M_{\rm vir}$$

$$\rho_g \sim M_g r_{\rm vir}^{-3} = f_g M_{\rm vir} r_{\rm vir}^{-3}$$

where $f_g = M_g/M_{vir}$ is the gas fraction.

$$L_X \propto f_g^2 M_{\rm vir}^{4/3} \propto f_g^2 T^2$$

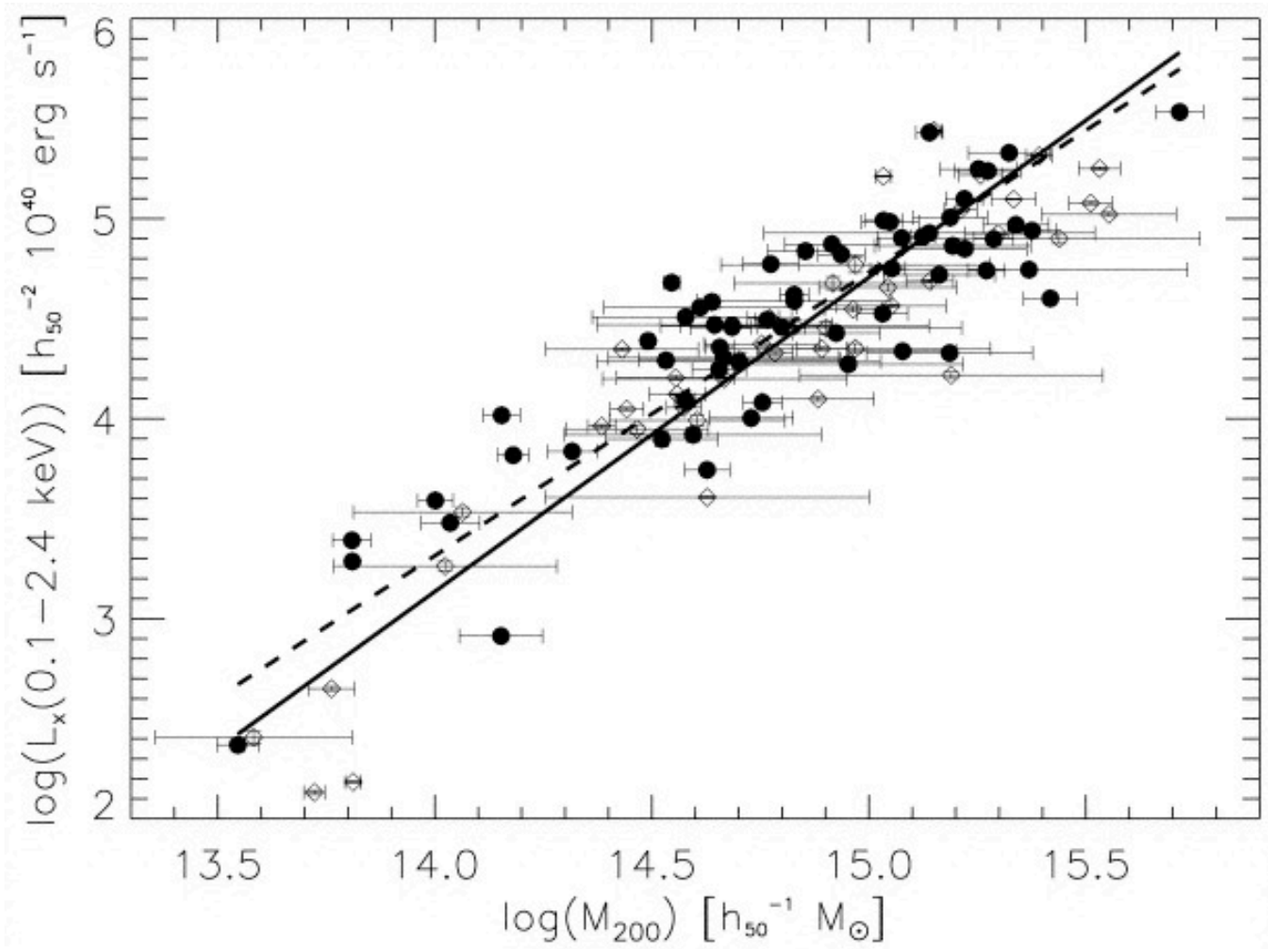

M–L and L–T relations

$$T \propto= \frac{M_{200}}{r_{200}} \propto r_{200}^2 \propto M^{2/3}$$

From Bremmstrahlung radiation, we have:

$$L_X \propto \rho_g^2 T^{1/2} r_{\rm vir}^3 \propto \rho_g^2 T^{1/2} M_{\rm vir}$$

$$\rho_g \sim M_g r_{\rm vir}^{-3} = f_g M_{\rm vir} r_{\rm vir}^{-3}$$

where $f_g = M_g/M_{vir}$ is the gas fraction.

$$L_X \propto f_g^2 M_{\rm vir}^{4/3} \propto f_g^2 T^2$$

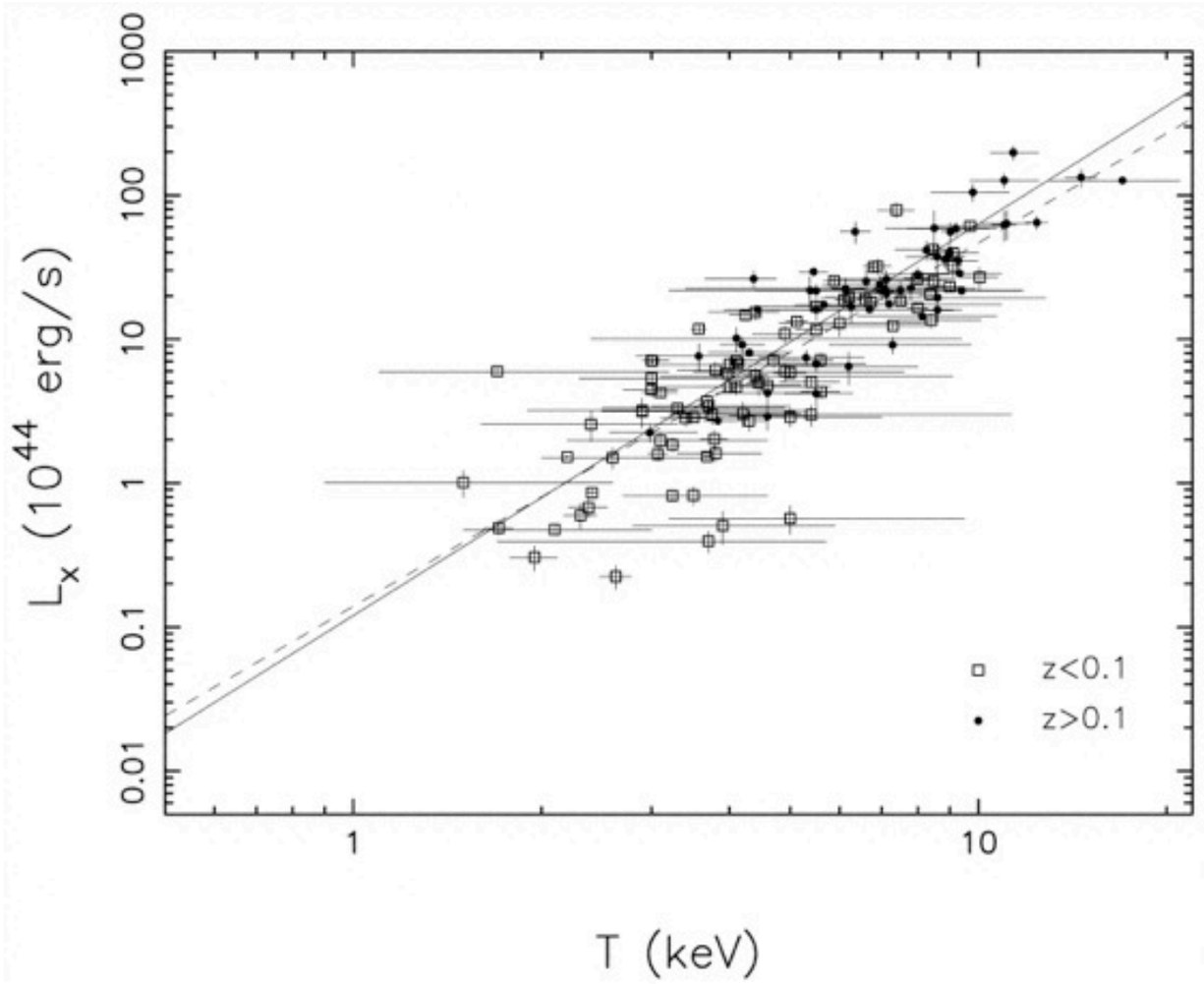

Measured slopes are $L \sim T^A$ with A=2.5-2.9.

SZ scaling relations

$$Y \equiv \int_\Omega y\, d\Omega = \frac{1}{D_A^2}\left(\frac{k_\mathrm{B}\sigma_T}{m_e c^2}\right)\int_0^\infty dl \int_A n_e T_e\, dA,$$

$$YD_A^2 \propto T_e \int n_e\, dV = M_\mathrm{gas} T_e = f_\mathrm{gas} M_\mathrm{tot} T_e.$$

$$YD_A^2 \propto f_\mathrm{gas} T_e^{5/2}$$
$$YD_A^2 \propto f_\mathrm{gas} M_\mathrm{tot}^{5/3}$$
$$YD_A^2 \propto f_\mathrm{gas}^{-2/3} M_\mathrm{gas}^{5/3}$$

Planck collaboration (2011)

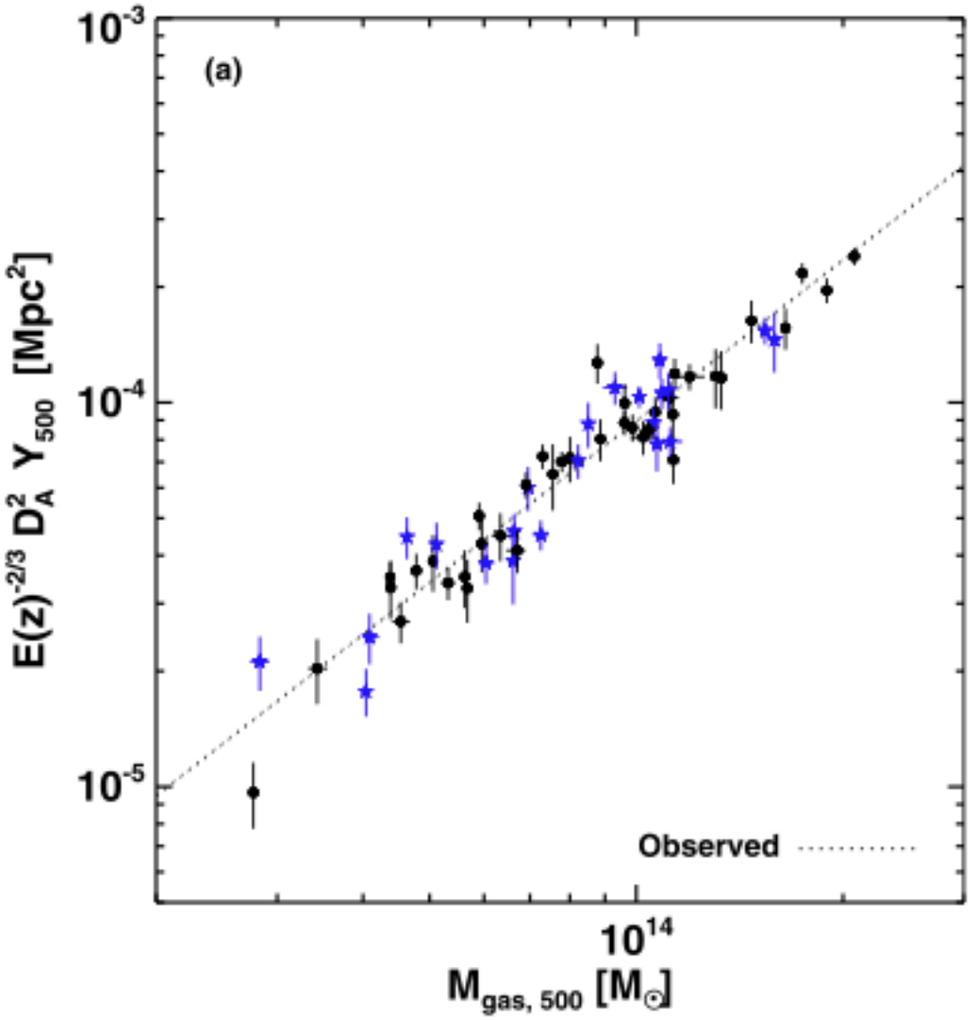

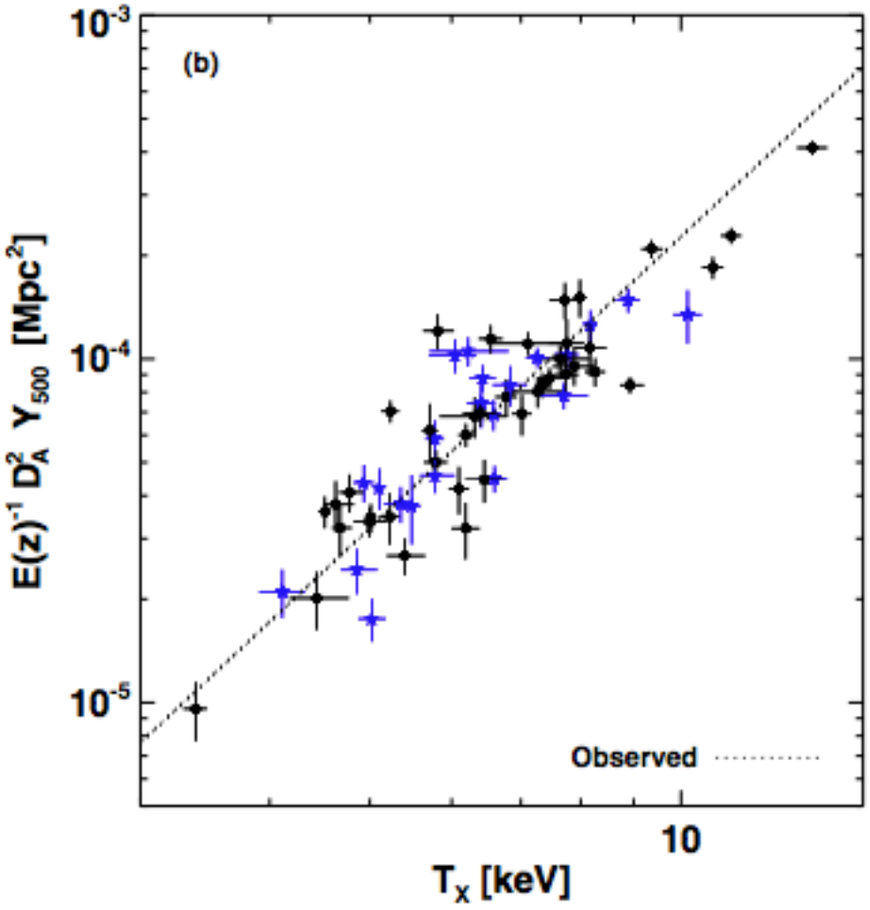

Scaling relation biases

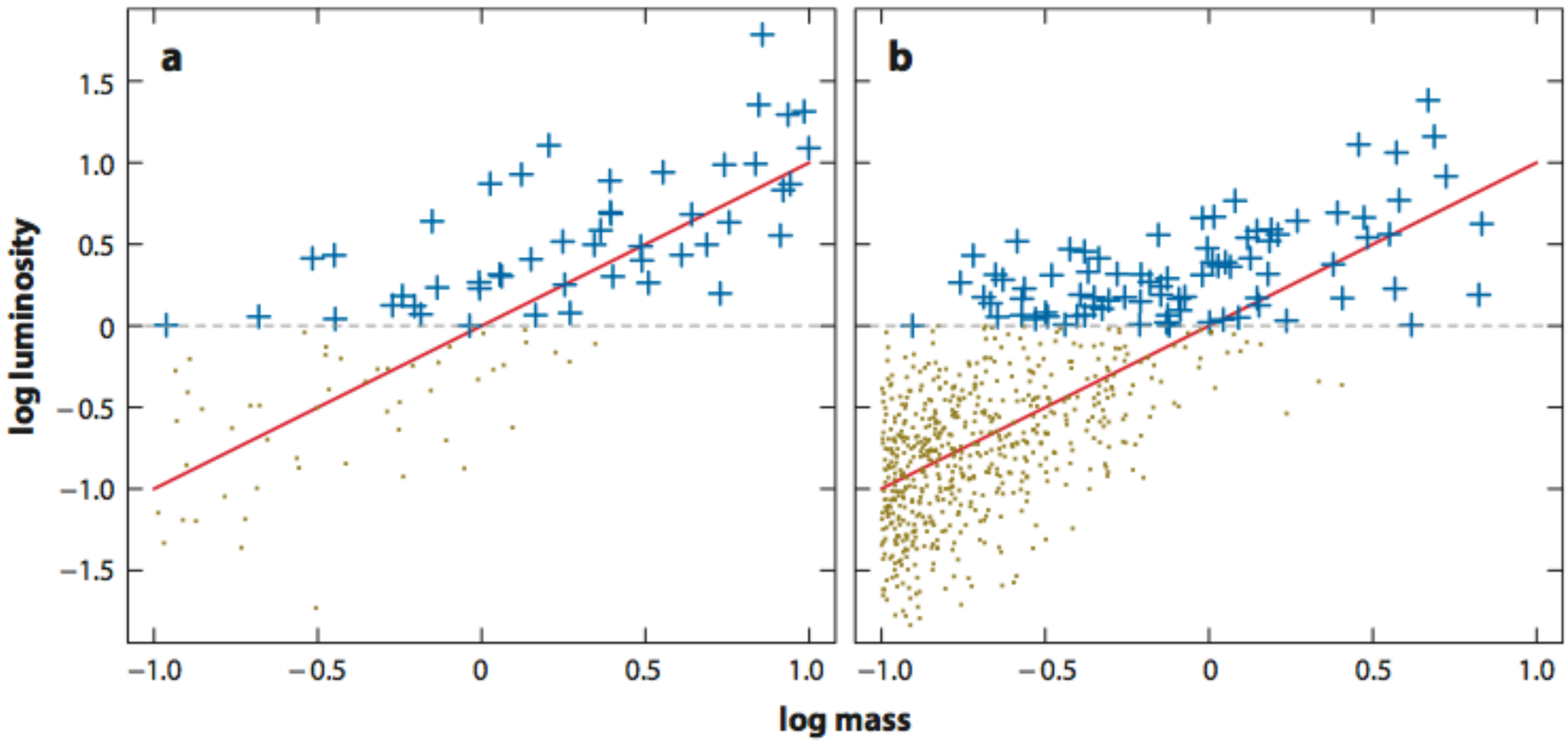

Figure 5

Diagrams illustrating generically how the distribution of observed scaling relation data (*blue crosses*) do not reflect the underlying scaling law (*red line*) due to selection effects (e.g., a luminosity threshold; *dashed gray line*). Dark yellow dots indicate undetected sources. (*a*) An unphysical case in which cluster log masses are uniformly distributed; (*b*) a case with a more realistic, steeper mass function than in panel *a* (normalized to produce roughly the same number at high masses). The steepness of the mass function has a clear effect on the degree of bias in the detected sample. To recover the correct scaling relation, an analysis must account for both the selection function of the data and the underlying mass function of the cluster population. Adapted from Mantz et al. (2010a).

Allen, Evrard, Mantz (2011)

Biases in selection

Different observable, but one still gets a bias from correlation between observables

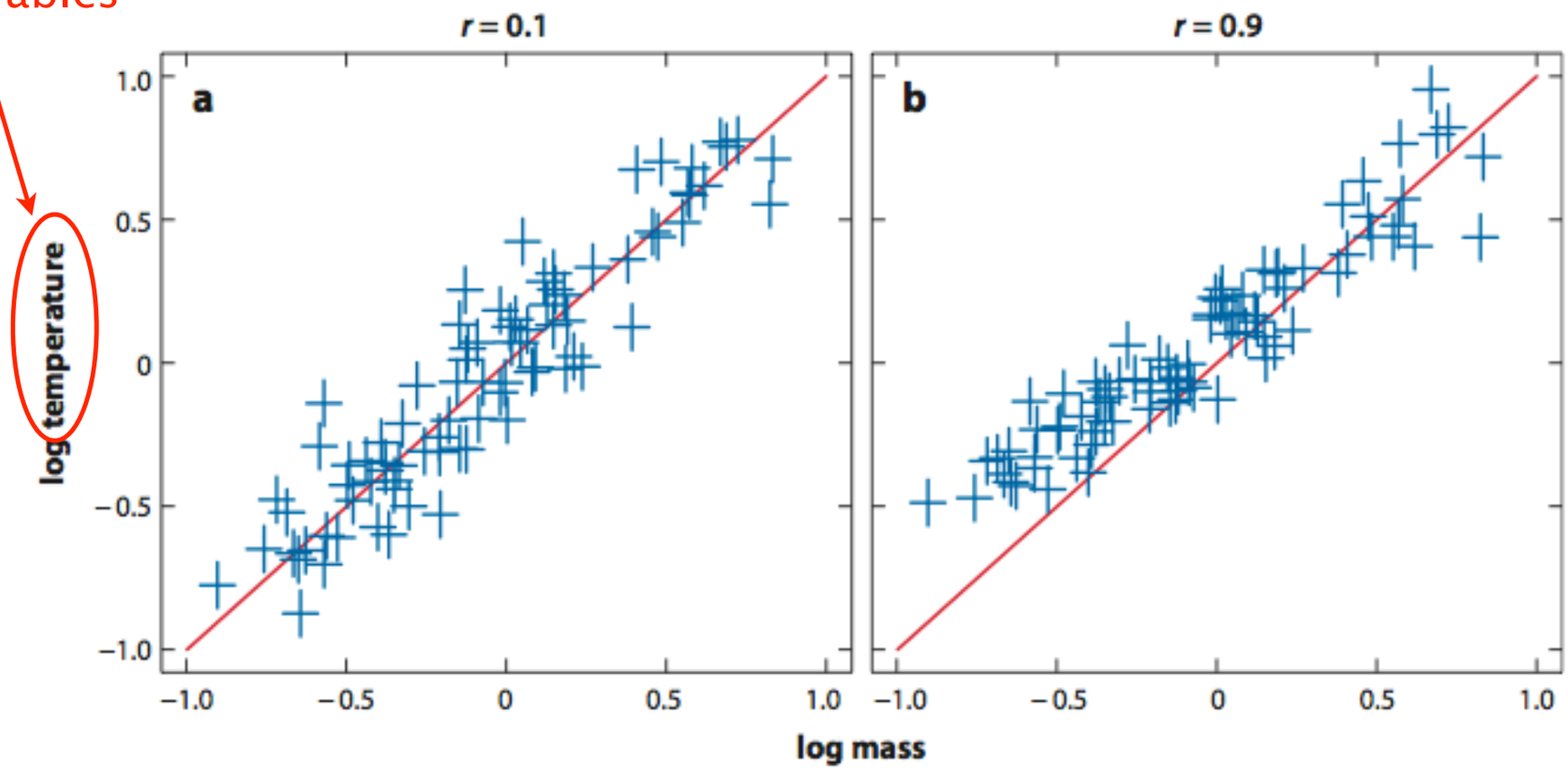

Figure 6

Example scaling relations where the observable of interest is not the basis of cluster selection. In both panels, the red line indicates the true scaling relation, and the blue crosses correspond to the detected clusters in **Figure 5*b***. The marginal scatter in this relation is chosen to be smaller than that in **Figure 5**, consistent with measured values of the luminosity-mass and temperature-mass intrinsic scatters (Section 3.3.4). The intrinsic temperature-luminosity correlation at fixed mass is relatively small in panel *a* ($r = 0.1$) and large in panel *b* ($r = 0.9$); in the latter case, the observed data are significantly influenced by selection bias despite the fact that the selection was made using a different observable.

Allen, Evrard, Mantz (2011)

Astrophysical biases: X-ray cool-cores

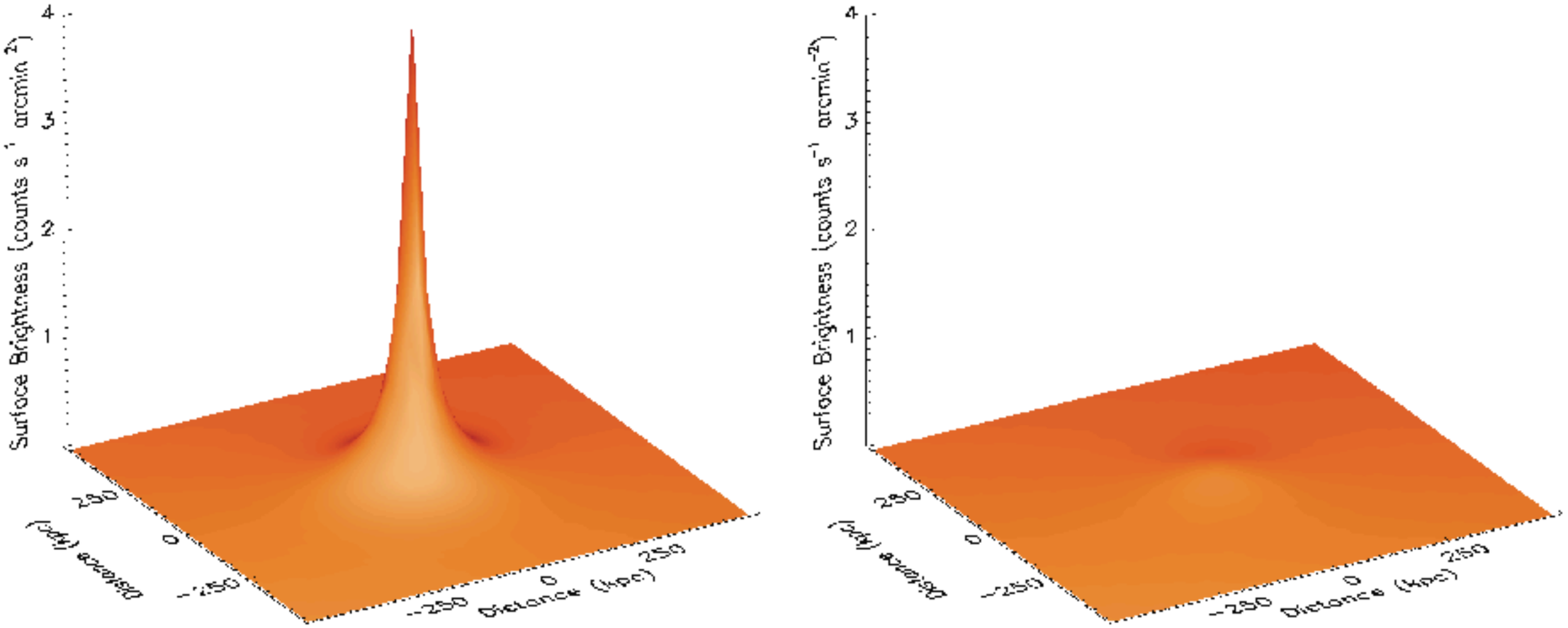

Figure 7. The three-dimensional representation of the projected surface brightness for the cool-core cluster Abell 2029 (left-hand panel) and the radio halo cluster Abell 2319 (right-hand panel) scaled to appear as they would if observed at the same redshift. The flat surface brightness core of Abell 2319 with respect to that of Abell 2029 (core radius of 120 versus 20 kpc, respectively) is the most obvious morphological distinction and impacts on the relative importance of projection effects in the two systems. The *X*- and *Y*-axes span 1 Mpc on a side. The *Z*-axis shows the surface brightness in units of counts s^{-1} $arcmin^{-2}$.

From Million & Allen (2009)

Cool-core bias in L–T scaling

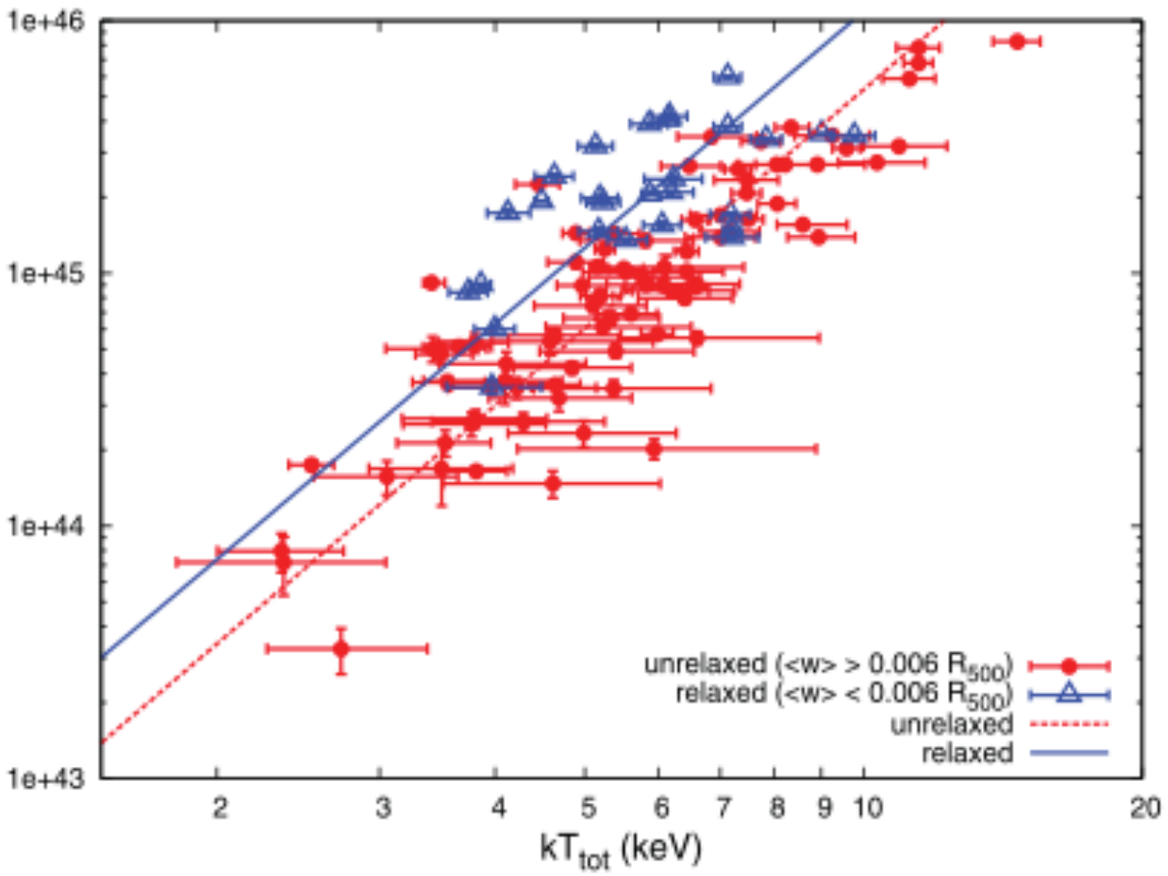

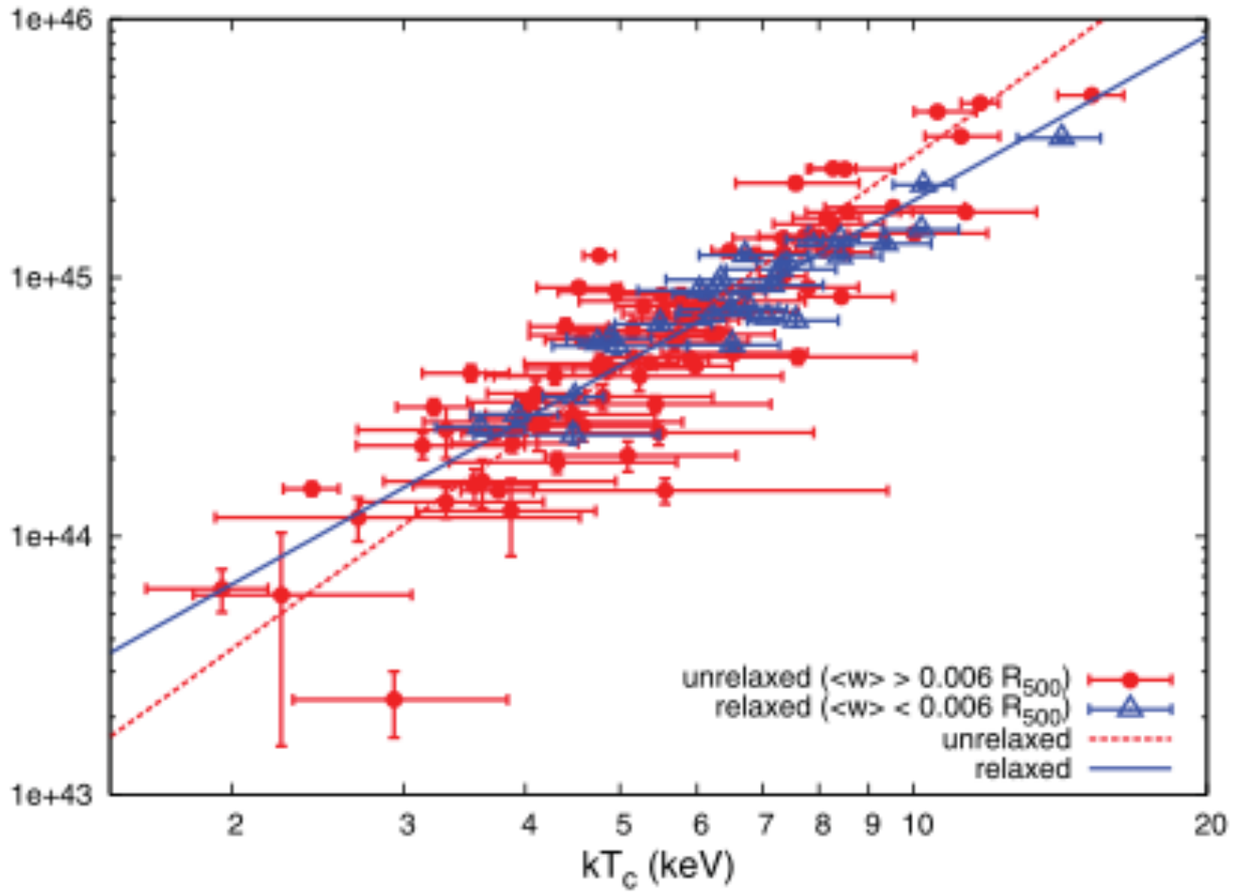

L–T relation for relaxed and non-relaxed clusters, before and after removing the core component (from Maughan et al. 2012)

Example of violation of self-similar scaling!

Y_X: a low-scatter X-ray mass proxy

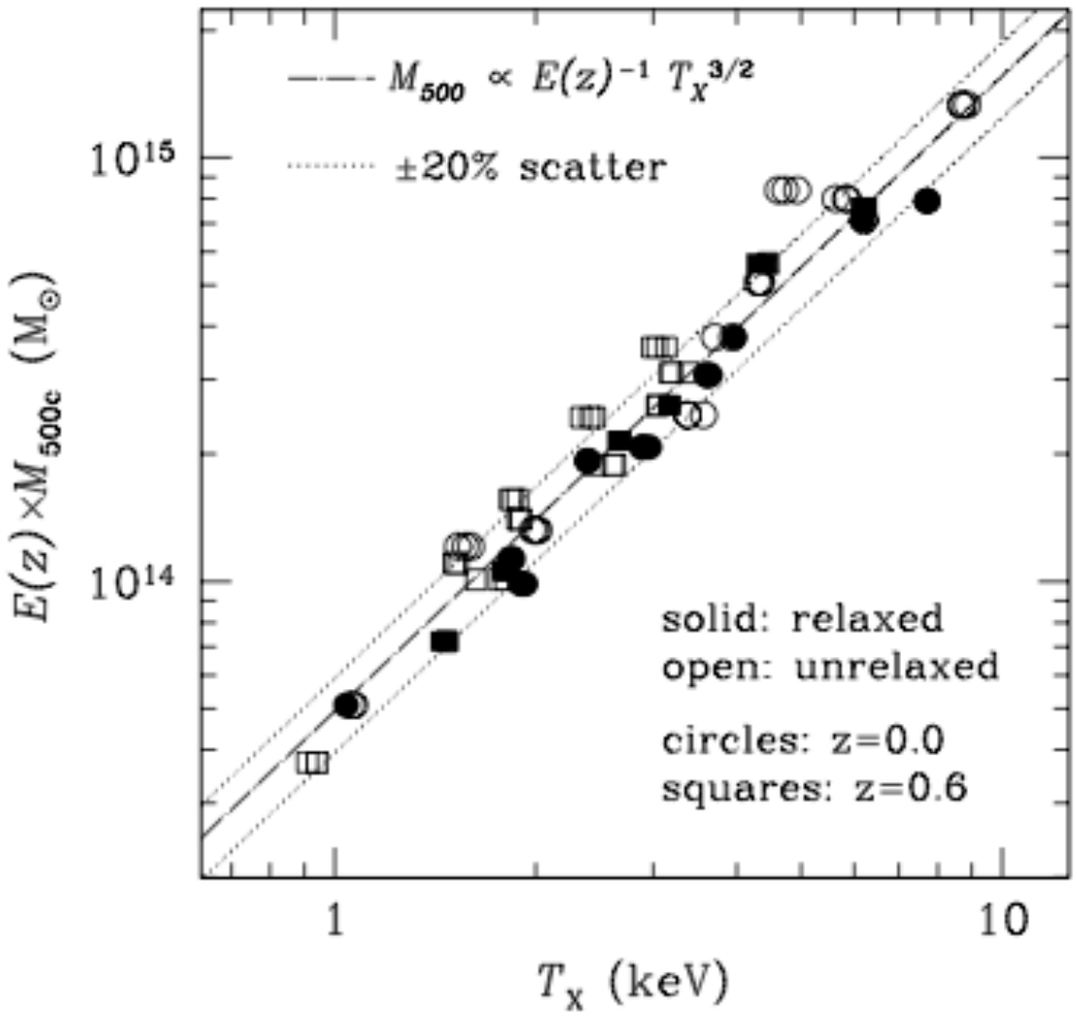

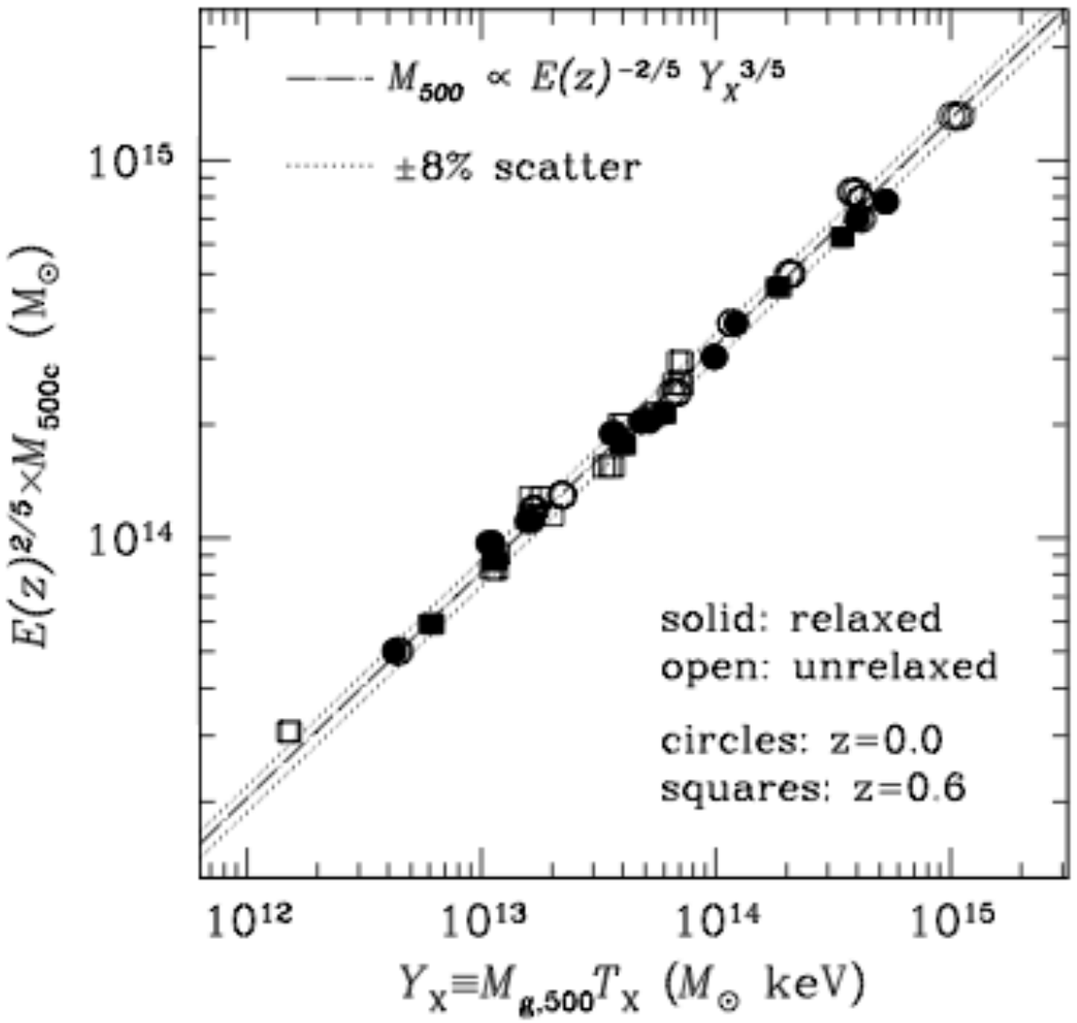

M_{gas} is also good mass proxy, but relatively larger scatter (~15%)

Figure from Kravtsov, Vikhlinin & Nagai (2006)

Y_X: a low-scatter mass proxy

$$Y_{\rm X} \equiv M_{g,500} T_{\rm X}$$

Yx is defined analogous to SZ integrated Y parameter: it is the X-ray analogue of total thermal pressure

We expect Y_X to be proportional to Y_{SZ}:

$$Y d_A^2 \propto Y_X,$$

but this relation is not exactly 1:1 because the two signals weigh the gas temperature differently.

Observationally, Y d_A^2 is proportional to $Y_X^{0.85 - 0.9}$

Y_X and Y_{SZ} comparison

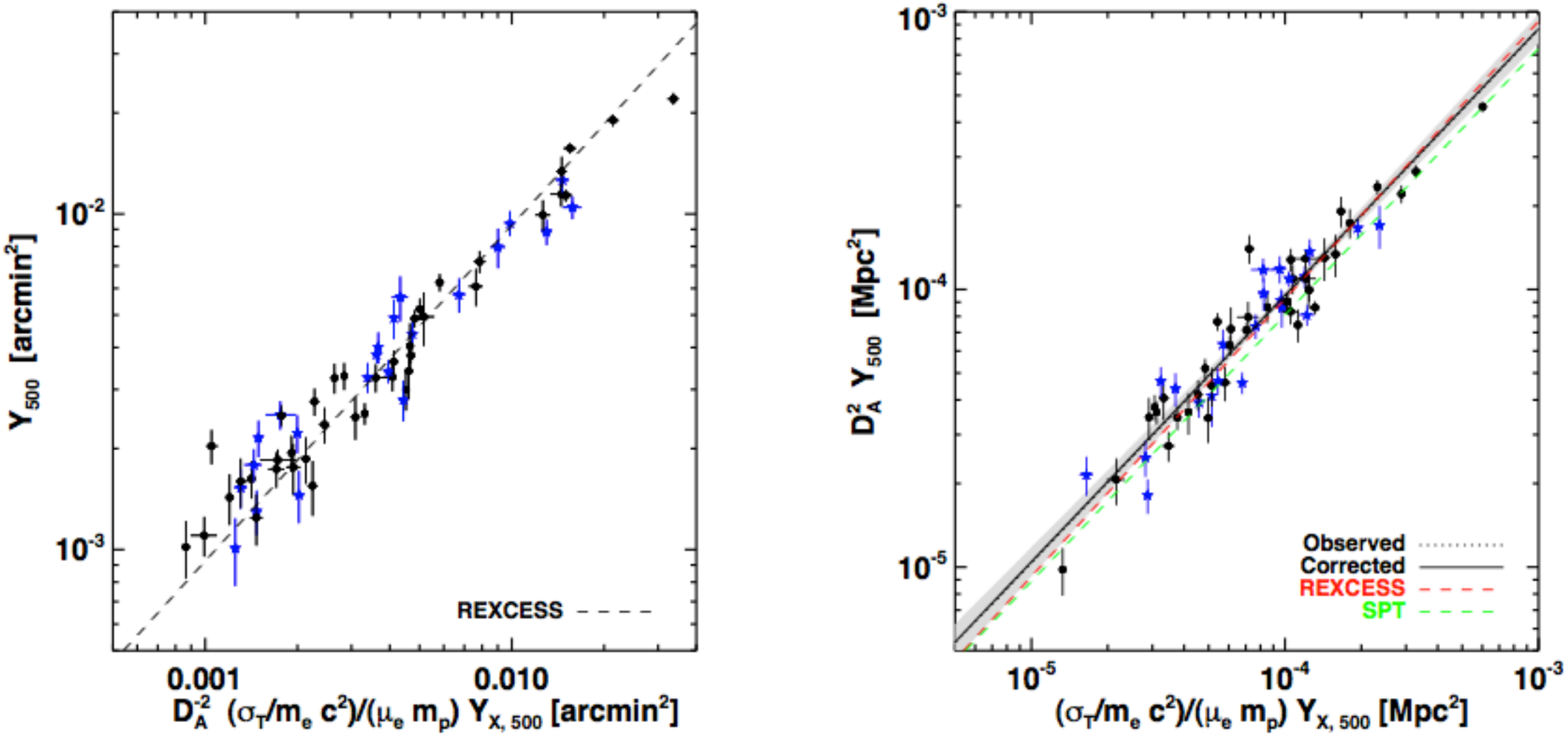

Fig. 4: SZ flux vs X-ray prediction. Blue stars indicate cool core systems. *Left panel:* Relation plotted in units of arcmin^2. The dashed line is the prediction from REXCESS X-ray observations (Arnaud et al. 2010). *Right panel:* Relation plotted in units of Mpc^2. The *SPT* results are taken from Andersson et al. (2010).

From Planck collaboration (2011)

Questions?